

26884



National Library of Canada

Bibliothèque nationale du Canada

CANADIAN THESES ON MICROFICHE

THÈSES CANADIENNES SUR MICROFICHE

NAME OF AUTHOR / NOM DE L'AUTEUR EKWERE JOHNSON PETERS

TITLE OF THESIS / TITRE DE LA THÈSE PATTERN OVERSWEEP IN FIVE AND NINE-SPOT WATERFLOOD PILOTS

UNIVERSITY / UNIVERSITÉ _____

DEGREE FOR WHICH THESIS WAS PRESENTED / GRADE POUR LEQUEL CETTE THÈSE FUT PRÉSENTÉE M.Sc. PETROLEUM ENGINEERING

YEAR THIS DEGREE CONFERRED / ANNÉE D'OBTENTION DE CE GRADE 1975

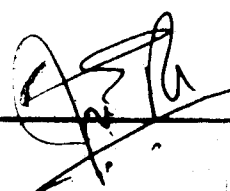
NAME OF SUPERVISOR / NOM DU DIRECTEUR DE THÈSE P. M. DRANCHUK

Permission is hereby granted to the NATIONAL LIBRARY OF CANADA to microfilm this thesis and to lend or sell copies of the film.

L'autorisation est, par la présente, accordée à la BIBLIOTHÈQUE NATIONALE DU CANADA de microfilmer cette thèse et de prêter ou de vendre des exemplaires du film.

The author reserves other publication rights, and neither the thesis nor extensive extracts from it may be printed or otherwise reproduced without the author's written permission.

L'auteur se réserve les autres droits de publication; ni la thèse ni de longs extraits de celle-ci ne doivent être imprimés ou autrement reproduits sans l'autorisation écrite de l'auteur.

DATED / DATE October 20, 1975 SIGNED / SIGNÉ 

PERMANENT ADDRESS / RÉSIDENCE FIXE 2005 GALBRAITH HOUSE
MICHENER PARK
EDMONTON, ALBERTA

THE UNIVERSITY OF ALBERTA

PATTERN OVERSWEEP IN FIVE AND NINE-SPOT WATERFLOOD PILOTS

by

Ekwere J. Peters



A THESIS

SUBMITTED TO THE FACULTY OF GRADUATE STUDIES AND RESEARCH
IN PARTIAL FULFILMENT OF THE REQUIREMENTS FOR THE DEGREE
OF MASTER OF SCIENCE IN PETROLEUM ENGINEERING .

DEPARTMENT OF MINERAL ENGINEERING

EDMONTON, ALBERTA

FALL, 1975

THE UNIVERSITY OF ALBERTA

FACULTY OF GRADUATE STUDIES AND RESEARCH

The undersigned certify that they have read, and recommend to the Faculty of Graduate Studies and Research, for acceptance, a thesis entitled "Pattern Oversweep in Five and Nine-Spot Waterflood Pilots" submitted by Ekwere J. Peters in partial fulfillment of the requirements for the degree of Master of Science in Petroleum Engineering.

Mr. Daubech
.....
Supervisor

Canon Bentzen
.....

B. Maddox
.....

Date October 17, 1975
.....

ABSTRACT

A laboratory model study has been conducted on isolated and partially confined five and nine-spot waterflood pilots to examine the problem of overly optimistic oil recoveries often observed in such pilots.

The model consisted of an unconsolidated pack of strongly water-wet glass beads sandwiched between two transparent lucite plates. Colored injection water permitted direct visual observation of the flood fronts. Three mobility ratios were studied, and in every case, initial water saturation was present.

The results indicate that both isolated five and nine-spot pilots continue to recover oil with continued water injection. However, when surrounded by a ring of eight similar patterns, both pilots behave as if confined provided the injection rates are sufficiently high to ensure stabilized floods. The higher the mobility ratio, the lower the injection rate required to ensure stabilized floods.

Despite the differences in the breakthrough oil recoveries, the ultimate recoveries from the stabilized five and nine-spot patterns are identical for the range of mobility ratios studied. This result is important from a practical standpoint. If field pilots behave as laboratory pilots, then a limited number of nine-spots, such as presented in this study, may be employed to expedite the feasibility studies of large scale five-spot floods in situations in which the lead time, rather than the cost of the project, is the overriding factor.

Also, a mathematical theory of two-phase immiscible fluid displacement in porous media has been employed to demonstrate the principles of model scaling of laboratory floods. This approach highlights the underlying assumptions and limitations of two-dimensional reservoir models. Furthermore, the scaling procedure proposed in the literature for five-spot floods has been successfully extended to nine-spot floods.

ACKNOWLEDGEMENTS

The author gratefully appreciates the able guidance provided by Professor P. M. Dranchuk who supervised this study.

Acknowledgement is also made to Dr. R. G. Bentsen for his helpful comments and suggestions regarding Model Scaling, Mr. D. Shaw of the Energy Resources Conservation Board for suggesting the oils used in this study, and to Imperial Oil Refinery for generously donating these oils.

The author also wishes to express his appreciation to the Canadian Commonwealth Scholarship and Fellowship Committee, the National Research Council and the Department of Energy, Mines and Resources for the financial support that made this study possible.

Finally, the author is grateful to his wife, Unwa, whose patience and understanding contributed immensely to the successful completion of this study.

TABLE OF CONTENTS

	PAGE
LIST OF TABLES	ix
LIST OF FIGURES	x
LIST OF PLATES	xii
I. INTRODUCTION	1
II. LITERATURE REVIEW	3
Optimistic Pilot Oil Recoveries	3
Pessimistic Pilot Oil Recoveries	4
Interpretation of Pilot Oil Recovery Data	5
Theory of Immiscible Fluid Displacement	6
1. Effect of Rate and Capillarity	7
2. Effect of Mobility Ratio	9
Five-Spot and Nine-Spot Sweep Efficiency	12
Summary	13
III. MODEL SCALING	14
Derivation of Equations	15
1. Dimensionless Form of the Combined Equation	18
1.1 One-Dimensional Horizontal Flow, No Gravity, No Capillarity	19
1.2 One-Dimensional Horizontal Flow, No Gravity	19
1.3 Two-Dimensional Horizontal Flow, No Gravity	20
Viscous Fingering	22
Scaling Applied to Five-Spot and Nine-Spot Patterns	23
IV. EXPERIMENTAL PROCEDURE AND MATERIALS	26
Patterns Studied	26
Equipment	26
Model and Fluid Properties	29
Procedure	33
V. EXPERIMENTAL RESULTS AND OBSERVATIONS	35
Isolated Pilot Performances	35
Pattern Confinement	42
Breakthrough Oil Recoveries	42
Confined Pilot Performance	50
Pilot Scaling	50

	PAGE
VI. DISCUSSION OF RESULTS	62
Isolated Pilot Performances	62
Pattern Confinement	63
Mechanism of Oversweep	63
Pilot Scaling	65
Effect of Mobility Ratio	66
Five-Spot versus Nine-Spot Performance	67
VII. SUMMARY AND CONCLUSIONS	70
Recommendations	71
NOMENCLATURE	72
REFERENCES	74
BIBLIOGRAPHY	80
APPENDIX A: Determination of the Permeability and Porosity of the Model	82
APPENDIX B: Flooding Results	86
APPENDIX C: Determination of Mobility Ratios	116
APPENDIX D: Calculation of Scaling Coefficients	117

LIST OF TABLES

TABLE		PAGE
1	Calibration of Injection Cylinders	30
2	Summary of Model Properties	32
3	Fluid Properties at 70°F	32

LIST OF FIGURES

FIGURE		PAGE
1	Pattern Arrangements	27
2.	Effect of Injection Rate on Oil Recovery from an Isolated 5-Spot Pattern. Mobility Ratio = 2.63	36
3.	Effect of Injection Rate on Oil Recovery from an Isolated 5-Spot Pattern. Mobility Ratio = 14.09	37
4.	Effect of Injection Rate on Oil Recovery from an Isolated 5-Spot Pattern. Mobility Ratio = 20.61	38
5.	Effect of Injection Rate on Oil Recovery from an Isolated 9-Spot Pattern. Mobility Ratio = 2.63	39
6.	Effect of Injection Rate on Oil Recovery from an Isolated 9-Spot Pattern. Mobility Ratio = 14.09	40
7.	Effect of Injection Rate on Oil Recovery from an Isolated 9-Spot Pattern. Mobility Ratio = 20.61	41
8.	Effect of Injection Rate on Oil Recovery from a Modified 5-Spot Pattern. Mobility Ratio = 2.63	43
9.	Effect of Injection Rate on Oil Recovery from a Modified 5-Spot Pattern. Mobility Ratio = 14.09	44
10.	Effect of Injection Rate on Oil Recovery from a Modified 5-Spot Pattern. Mobility Ratio = 20.61	45
11.	Effect of Injection Rate on Oil Recovery from a Modified 9-Spot Pattern. Mobility Ratio = 2.63	46
12.	Effect of Injection Rate on Oil Recovery from a Modified 9-Spot Pattern. Mobility Ratio = 14.09	47
13.	Effect of Injection Rate on Oil Recovery from a Modified 9-Spot Pattern. Mobility Ratio = 20.61	48
14.	Effect of Rate on Breakthrough Oil Recovery from Modified 5 and 9-Spot Patterns. Mobility Ratio = 2.63	49
15.	Effect of Rate on Breakthrough Oil Recovery from Modified 5 and 9-Spot Patterns. Mobility Ratio = 14.09	51

16	Effect of Rate on Breakthrough Oil Recovery from Modified 5 and 9-Spot Patterns. Mobility Ratio = 20.61	52
17	Comparison of Stabilized Oil Recovery Profiles from the Modified 5 and 9-Spot Patterns. Mobility Ratio = 2.63	53
18	Comparison of Stabilized Oil Recovery Profiles from the Modified 5 and 9-Spot Patterns. Mobility Ratio = 14.09	54
19	Comparison of Stabilized Oil Recovery Profiles from the Modified 5 and 9-Spot Patterns. Mobility Ratio = 20.61	55
20	Effect of Mobility Ratio on Stabilized Oil Recovery from the Modified 5 and 9-Spot Patterns	56
21	Variation of Oil Recovery with Scaling Coefficient at 1 Pore Volume Liquid Production. Viscosity Ratio = 1.32	58
22	Variation of Oil Recovery with Scaling Coefficient at 2 Pore Volumes Liquid Production. Mobility Ratio = 2.63	59
23	Variation of Oil Recovery with Scaling Coefficient at 1 Pore Volume Liquid Production. Mobility Ratio = 14.09	60
24	Variation of Oil Recovery with Scaling Coefficient at 2 Pore Volumes Liquid Production. Mobility Ratio = 14.09	61
25	Variation of Pressure Drop with Injection Rate into a 5-Spot Pattern	84

LIST OF PLATES

PLATE		PAGE
1	Reservoir Model with Injection Manometers	28
2	Injection Cylinders	31
3	Breakthrough Areal Coverage for a Confined 5-Spot Pattern	69
4	Breakthrough Areal Coverage for a Confined 9-Spot Pattern	* 69

I. INTRODUCTION

A widely accepted method of studying the feasibility of large scale waterfloods is by the use of pilot waterfloods which usually consist of isolated patterns located in some representative portion of the field. The object is that the recoveries from these isolated pilots can be used as a measure of the oil recoveries to be expected from the large scale floods.

There may be situations in which such uncorrected pilot data may reliably predict large scale flood recoveries. However, in most cases, these isolated pilots have proved unreliable in predicting oil recoveries from fully developed floods. This unreliability stems from the freedom with which fluids can migrate into and out of the pilot area.

Several laboratory experiments have demonstrated that the oil recoveries from isolated or unconfined pilots can be extremely misleading. Some investigators (1, 2, 3, 4, 5) have shown that there are situations in which pilot flood oil recoveries are far too optimistic. Others (6, 7, 8) have shown that pilot recoveries can also be pessimistic, especially if the pilots are initiated in already depleted fields having low reservoir pressures.

This study was concerned with the problem of oversweep, which is the tendency of waterflood pilots to yield rather optimistic oil recoveries. Most of the existing attempts to allow for oversweep in interpreting pilot recovery data consist largely of history matching in which arbitrary correction factors are used to scale down pilot data (9, 10). A major limitation of this approach is that the empirical

correction factors are unknown functions of both fluid and reservoir properties and as such, are not easily predictable. Moreover, implicit in the idea of correction factors is an assumption that the ultimate recovery for the fully developed flood is known by some independent means. Very often, this is not the case.

Therefore, a more desirable solution to the problem of oversweep would be to operate the pilot in such a manner as to minimise oversweep if not completely eliminate it; that is, the pilot should be made to approach confined behaviour. The production history from such pilots may then be applied directly as an estimate of the recovery of the fully developed waterflood.

It was the purpose of this study to examine how pilot confinement may be achieved by judicious choices of injection rates and pattern configurations. These are some of the factors that can be easily controlled by the operator of the pilot. In view of the large number of possible pattern configurations, it would be necessary to limit the choice of patterns if the study is to be manageable. It was therefore decided to restrict the present study to two basic patterns: the popular and widely used five-spot pattern and the potentially advantageous normal nine-spot scheme. In particular, it would be of interest to compare the performances of these two patterns. Since fluid migration is influenced by mobility ratio, this factor was included in the study.

A secondary but important aim of this study was to develop a scaling procedure for the nine-spot pattern. This subject has received little or no attention in the literature to date.

II. LITERATURE REVIEW

Optimistic Pilot Oil Recoveries

Excessive oil recoveries from laboratory waterflood pilots have been documented by several investigators (11, 12, 13, 14, 15, 16). In some cases, recoveries of up to four times the oil originally contained within the pilot area have been reported (17).

Caudle and Loncaric (18) studied pilot oil recoveries using an artificially consolidated sandstone model and miscible fluids. Their model, consisting of one-eighth of a five-spot pattern, was partially confined because it extended beyond the pilot area by three well lengths giving rise to the possibility of oil migration into and out of the pilot area.

Their results, reported as functions of injection to production rate ratios, indicate a marked dependence of pilot oil recoveries on injection and production rates. For a rate ratio of unity, oil recovery of up to four times the displaceable pilot oil volume was recorded. But as the rate ratios increased, the oil recovery approached that of the confined or fully developed flood. This observation is important, for it suggests that for sufficiently high injection rates, isolated pilots tend to behave as if confined. If this is true, then injection rate control may be used to ensure flood confinement.

Drychuk and Jain (19) examined the effect of surrounding a normal five-spot pattern with a ring of eight like patterns. In their study, an injection rate in excess of that required by Rapoport, Carpenter and Leas (20) scaling criterion was employed to ensure stabilized floods.

A significant conclusion of this study was that while surrounding the five-spot with eight like-patterns limited the extent of oversweep, it was nevertheless insufficient to ensure effective pattern confinement for the injection rate used.

Pessimistic Pilot Oil Recoveries

Not all laboratory pilots yield optimistic oil recoveries. Some investigators have shown that under certain conditions, laboratory and field pilot recoveries may in fact be pessimistic.

Dalton, Rapoport and Carpenter (21) noted that the recovery history of waterflood pilots depended greatly on the ability of the producers within the pilots to compete for fluid with other producers in the field. If reservoir pressure is low, it is not possible for the producers to provide the sizeable pressure sink required to attract large quantities of oil and injected fluid. In this situation, it is possible that substantial oil migration would occur from the pilot area resulting in a pessimistic pilot recovery. On the other hand, if the reservoir pressure is high and the pressure at the producing wells low, the area supplying oil to the pilot producers can substantially exceed that contained by the basic pilot area. This situation results in optimistic oil recoveries. Dalton et al characterized this pressure influence on pilots by the π -ratio, defined as a dimensionless ratio of the reservoir to injection pressure.

Craig (22) similarly observed that pilot recovery history was a function of the productivity of the pilot producer. He studied the oil recovery performance of a laboratory five-spot surrounded by two rings of competing producers and concluded that such a pilot would

correctly predict fully developed flood recovery if the Condition Ratio of the pilot producer was at least 2.22. The Condition Ratio is equivalent to the ratio of a well's actual productivity to the productivity of an undamaged, non-stimulated, normal-sized well in the same formation. Craig's Condition Ratio concept is analogous to Dalton, Rapoport and Carpenter's (23) π -ratio concept in that both represent a measure of the pilot producer's ability to capture fluid.

Other aspects of Craig's study merit detailed examination. He observed that fluid migration across the pilot perimeter was minimized by the presence of radial waterflood fronts around the pilot injectors. When these fronts coalesced, the pilot area was effectively shielded from extraneous oil. The formation of these radial water banks was facilitated by an initial gas saturation and by the presence of competing producers around the pilot. As these conditions are usually present in the field, it may be inferred from Craig's observations that field pilots are unlikely to yield optimistic recoveries. In fact, if the Condition Ratios of the pilot producers are less than 2.22, pessimistic oil recoveries would result.

Interpretation of Pilot Recovery Data

To allow for the discrepancy between pilot and fully developed waterflood recoveries, Caudle et al (24) and Dalton et al (25) propose the use of correction factors.

Caudle's correction factors rely on a prior knowledge of the recovery performance of the fully developed flood while those of Dalton et al are based on the areal recovery factor, defined as the area which supplies oil to the basic pilot producer. In either case, application

of the laboratory results is achieved by adjusting the recovery curve of the field pilot conducted at a set rate or π -ratio to the confined pattern recovery values by the appropriate correction factors. Practical application of this technique is somewhat limited because neither the fully developed recovery history nor the areal recovery factor can be easily predicted.

Theory of Immiscible Fluid Displacement

The behaviour of laboratory and indeed field waterflood pilots are determined to a great extent by the factors that govern the immiscible displacement of one fluid by another in porous media. Any attempts to explain or predict waterflood performance must of necessity be preceded by an understanding of these factors.

A detailed derivation of the equations of immiscible fluid flow in porous media is presented under "Model Scaling". However, some of the factors that govern the displacement process may be deduced from the simple mathematical two-phase displacement model proposed by Buckley and Leverett (26). By applying Darcy's law to each of the phases, the authors derived their pioneering fractional flow equation:

$$f_w = \frac{1 + \frac{Kk_{ro}}{u^* \mu_o} \left(\frac{\partial P_c}{\partial x} - g\Delta\rho \cos\alpha \right)}{1 + \frac{k_{ro} \mu_w}{\mu_o k_{rw}}} \quad 1$$

where

f_w = fraction of water in the flowing stream passing any point in the medium

K = absolute permeability of the medium

k_{ro} = relative permeability to oil

- k_{rw} = relative permeability to water
- μ_o = oil viscosity
- μ_w = water viscosity
- u^* = total fluid velocity
- P_c = capillary pressure
- x = distance along direction of movement
- g = acceleration due to gravity
- $\Delta\rho$ = water-oil density difference
- α = angle of the formation dip to the vertical

Examination of the fractional flow equation reveals that the displacement process is influenced explicitly by (a) the rate of fluid movement (b) the rock properties through the absolute and relative permeability terms and (c) the fluid densities and viscosities. Other factors which indirectly enter the fractional flow equation include: wettability, surface and interfacial tensions and fluid saturation geometries, due to the inclusion of the capillary pressure term; rock grain size, composition and cementation, all of which influence the permeability of the porous medium.

1. Effect of Rate and Capillarity

Investigators disagree on the effect of production or injection rate on waterflood oil recovery. Some maintain that recovery decreases with increasing rate while others maintain that the opposite is true. And still others maintain that recovery is independent of rate.

Richardson and Perkins (27) concluded from their laboratory investigation that waterflood oil recovery was independent of rate over

a wide range of operating conditions, while Rapoport et al (28, 29), working with oil-wet porous media, observed that recovery increased with increasing rate but became rate independent at a sufficiently high rate. At this stage, the flood was said to have stabilized and the rate beyond which stabilization occurred was termed the critical rate. de Haan (30) confirmed that recovery increased with rate up to a point, but that further rate increase resulted in decreasing oil recovery especially at high oil-water viscosity ratios. Both de Haan (31) and Engelbert et al (32) attribute this reduction in recovery at high oil-water viscosity ratios to the phenomenon of "viscous fingering".

Theoretical calculations as well as experimental results indicate that the effect of rate on the efficiency of immiscible fluid displacement manifests itself almost entirely through the influence of capillarity. It is generally accepted that at very low rates, capillary forces dominate the displacement process; but as the rate increases, the influence of capillary forces diminishes until at sufficiently high rates, the rate dependent capillary terms of the fractional flow equation become negligible, making the displacement process effectively independent of rate. These observations are supported by the experimental results of Rapoport et al (33, 34) and the theoretical calculations of Douglas, Blair and Wagner (35).

Douglas et al (36) obtained numerical solutions for the fractional flow equation with capillarity at various dimensionless rates. Their results show that at high rates, a sharp water saturation front exists so that the displacement mechanism approximates the Buckley-Leverett model without capillarity. The formation of a sharp front

results in a very efficient, piston-like displacement. At low rates, no distinct water saturation front exists; as a result, the displacement process is inherently inefficient.

Capillary forces affect laboratory displacement experiments in other ways. Several investigators have observed that certain displacement experiments exhibit delayed water production (37, 38, 39). That is, the production of water occurs long after the water has first arrived at the outflow end of the core. The result is that the breakthrough recoveries obtained from such experiments are too high. This is the so-called capillary end effect. As pointed out by Leverett (40), the capillary end effect may be so severe in some systems as to completely invalidate the displacement results.

From theoretical considerations, it is clear that the capillary end effect is due mainly to the capillary pressure discontinuity at both the inlet and outlet ends of the core. The effect is known to be particularly severe at low displacement rates in short cores. It is to minimize the end effects that most experimenters recommend the use of long cores and high displacement rates.

2. Effect of Mobility Ratio

The effects of fluid viscosities and relative permeabilities on waterflooding are best studied through the concept of mobility ratio. Fluid mobility is the ratio of the effective permeability to fluid viscosity. Conventionally, mobility ratio is defined as the ratio of the displacing fluid mobility to that of the displaced phase. By this convention, mobilities less than unity are considered favorable while those greater than unity are unfavorable.

It is generally accepted that mobility ratio determines the breakthrough areal sweep efficiency of pattern floods. The areal sweep efficiency is that fraction of the pattern area contacted by the displacing fluid. The effect of mobility ratio on the areal sweep efficiency at breakthrough for a confined five-spot well pattern has been studied by Aronofsky and Ramey (41) with an electrolytic tank; by Dyes, Caudle and Erickson (42) and Caudle, Erickson and Slobod (43), by means of porous plate models and x-ray shadowgraph techniques; by Fay and Prats (44) and by Bradley, Heller and Odeh (45), with potentiometric models.

The results of five-spot sweep efficiencies obtained by the above methods have been summarized by Bradley et al (46). Their summary shows fair agreement among the methods in the region of unit mobility ratio and wide differences at low and high mobility ratios. Generally, the efficiencies based on the electrical analog of fluid flow tend to be optimistic by comparison to those obtained from models using porous media.

Practical difficulties arise in determining the mobility ratio for an immiscible fluid displacement. Many of the early mobility ratio studies, especially those based on the electrical analog of fluid flow, assumed piston-like displacement with only the displaced fluid flowing ahead of the front and the displacing fluid behind the front. In this situation, the mobilities of the displacing and displaced phases are unique and single-valued. In the case of immiscible displacement however, the situation is not as clearcut. The leaky-piston displacement model of Buckley-Leverett (47) has shown that two-phase flow occurs

behind the front. Thus behind the front, the mobility of the displacing phase is continuously changing in accordance with the relative permeability-saturation behaviour of the porous medium, rising from zero at the beginning of the displacement to a maximum at floodout.

To overcome this difficulty, Craig, Geffen and Morse (48) propose that the mobility of the displacing phase be determined at the average displacing phase saturation behind the front. The authors recognize that this choice is somewhat arbitrary but maintain that mobility ratios defined on this basis have been successfully used to correlate waterflood recoveries. On the other hand, Perkins and Collins (49) have pointed out that the mobility ratio defined at residual fluid saturations constitutes a useful scaling group in laboratory waterflood studies.

Some investigators have used miscible fluids to study mobility ratio effect on sweep efficiencies (50, 51). Miscible fluids have the advantage of eliminating capillary effects. Moreover, the mobility ratio simplifies to the viscosity ratio of the displaced to the displacing phases. However, results obtained by the use of miscible fluids may be affected by the presence of mixing or transition zones. This effect is believed to be responsible for the consistently lower sweep efficiencies attributed to the five-spot pattern by Caudle et al (52) and Dyes et al. (53) as compared to those of other workers.

Despite differences in quantitative and definitional details, there is general agreement on the broad effects of mobility ratio on waterflood recovery. At favorable mobility ratios, the areal sweep efficiency is high and much of the oil recovery is achieved at break-

through. Injection of water beyond breakthrough results in almost 100 percent coverage at a low watercut. At adverse mobility ratios however, the results are reversed. Breakthrough sweep efficiency is low and much of the oil is recovered during the so-called subordinate displacement phase which follows the initial water breakthrough. Injection beyond water breakthrough leads to a rapid increase in water-oil ratios. Although potentially the same ultimate recovery is obtainable over a wide range of mobility ratios, the rapid increase in water-oil ratios usually leads to early flood abandonment and hence less oil recovery in unfavorable mobility ratio situations.

Five-spot and Nine-spot Sweep Efficiencies

The areal sweep efficiency for the five-spot pattern has received considerable attention in the literature (54, 55, 56, 57, 58). Although the summary of Bradley et al (59) shows wide differences in the breakthrough sweep efficiencies attributed to the five-spot by various investigators, the consensus is that at unit mobility ratio the efficiency is about 72 percent. It must be emphasized that this is the efficiency under highly idealized conditions. In practice, field conditions differ considerably from the ideal and as such, the five-spot sweep efficiency under field conditions may be much lower than 72 even at more favorable mobility ratios.

Unlike the five-spot pattern, very little has been published on nine-spot sweep efficiencies. By means of potential theory calculations, Krutter (60) arrived at a breakthrough sweep efficiency of 52 percent for unit mobility ratio and concluded that the nine-spot was inferior to the five-spot flooding pattern. Muskat (61) extended

Krutter's results and showed that the efficiency varied from 50 to 78 percent depending on the rate ratio of the corner to side wells. At a rate ratio of 1, that is when the injection or production rates of the corner and side wells were equal, the areal sweep at breakthrough was about 50 percent. A maximum sweep of 78 percent was achieved at a rate ratio of 10.6. For large rate ratios, equivalent to closing in the side wells, the sweep efficiency approached 72 percent which is that for a five-spot pattern.

Thus, under certain conditions, the breakthrough efficiency of the five-spot is superior to that of the nine-spot pattern. However, Crawford (62) has reported that a comparative study of the five and nine-spot patterns yielded identical ultimate recoveries.

Summary

A review of the literature has shown that surrounding an isolated five-spot pilot with a ring of eight like patterns limits the extent of oversweep (63) and that oversweep decreases with increasing injection to production rate ratios (64). It is apparent, therefore, that a combination of the above pattern arrangement with the observed rate effect may be employed to minimize oversweep in waterflood pilots, if not completely eliminate it. The present study is based on this premise.

III. MODEL SCALING

If laboratory displacement experiments are to be successfully used to predict multi-phase fluid flow behaviour in petroleum reservoirs, such experiments must be "properly scaled". Apart from the obvious differences in dimensions between the model and the prototype, the flow regimes in both systems may differ considerably. For instance, forces that have practically no effect on the behaviour of the prototype, may significantly affect the behaviour of the model. An example is the capillary end effect encountered in laboratory displacements.

Generally, complete scaling cannot be achieved; for example, an oil well in the field would scale to microscopic dimensions in any laboratory model. This is not a serious problem because in certain situations, some of the scaling criteria may be relaxed without undue loss of analogy between the model and the prototype. Often the purpose is not to achieve complete scaling but rather to recognize the extent to which the inevitable imperfections of the model limits extrapolation of the laboratory results to field conditions.

Two general methods are available for deriving dimensionless scaling groups. The first and older of the two is dimensional analysis which is essentially a trial and error procedure. Successful application of this method depends on a sound knowledge of the complete set of relevant variables. The second and newer method is inspectional analysis which depends on the dimensional homogeneity of the equations describing the behaviour of the system. A fundamental requirement of inspectional analysis is that the process under study be expressible by a mathematical equation.

The main disadvantage of dimensional analysis is that the physical meaning of the similarity groups obtained by this method is usually less apparent than that obtained by inspectional analysis. On the other hand, the formulation of the mathematical equations required by inspectional analysis usually involves making simplifying assumptions with the consequence that certain groups which can be important in less ideal conditions may be omitted (65).

The use of dimensionless groups in studying water drive processes was pioneered by Leverett, Lewis and True (66). Engelberts and Klinkenberg (67) extended their work. A detailed use of inspectional analysis for model scaling has been published by Rapoport (68). Also, Rapoport and Leas (69) used inspectional analysis to scale a linear laboratory displacement experiment. Geertsma, Croes and Schwarz (70) combined dimensional and inspectional analyses in deriving their scaling groups.

In what follows, inspectional analysis is used to derive some of the dimensionless scaling groups for two-phase incompressible flow in porous media. This is undertaken to point out in a systematic manner the various underlying assumptions and hence the justification for the use of two-dimensional models in laboratory simulation of reservoir displacement mechanisms. The equations are similar to those derived by Spivak (71).

Derivation of Equations

The partial differential equation describing two-phase immiscible and incompressible flow in three-dimensions follows from combination of Darcy's law with the law of conservation of matter.

Darcy's law for the oil and water phases respectively is

$$\vec{u}_o = -K \frac{k_{ro}}{\mu_o} (\nabla P_o - \rho_o g \nabla Z) \quad 2-a$$

$$\vec{u}_w = -K \frac{k_{rw}}{\mu_w} (\nabla P_w - \rho_w g \nabla Z) \quad 2-b$$

The continuity equations which express the conservation of volume may be written as

$$\nabla \cdot (\vec{u}_o) = \nabla \cdot \left(-K \frac{k_{ro}}{\mu_o} (\nabla P_o - \rho_o g \nabla Z) \right) = -\phi \frac{\partial S_o}{\partial t} - q_{vo} \quad 3-a$$

$$\nabla \cdot (\vec{u}_w) = \nabla \cdot \left(-K \frac{k_{rw}}{\mu_w} (\nabla P_w - \rho_w g \nabla Z) \right) = -\phi \frac{\partial S_w}{\partial t} - q_{vw} \quad 3-b$$

Addition of 3-a and 3-b yields

$$\nabla \cdot (\vec{u}_o + \vec{u}_w) = \nabla \cdot (\vec{u}) = -(q_{vo} + q_{vw}) = -q_v \quad 4$$

The set of Equations 3 with appropriate initial and boundary conditions completely describes two-phase, incompressible, immiscible fluid flow in porous media. Defining capillary pressure as $P_o - P_w = P_c$ and K_m for phase m as $(k_r/\mu)_m$ and substituting, then Equation 2-a becomes,

$$\begin{aligned} \vec{u}_o &= -KK_o (\nabla (P_w + P_c) - \rho_o g \nabla Z) \\ &= -KK_o \nabla P_w - KK_o \nabla P_c + KK_o \rho_o g \nabla Z \end{aligned} \quad 5$$

Combining 2-b and 5,

$$\begin{aligned} \vec{u}_o + \vec{u}_w = \vec{u} &= -K (K_o + K_w) \nabla P_w - KK_o \nabla P_c \\ &\quad + Kg(K_o \rho_o + K_w \rho_w) \nabla Z \end{aligned} \quad 6$$

Therefore

$$\nabla P_w = \frac{-\vec{u}}{K(K_o + K_w)} - \frac{K_o}{K_o + K_w} \nabla P_c + \frac{K_o \rho_o g + K_w \rho_w g}{K_o + K_w} \nabla Z \quad 7$$

Substituting 7 into 3-b gives

$$\nabla \cdot \left(\frac{K_w}{K_o + K_w} \vec{u} + K \frac{K_w K_o}{K_o + K_w} \nabla P_c + K \Delta \rho g \frac{K_w K_o}{K_o + K_w} \nabla Z \right) = -\phi \frac{\partial S_w}{\partial t} - q_{vw} \quad 8$$

where $\Delta \rho = \rho_w - \rho_o$

Defining the dimensionless quantities

$$f(S_w) = \frac{K_w}{K_o + K_w}$$

and

$$\psi(S_w) = k_{ro}(S_w) \cdot f(S_w),$$

Equation 8 becomes

$$\nabla \cdot \left(f \vec{u} + \frac{K}{\mu_o} \psi \nabla P_c + \frac{K}{\mu_o} g \Delta \rho \psi \nabla Z \right) - q_{vw} = \phi \frac{\partial S_w}{\partial t} \quad 9$$

or, since $\nabla \cdot (f \vec{u}) = f \nabla \cdot \vec{u} + \vec{u} \cdot \nabla f$

$$f \nabla \cdot \vec{u} + \vec{u} \cdot \nabla f + \nabla \cdot \left(\frac{K}{\mu_o} \psi \nabla P_c + \frac{K}{\mu_o} g \Delta \rho \psi \nabla Z \right) = -\phi \frac{\partial S_w}{\partial t} - q_{vw} \quad 10$$

Defining q_{vw} at a point as $f q_v$ where q_v is the total source or sink term, then using 4, Equation 10 becomes

$$\vec{u} \cdot \nabla f + \nabla \cdot \left(\frac{K}{\mu_o} \psi \nabla P_c \right) + \nabla \cdot \left(\frac{K}{\mu_o} g \Delta \rho \psi \nabla Z \right) = -\phi \frac{\partial S_w}{\partial t} \quad 11$$

Equation 11 will be referred to as the combined displacement equation. It is interesting to note that the three terms on the left side of Equation 11 are the viscous, capillary and gravity terms usually referred to in the literature.

Equations 11 and 4 are two nonlinear partial differential equations in two dependent variables, $\vec{u}(x, y, z, t)$ and $S_w(x, y, z, t)$. If the flux vector \vec{u} is known, then Equation 11 alone completely

describes the problem. In cartesian coordinates for an anisotropic reservoir with constant dip angles, Equation 11 is written as

$$\begin{aligned}
 u_x \frac{\partial f}{\partial x} + u_y \frac{\partial f}{\partial y} + u_z \frac{\partial f}{\partial z} + \frac{\partial}{\partial x} \left(\frac{K_x}{\mu_o} \psi \frac{\partial P_c}{\partial x} \right) + \frac{\partial}{\partial y} \left(\frac{K_y}{\mu_o} \psi \frac{\partial P_c}{\partial y} \right) + \frac{\partial}{\partial z} \left(\frac{K_z}{\mu_o} \psi \frac{\partial P_c}{\partial z} \right) \\
 + \frac{\partial}{\partial x} \left(\frac{K_x}{\mu_o} \Delta \rho \cos \alpha_x \psi \right) + \frac{\partial}{\partial y} \left(\frac{K_y}{\mu_o} \Delta \rho \cos \alpha_y \psi \right) + \frac{\partial}{\partial z} \left(\frac{K_z}{\mu_o} \Delta \rho \cos \alpha_z \psi \right) \\
 = -\phi \frac{\partial S}{\partial t}
 \end{aligned} \tag{12}$$

Defining f' as $\frac{df}{dS}$, P'_c as $\frac{dP_c}{dS}$ and ψ' as $\frac{d\psi}{dS}$, Equation 12 becomes

$$\begin{aligned}
 f' (u_x \frac{\partial S}{\partial x} + u_y \frac{\partial S}{\partial y} + u_z \frac{\partial S}{\partial z}) + \frac{\partial}{\partial x} \left(\frac{K_x}{\mu_o} \psi P'_c \frac{\partial S}{\partial x} \right) + \frac{\partial}{\partial y} \left(\frac{K_y}{\mu_o} \psi P'_c \frac{\partial S}{\partial y} \right) \\
 + \frac{\partial}{\partial z} \left(\frac{K_z}{\mu_o} \psi P'_c \frac{\partial S}{\partial z} \right) + \frac{K_x}{\mu_o} \psi \cos \alpha_x \psi' \frac{\partial S}{\partial x} + \frac{K_y}{\mu_o} \Delta \rho \cos \alpha_y \psi' \frac{\partial S}{\partial y} + \frac{K_z}{\mu_o} \Delta \rho \cos \alpha_z \psi' \frac{\partial S}{\partial z} \\
 = -\phi \frac{\partial S}{\partial t}
 \end{aligned} \tag{13}$$

where the w subscripts have been omitted from S .

1. Dimensionless Form of the Combined Equation

The following dimensionless quantities are defined:

$$x_D = \frac{x}{L}$$

$$y_D = \frac{y}{L} \sqrt{\frac{K_x}{K_z}}$$

$$z_D = \frac{z}{L} \sqrt{\frac{K_x}{K_z}}$$

$$t_D = \frac{u^* t}{\phi L}$$

where u^* is some characteristic superficial velocity, for example, q/A for a linear flood,

$$\text{and } \bar{P}_c = \frac{P_c}{\sigma \cos \theta} \sqrt{\frac{K_x}{\phi}}$$

Substituting into Equation 13, the combined displacement equation in dimensionless form becomes

$$\begin{aligned} \frac{df}{dS} & \left(\frac{u_x}{u^*} \frac{\partial S}{\partial x_D} + \frac{u_y}{u^*} \frac{\partial S}{\partial y_D} \sqrt{\frac{K_x}{K_y}} + \frac{u_z}{u^*} \frac{\partial S}{\partial z_D} \sqrt{\frac{K_x}{K_z}} \right) \\ & + \frac{\sqrt{K_x} \phi}{\mu_o u^*} \sigma \cos \theta \left(\frac{\partial}{\partial x_D} \left(\frac{\bar{\psi}_c'}{L} \frac{\partial S}{\partial y_D} \right) + \frac{\partial}{\partial y_D} \left(\frac{\bar{\psi}_c'}{L} \frac{\partial S}{\partial y_D} \right) + \frac{\partial}{\partial y_D} \left(\frac{\bar{\psi}_c'}{L} \frac{\partial S}{\partial z_D} \right) \right) \\ & + \frac{\Delta \rho g}{\mu_o u^*} \left(K_x \cos \alpha_x \psi' \frac{\partial S}{\partial x_D} + \sqrt{K_x K_y} \cos \alpha_y \psi' \frac{\partial S}{\partial y_D} \right. \\ & \left. + \sqrt{K_x K_z} \cos \alpha_z \psi' \frac{\partial S}{\partial z_D} \right) = - \frac{\partial S}{\partial t_D} \end{aligned} \quad 14$$

Three special cases of Equation 14 are discussed below.

1.1 One-Dimensional Horizontal Flow, No Gravity, No Capillarity

In this case, Equation 14 becomes

$$\frac{df}{dS} \frac{\partial S}{\partial x_D} = - \frac{\partial S}{\partial t_D} \quad 15$$

This is the familiar Buckley-Leverett frontal advance equation for which there is an analytical solution (72).

1.2 One-Dimensional Horizontal Flow, No Gravity

In this case, Equation 14 becomes

$$\frac{df}{dS} \frac{\partial S}{\partial x_D} + \frac{\sigma \cos \theta \sqrt{K_x} \phi}{\mu_w u^* L} \frac{1}{\lambda} \frac{\partial}{\partial x_D} \left(\bar{\psi}_c' \frac{\partial S}{\partial x_D} \right) = - \frac{\partial S}{\partial t_D} \quad 16$$

where $\lambda = \mu_o / \mu_w$

Equation 16 is a more complete form of the linear displacement equation derived by Rapoport and Leas (73). It will be noted that the dimensionless group $L\mu_w u^*/\sigma \cos\theta \sqrt{K_x \phi}$ is a popular scaling coefficient for linear immiscible displacement studies. Rapoport and Leas (74) have successfully employed a modified form of this coefficient to demonstrate the principles of scaling linear laboratory floods for an oil-wet system.

1.3 Two-Dimensional Horizontal Flow, No Gravity

In this case, u^* is chosen as the average superficial velocity in the areal direction and in general, $u_z = 0$ and u_x and u_y are assumed constant and equal to u^* . Also, $\cos\alpha_x = \cos\alpha_y = 0$ and $\cos\alpha_z = 1$. Further, for an isotropic medium, $K_x = K_y = K_z = K$. Since the flow is invariant in the z -direction, Equation 14 reduces to

$$\frac{df}{dS} \left(\frac{\partial S}{\partial x_D} + \frac{\partial S}{\partial y_D} \right) + \frac{\sigma \cos\theta \sqrt{K\phi}}{\mu_w u^* L} \frac{1}{\lambda} \left\{ \frac{\partial}{\partial x_D} \left(\psi_c \frac{\partial S}{\partial x_D} \right) + \frac{\partial}{\partial y_D} \left(\psi_c \frac{\partial S}{\partial y_D} \right) \right\} = - \frac{\partial S}{\partial t_D} \quad 17$$

where $\lambda = \mu_o / \mu_w$

Equation 17 provides the basis for scaling two-dimensional immiscible fluid displacements. In deriving this equation, it has been assumed that the flow is everywhere horizontal, the fluids incompressible, the reservoir properties isotropic and that the model is sufficiently thin to render the effects of gravity segregation negligible. Furthermore, Darcy's law is assumed to apply. Subject to these assumptions, Equation 17 shows that the flooding behaviour is controlled by the dimensionless similarity group

$$C_1 = \frac{\mu_w u^* L}{\sigma \cos \theta \sqrt{K\phi}}$$

This group defines the relative importance of the capillary forces in the displacement of oil by water. For a given value of C_1 all porous systems of given geometry operated under similar boundary conditions, and characterized by the same oil to water viscosity ratio and the same f , ψ and \bar{P}_c , will yield the same flooding behaviour. Thus C_1 represents a scaling factor which can be used to relate the results of flow model experiments to field performance. For correct scaling, the laboratory flood must be operated such that

$$\left[\frac{\mu_w u^* L}{\sigma \cos \theta \sqrt{K\phi}} \right]_{\text{model}} = \left[\frac{\mu_w u^* L}{\sigma \cos \theta \sqrt{K\phi}} \right]_{\text{prototype}}$$

The requirement that the capillary pressure and relative permeability relations must be the same functions of saturation in the model and its prototype is rather restrictive. To overcome this difficulty, Perkins and Collins (75) redefined the relative permeabilities and saturations in a way which permits different relative permeability and capillary pressure relations in the model and prototype.

They defined dimensionless saturation as follows:

$$\bar{S}_w = \frac{S_w - S_{cw}}{1 - S_{ro} - S_{cw}}$$

where S_{cw} = residual water saturation

S_{ro} = residual oil saturation

The relative permeabilities were defined as follows:

$$\bar{K}_w = \frac{k_w}{k_{wro}}$$

and

$$\bar{K}_o = \frac{k_o}{k_{ocw}}$$

where k_{wro} = effective permeability to water at residual oil saturation

k_{ocw} = effective permeability to oil at residual water saturation

This approach results in the introduction of mobility ratio,

$$M = \frac{k_{wro} \mu_o}{k_{ocw} \mu_w}$$

as an additional dimensionless scaling group. The group involving the ratio of capillary to viscous forces takes on the form:

$$\frac{\sigma \cos \theta k_{wro}}{u \mu_w L} \sqrt{\frac{\phi}{K}}$$

Then for exact compliance with the scaling criteria, \bar{K}_o , \bar{K}_w and $\bar{P}'_c(\bar{S}_w)$ must be the same function of the dimensionless saturation \bar{S}_w in the model and prototype.

Viscous Fingering

When oil is displaced from a porous medium by water having a lower viscosity than the oil, the oil-water interface is essentially unstable and tends to break up into "fingers". This phenomenon has been termed "viscous fingering" in the literature.

The onset of the instability that leads to viscous fingering has been predicted mathematically by van Meurs et al (76) and Chuoke et al (77). In certain situations, this instability may exert sufficient influence on the oil-water displacement process as to warrant a separate scaling consideration. However, Rachford (78) has pointed out that in water-wet systems containing initial water saturations, the presence of transition zones tend to dampen the growth of fingers. For such systems, Rachford (79) concludes that the effects of viscous fingering are minimal and as such, no separate scaling requirements appear necessary to account for this phenomenon.

Scaling Applied to Five-Spot and Nine-Spot Patterns

The major difficulty in applying the outlined scaling procedure to two-dimensional systems such as a five-spot or a nine-spot flooding pattern lies in the choice of the flux vector, u^* . Application to a linear system is a relatively simple matter since u^* may be chosen as the superficial fluid velocity (q/A). Moreover, in this case, u^* has an unmistakable physical significance. Unlike the linear case, no representative velocity flux exists in the two-dimensional case. To overcome this problem, Rapoport and Leas (80) proposed the use of a linear approximation of the five-spot pattern based on the direction of the predominant streamlines in an infinitely confined five-spot flow regime.

Rapoport, Carpenter and Leas (81) employed such an approximation to study the scaling of a five-spot model. They used the scaling group

$$C_2 = \frac{(q/L)\mu_w}{\sigma\sqrt{K\phi}} = \frac{Q\bar{\mu}_w}{\sigma\sqrt{K\phi}}$$

where Q = volumetric rate per unit thickness of
the porous medium

It is apparent that C_2 is equivalent to C_1 with u^* chosen as q/L^2 . Also, $\cos\theta$ which is a measure of wettability of the porous medium, does not appear explicitly in C_2 . This is because the magnitude of $\cos\theta$ is unity for either a strongly water-wet or oil-wet system.

For sufficiently large values of the scaling coefficient (C_2), Rapoport et al (82) observed that the flooding behaviour became independent of the scaling coefficient. The value of C_2 at which stabilization was first observed was termed the critical scaling coefficient. They observed further that for their particular system, the critical scaling coefficient was 3.5×10^{-3} for a viscosity ratio of unity. A similar calculation for a typical oil reservoir led the authors to conclude that field waterfloods are always stabilized. Hence, to properly simulate field conditions, laboratory displacement models must be operated under stabilized conditions.

To date, no attempt has been made to extend the scaling laws to nine-spot floods. If stabilization occurs in nine-spot floods, the theory of immiscible fluid displacement indicates that a critical scaling group must exist for this pattern. Moreover, Equation 17 shows that for scaling coefficients greater than the critical, the recovery performance of the five-spot and nine-spot floods operated under similar conditions would be identical.

The above considerations suggest that the application of the scale-up laws to nine-spot floods may proceed along lines similar to those used by Rapoport et al (83) for the five-spot. In the present

study, it is proposed to use the production rate of the central production well in the calculation of the scaling coefficients. For a confined five-spot, the production rate (q) is equal to the injection rate per well since the production well receives one-quarter of the fluid from each of the four injectors. For the confined nine-spot; similar considerations lead to

$$q = q_1 + 2q_2$$

where q_1 and q_2 are the injection rates of the corner and side wells, respectively.

IV. EXPERIMENTAL PROCEDURE AND MATERIALS

Patterns Studied

The primary concern of this study was to obtain pilot confinement using a limited number of well patterns. To this end, the recovery performances of unconfined or isolated five and nine-spot pilots were first studied over a wide range of injection rates; then, both pilots were each surrounded by a ring of eight similar patterns and their recovery performances re-examined in the light of this modification. These pattern arrangements are shown in figure 1.

Equipment

The reservoir model was an unconsolidated pack of 100 mesh industrial glass beads sandwiched between two transparent lucite plates. The medium had 185 fully penetrating wells spaced 7.25 cm apart in a square matrix. The model was mounted in a manner that permitted operation at any desired inclination. Because the thickness was very much smaller than the other dimensions, the model may be considered to be essentially two-dimensional. Details of design and construction may be found in reference (84). A photograph of the model is shown in Plate 1.

Water injection into the model was accomplished by an arrangement of forty injection cylinders actuated by a double acting master cylinder. The master cylinder was in turn driven hydraulically by a Ruska Proportioning Pump capable of fluid delivery at 28 rates. Because they were all bolted to the same 2-inch steel plate, the pistons moved in unison to ensure uniform water injection into all the injectors.

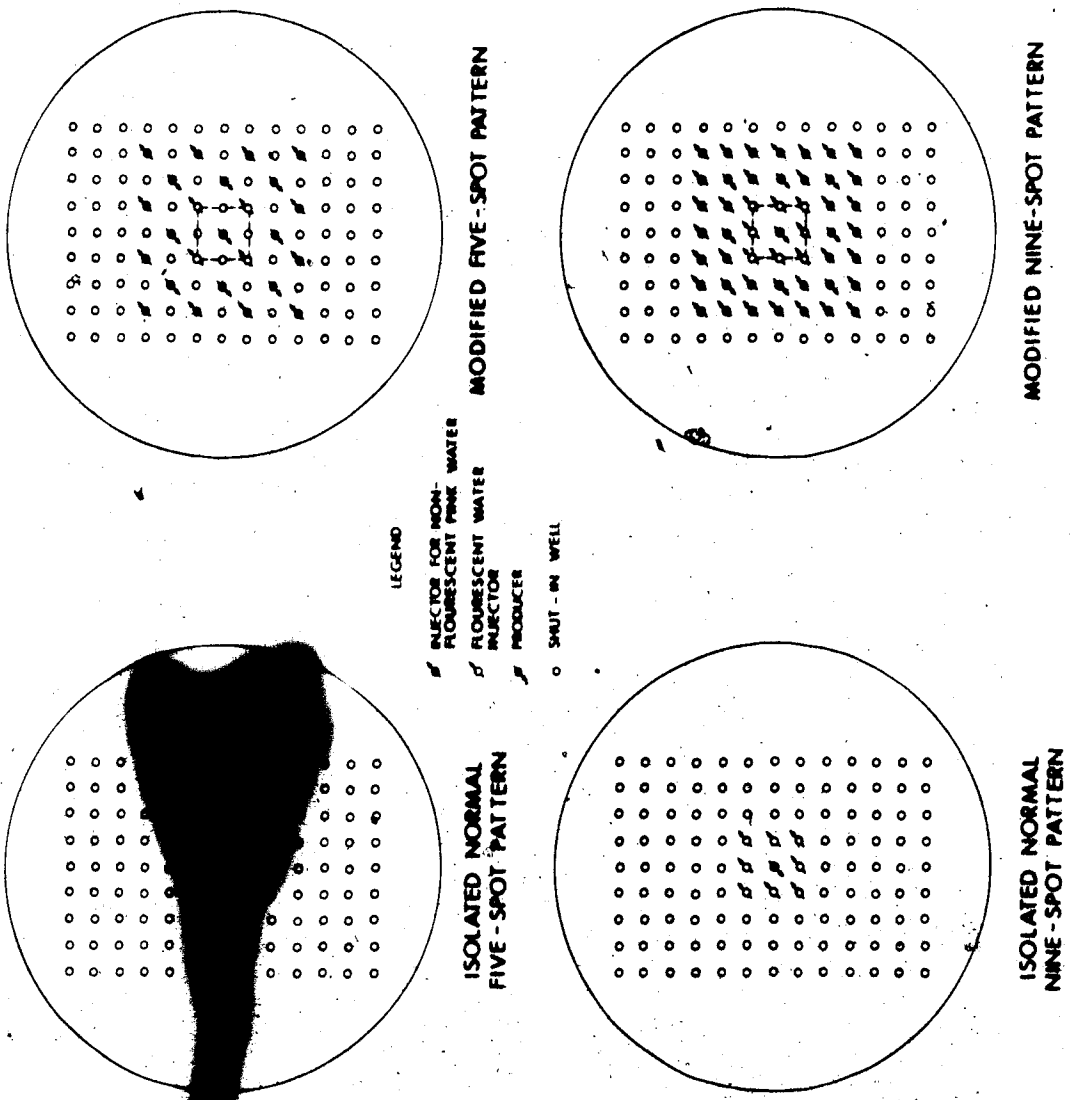


FIGURE 1. Pattern Arrangements

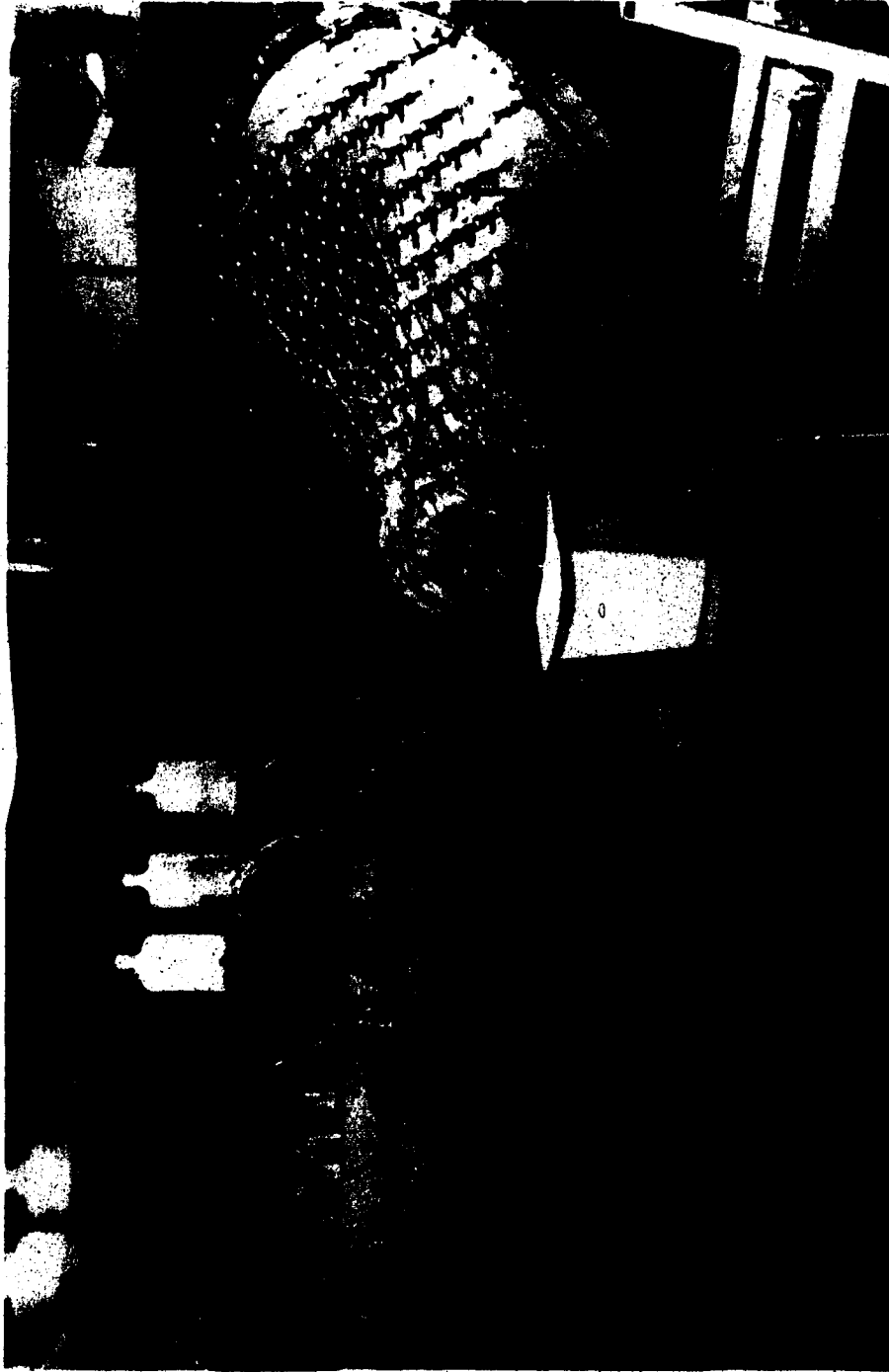


PLATE 1. Reservoir Model with Injection Manometers

The discharge rates from the injection cylinders were calibrated against the Ruska pump speeds. Table 1 presents a summary of this calibration. The numbers in bracket are the measured discharge rates from each cylinder for the corresponding pump speeds shown. Plate 2 is a photograph of the injection piston-cylinder arrangement. The injection pressures were measured with a bank of forty mercury manometers shown to the left of the inclined reservoir model in Plate 1.

To enable direct visual observation of the flood fronts, the innermost injection wells of each of the patterns received water colored with sodium fluorescein obtained from Fisher Scientific. A bright yellow fluorescence was obtained when the model was illuminated from beneath by ultraviolet lighting. Best results were obtained in a dark room. With this arrangement, it was possible to photograph the fronts at any desired stage of the flood. The remainder of the injection water was colored with a non fluorescent pink dye. This was necessary to facilitate visual observation of the displacement behaviour of the surrounding patterns. Specifically, it served to identify irregular pattern behaviour due to partially plugged wells.

Model and Fluid Properties

Before packing, the glass beads were washed with ordinary household detergent and thoroughly rinsed with distilled water. This rendered the beads strongly water-wet. During packing, the model was vibrated continuously with three, 60 cycle, electric vibrators for five days. This resulted in a uniform pack of porosity 36.42 percent and absolute permeability to water of 6.20 darcys. The properties of the model, the pilot and wellbore dimensions are summarized in Table 2.

Table 1
CALIBRATION OF INJECTION CYLINDERS

Gear Level	Pump Gear						
	1	2	3	4	5	6	7
A	2,500 (2.679)	3,125 (3.348)	3,750 (4.018)	5,000 (5.357)	6,250 (6.696)	7,500 (8.036)	8,750 (9.375)
B	10,000 (10.714)	12,000 (12.857)	15,000 (16.071)	20,000 (21.429)	25,000 (26.786)	30,000 (32.143)	35,000 (37.500)
C	40,000 (42.857)	50,000 (53.571)	60,000 (64.286)	80,000 (85.714)	100,000 (107.143)	120,000 (128.571)	140,000 (150.000)
D	160,000 (171.429)	200,000 (214.286)	240,000 (257.142)	320,000 (342.857)	400,000 (428.571)	480,000 (514.286)	560,000 (600.000)

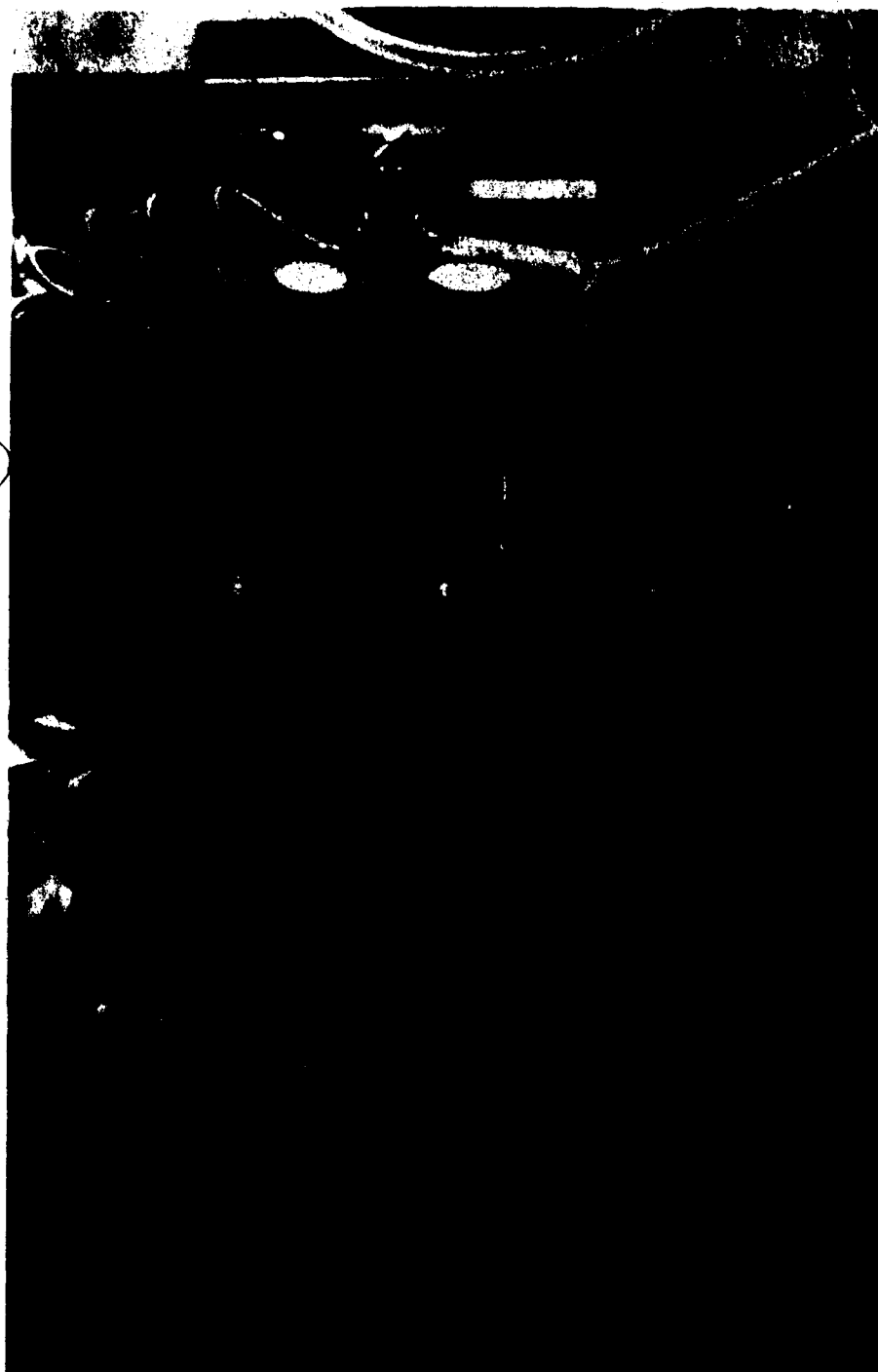


PLATE 2. Injection Cylinders

Details of permeability and porosity determination are given in Appendix A.

Table 2

SUMMARY OF MODEL PROPERTIES

Average grain size	100	mesh
Porosity	36.42	%
Absolute permeability	6.60	darcys
Diameter	121.92	cm
Area of unit pattern	210.25	cm ²
Average thickness	0.4967	cm
Pattern pore volume	38.034	cm ³
Wellbore radius	0.123	cm
Injection-production well distance (corner well)	10.25	cm
Injection-production well distance (side well)	7.25	cm

Three grades of refined petroleum products, obtained from Imperial Oil Refinery, were used to simulate the oil phases. The trade names together with the properties of the oils are given in Table 3. Interfacial tensions were measured with a DuNouy tensiometer and the viscosities with a modified Ostwald viscometer.

Table 3

FLUID PROPERTIES AT 70°F

Fluid Type	ρ gms/cc	μ cp	μ_o/μ_w -	σ dynes/cm
Dyed Water	0.9907	0.9907	-	-
Kerosene	0.7905	1.3043	1.3165	27.17
HGO	0.8508	8.5761	8.6566	27.23
✓DWO	0.8524	15.0790	15.2206	21.66

Procedure

Prior to every experimental run, initial water and oil saturations were established as follows. First, the model was fully saturated with distilled water and then clamped vertically. Oil was then injected into the top three peripheral wells while water was produced from the lowest peripheral well. This injection and production arrangement was adopted to take advantage of gravity segregation. After breakthrough, oil injection continued until no more water was produced. At this stage, a material balance calculation gave the initial fluid saturations.

The initial fluid saturations having been established, the model was clamped horizontally in readiness for the experimental run. After selecting the flood pattern of interest, the injection and production wells were opened to allow the model to attain pressure equilibrium. With the gear selected to give the desired injection rate, the pump was started to initiate the flood.

During flooding, the injection pressures were closely observed to detect partially plugged wells. High injection pressure into a well relative to other wells was an indication that the well was partially plugged. In such a case, the experimental results were discarded and the run repeated after cleaning out the plugged well.

The fluids from the pilot producer were collected in a bank of graduated test tubes, the first tube being used to collect clean oil prior to water breakthrough. Subsequent tubes received water-oil mixtures. When the pilot was surrounded by like patterns, the production from the surrounding producers was collected in the same vessel. No

attempt was made to measure the production from these wells. However, to ensure uniform flood development, it was often necessary to adjust the production rates from these wells.

By means of ultraviolet lighting, the area contacted by the fluorescent injection water was photographed at any desired stage of the flood. Of particular interest was the areal coverage at water breakthrough.

Each experimental run was arbitrarily terminated when the equivalent of three to four pattern pore volumes of fluids were produced. The recoveries from the pilot producer were used to calculate the recovery profiles employed in this study. After each run, the model was flushed with about thirty pore volumes of distilled water before resaturating for the next run.

V. EXPERIMENTAL RESULTS AND OBSERVATIONS

In all, 51 flood tests were made. The results are presented in Appendix B as Runs 1 through 51. Mobility ratios (M) of 2.63, 14.09 and 20.61 were studied. The fluid mobilities were determined at residual saturations as suggested by Perkins and Collins (85). The details of the mobility calculations are shown in Appendix C.

Isolated Pilot Performances

Figures 2, 3 and 4 give the oil recovery profiles for the isolated five-spot pilot at the three mobility ratios. The injection rates studied ranged from 16.1 to 514.3 cc/hr/well. It may be observed from figure 2 that for $M = 2.63$, considerable oversweep occurs at low injection rates. At successively higher rates, the oil recovery decreases but oversweep persists nonetheless.

For $M = 14.09$ and 20.61, the isolated five-spot recovery profiles exhibit the same rate sensitivity observed at $M = 2.63$; that is, the oil recoveries decrease with increasing injection rate. It may be observed from figures 3 and 4 that oversweep occurs also at these adverse mobility ratios, even though the general level of oil recoveries are lower than at $M = 2.63$.

The corresponding recovery profiles for the isolated nine-spot pilots are shown in figures 5, 6 and 7. These recovery profiles are, in general, similar to those of the five-spot. As before, oversweep is more pronounced at low rates and mobility ratios.

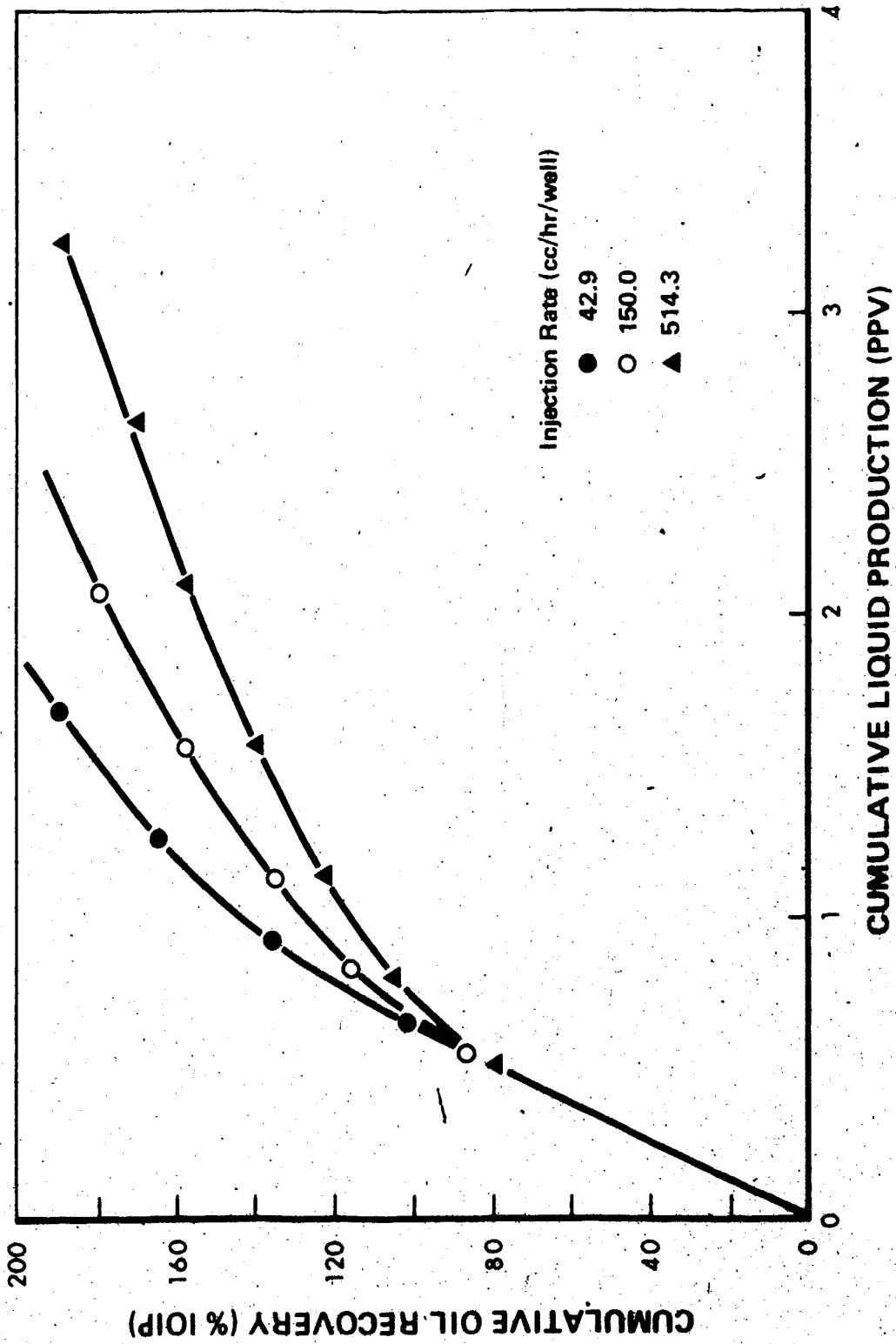


FIGURE 2. Effect of Injection Rate on Oil Recovery from an Isolated 5 - Spot Pattern.
Mobility Ratio = 2.63

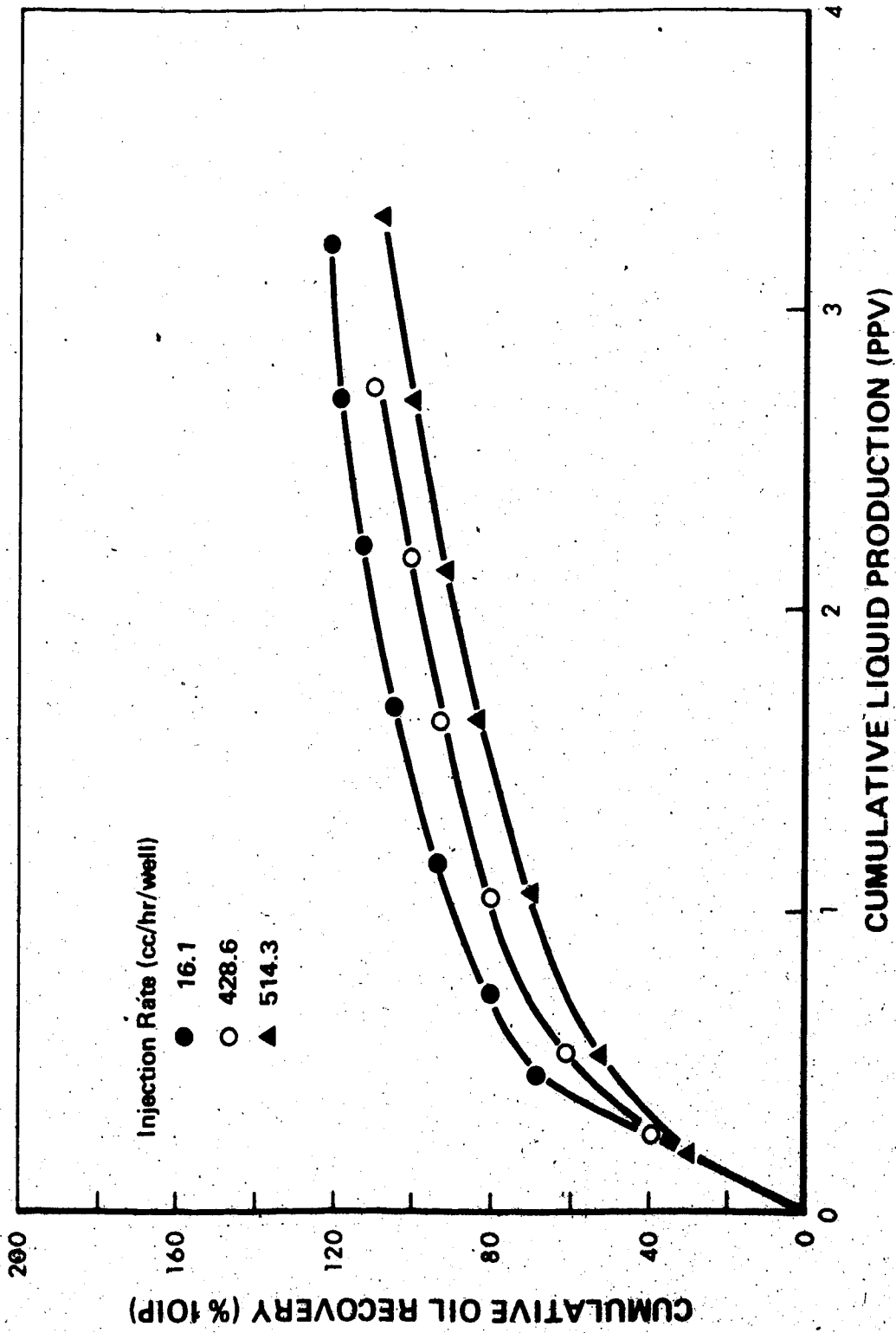


FIGURE 3. Effect of Injection Rate on Oil Recovery from an Isolated 5 - Spot Pattern.
Mobility Ratio = 14.09

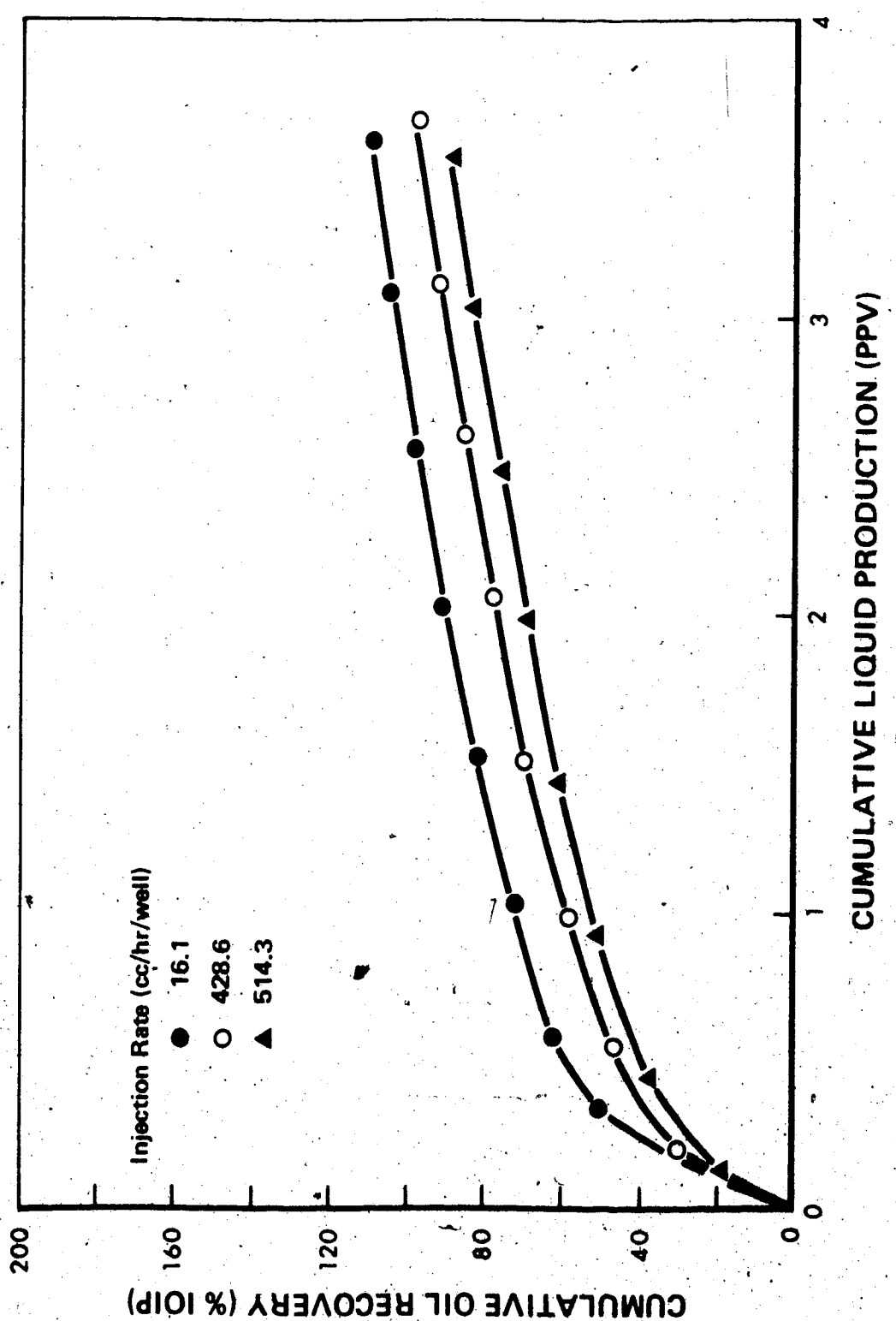


FIGURE 4. Effect of Injection Rate on Oil Recovery from an Isolated 5 - Spot Pattern.
Mobility Ratio = 20.61

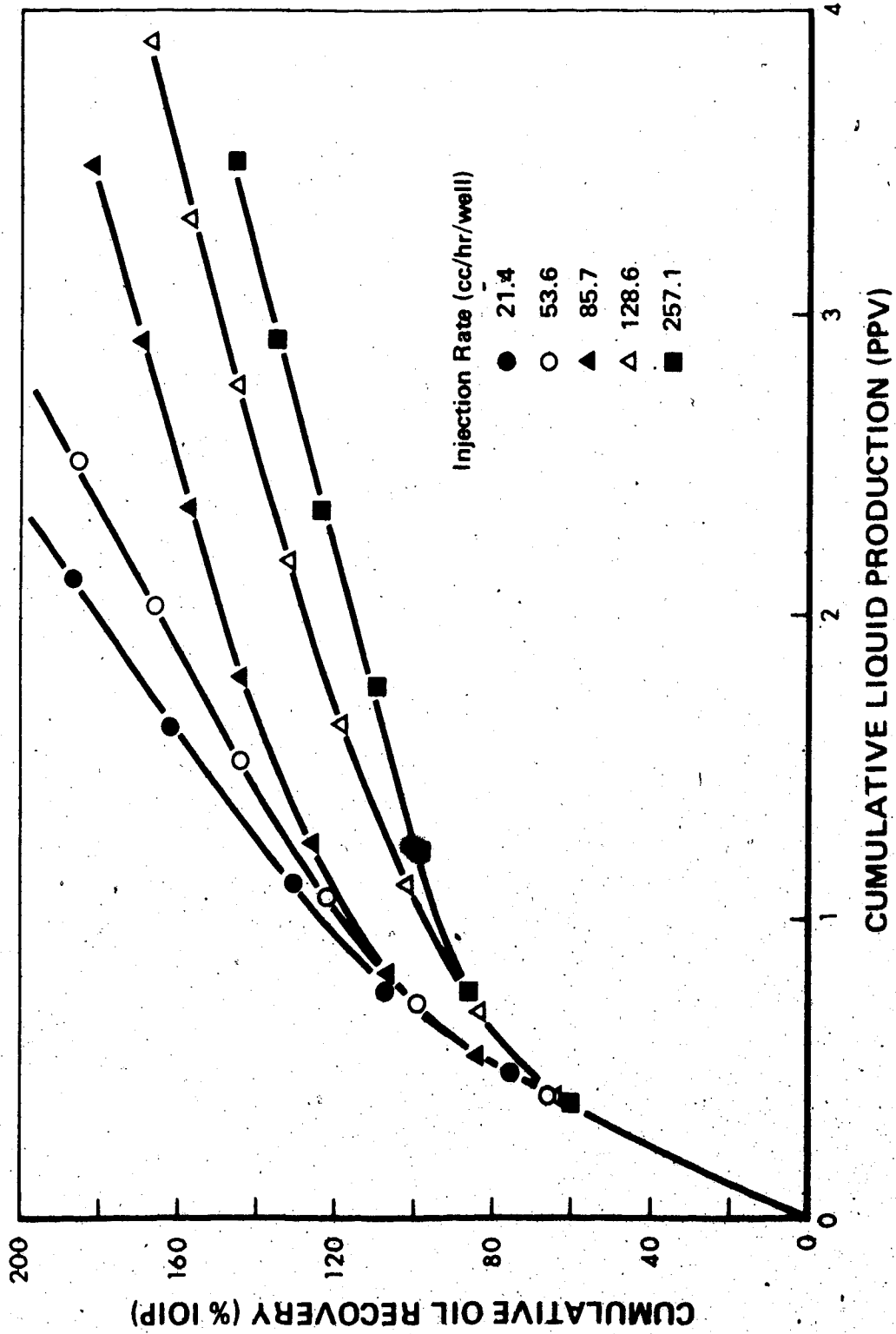


FIGURE 5. Effect of Injection Rate on Oil Recovery from an Isolated 9 - Spot Pattern.
 Mobility Ratio = 2.63

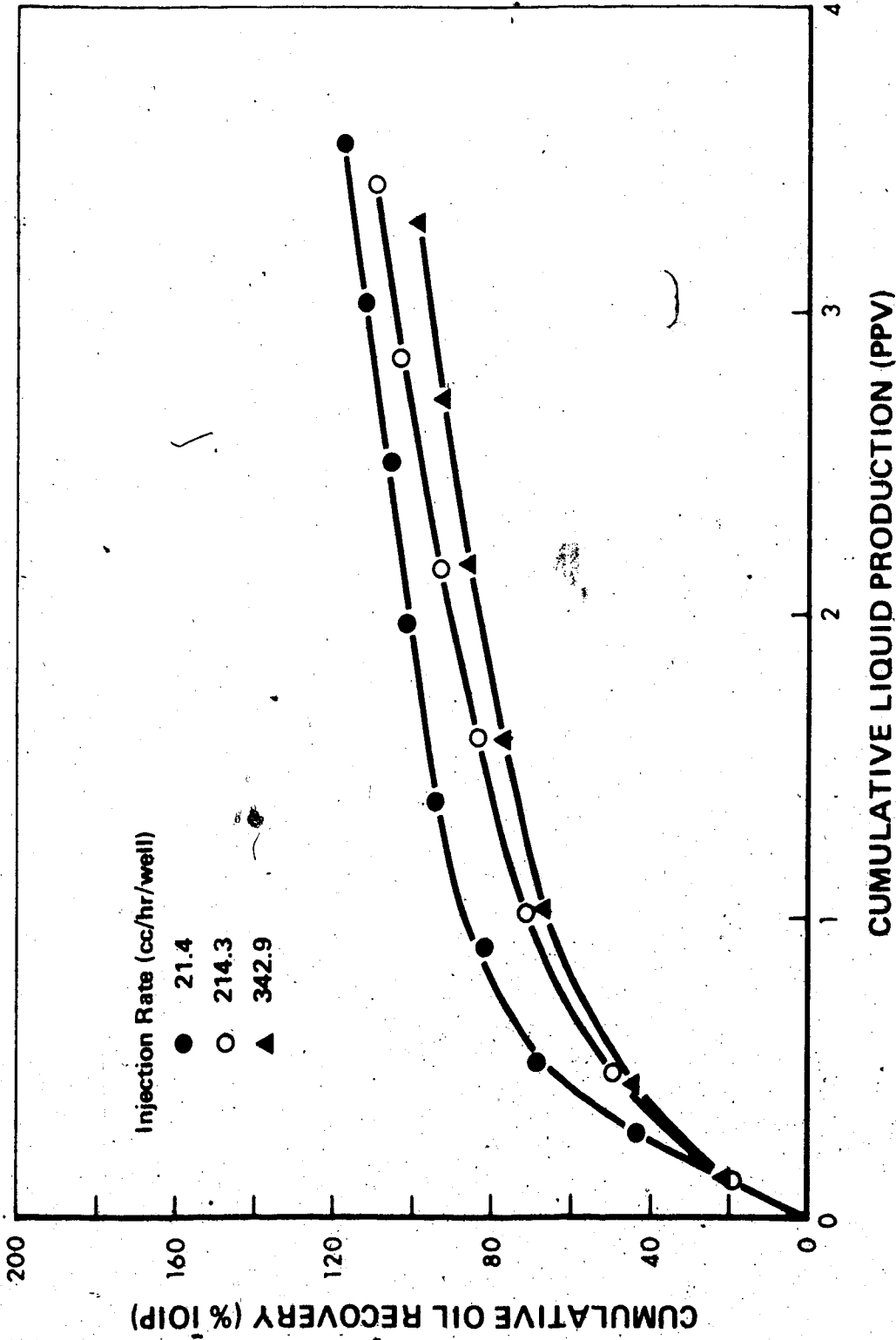


FIGURE 6. Effect of Injection Rate on Oil Recovery from an Isolated 9 - Spot Pattern.
Mobility Ratio = 14.09

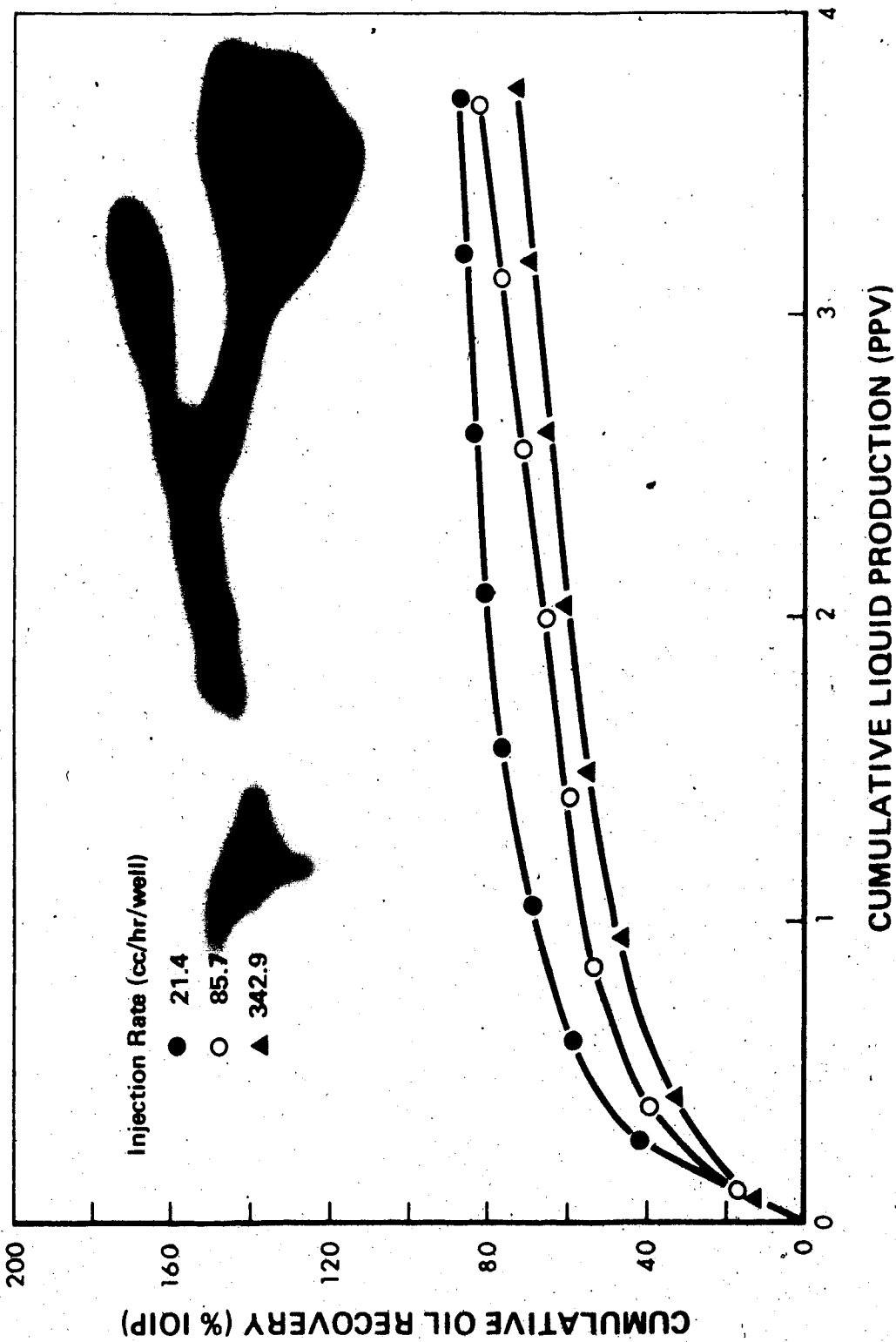


FIGURE 7. Effect of Injection Rate on Oil Recovery from an Isolated 9 - Spot Pattern.
 Mobility Ratio = 20.61

Pattern Confinement

Figures 8, 9 and 10 present the flooding results for the modified five-spot pilot. For $M = 2.63$, figure 8 indicates that the flood oversweeps the pattern at injection rates below 342.9 cc/hr/well. But at rates equal to and greater than 342.9 cc/hr/well, the pilot recovery becomes independent of rate and effective pilot confinement is achieved.

For $M = 14.09$ and 20.61 , figures 9 and 10 show that the modified five-spot recovery is less rate sensitive over a wider range of injection rates than was the case at $M = 2.63$. In fact, for all practical purposes, flood stabilization and effective confinement occur at rates as low as 32.1 cc/hr/well for these mobility ratios. Lower injection rates could not be studied because of the practical difficulties of obtaining uniform production distribution at such low rates.

The recovery performances of the modified nine-spot pilot are shown in figures 11, 12 and 13. For $M = 2.63$, the oversweep at low injection rates is more pronounced than in the modified five-spot. The pilot is effectively confined at rates of 128.6 cc/hr/well and greater. For $M = 14.09$ and 20.61 , figures 12 and 13 show that the modified nine-spot floods are stabilized and effectively confined over the range of injection rates studied.

Breakthrough Oil Recoveries

Breakthrough recoveries from the modified pilots are shown in figures 14, 15 and 16 as functions of production rate and mobility ratio. For $M = 2.63$, it is apparent from figure 14 that the breakthrough recoveries from both pilots are essentially independent of rate. On the

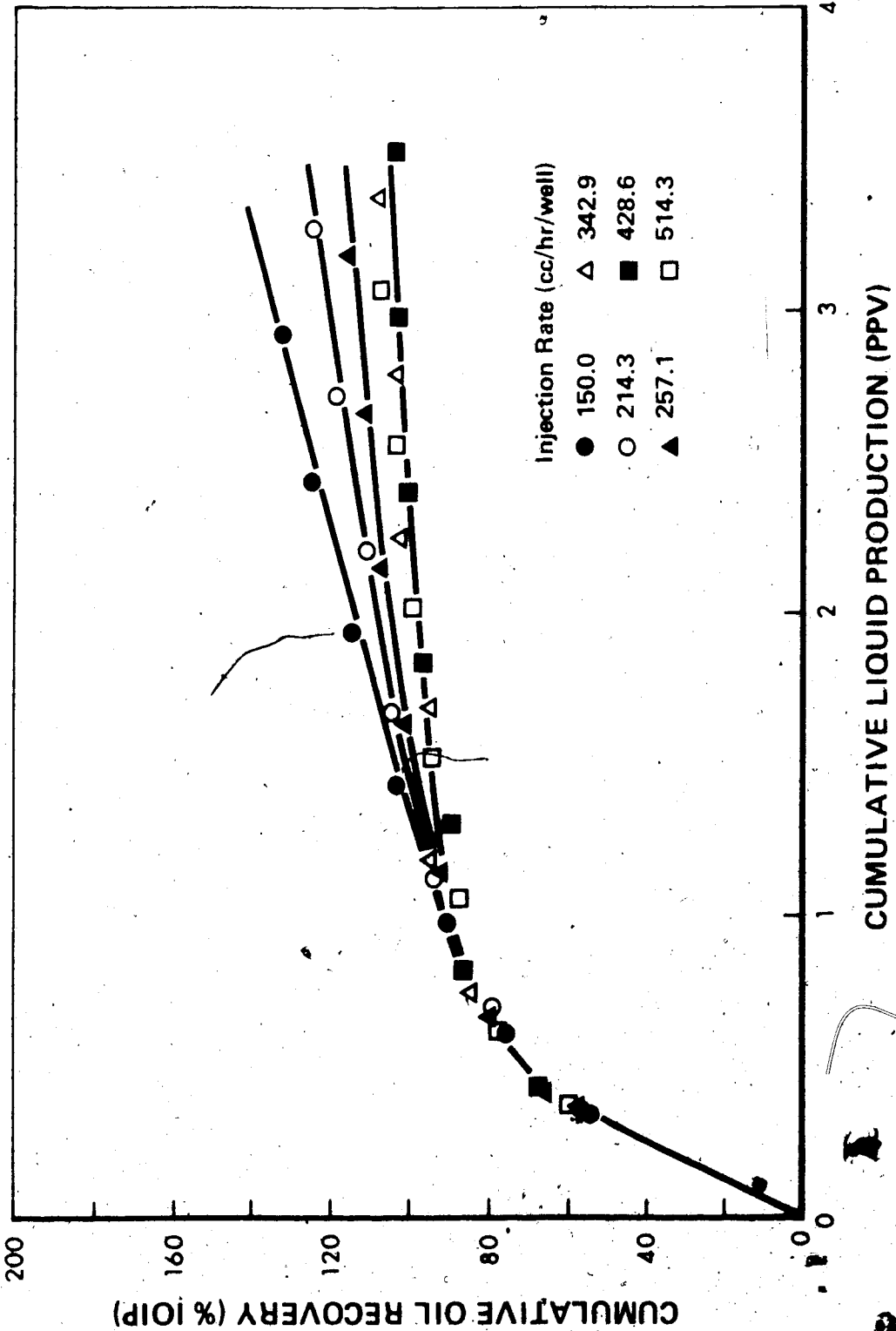


FIGURE 8. Effect of Injection Rate on Oil Recovery from a Modified 5 - Spot Pattern. Mobility Ratio = 2.63

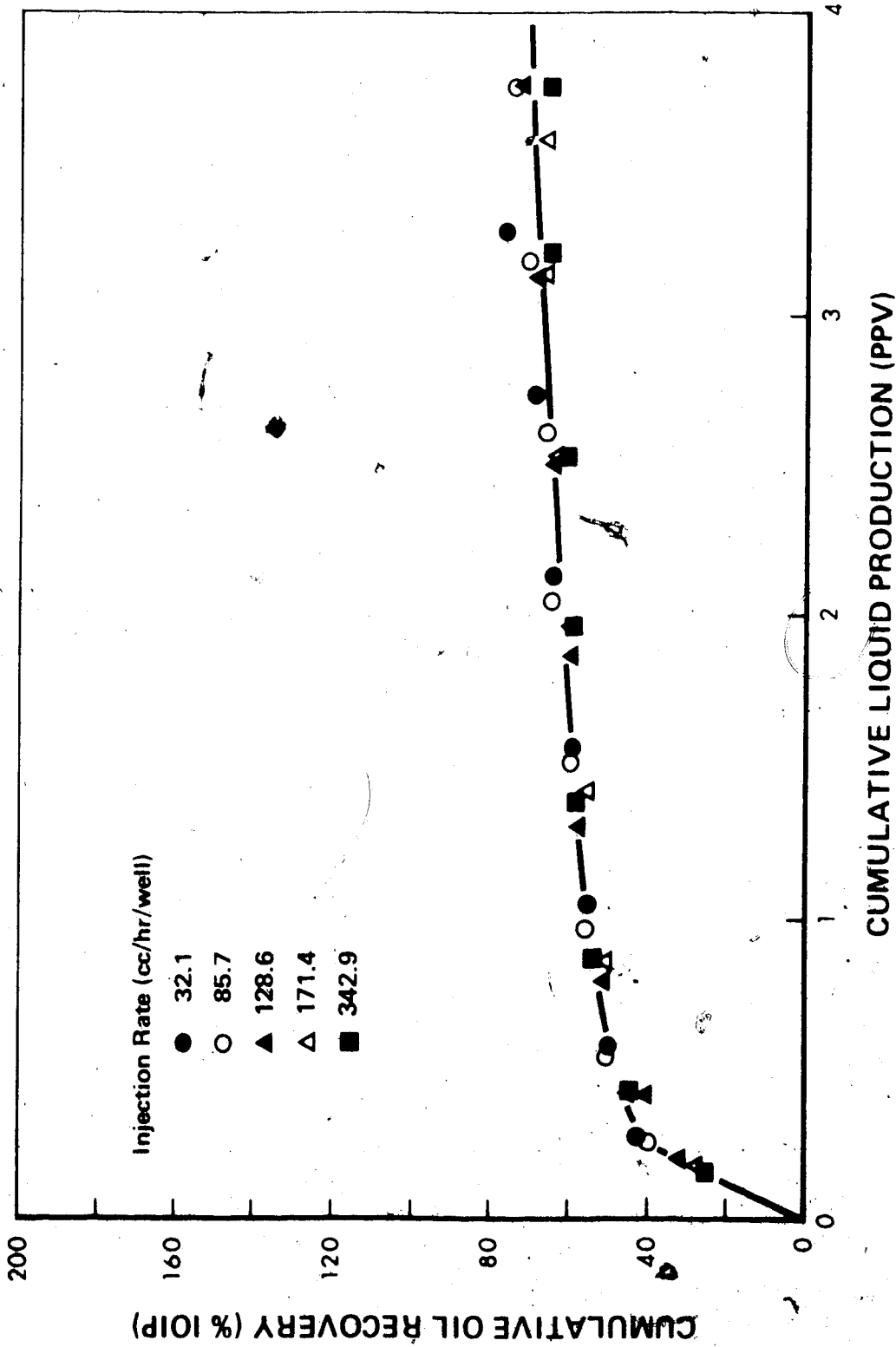


FIGURE 9. Effect of Injection Rate on Oil Recovery from a Modified 5 - Spot Pattern.
Mobility Ratio = 14.09

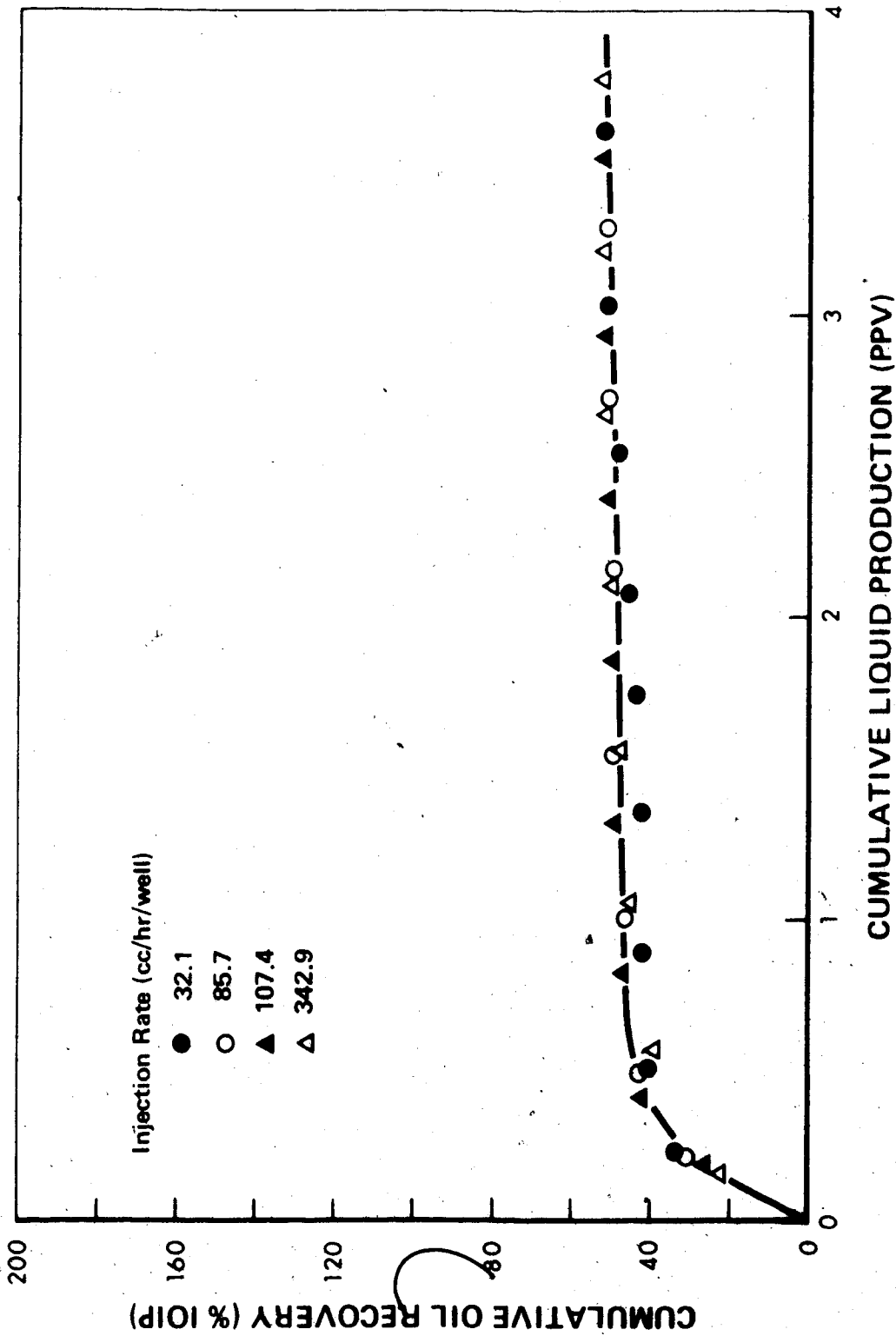


FIGURE 10. Effect of Injection Rate on Oil Recovery from a Modified 5-Spot Pattern.
 Mobility Ratio = 20.61

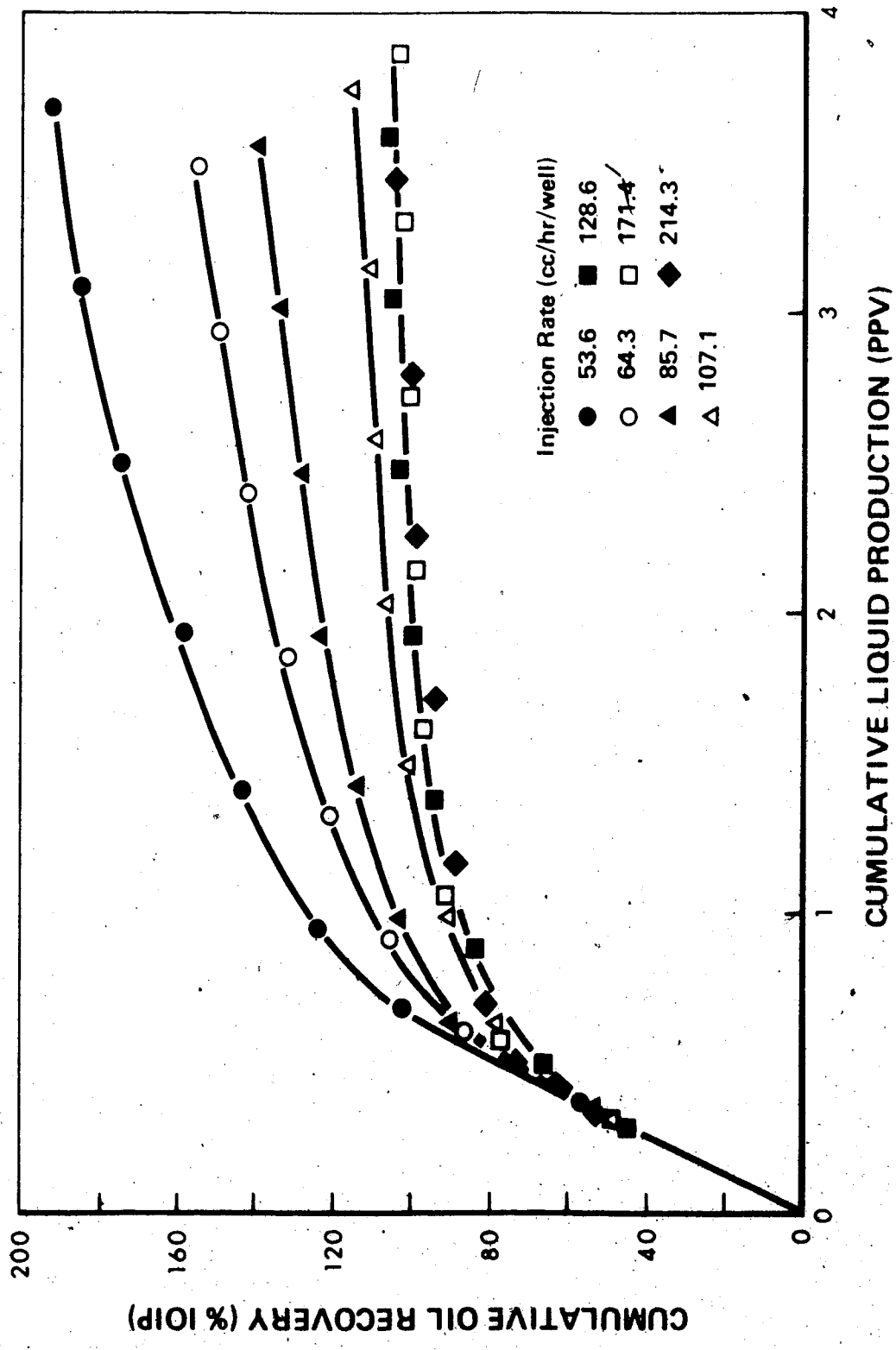


FIGURE 11. Effect of Injection Rate on Oil Recovery from a Modified 9 - Spot Pattern. Mobility Ratio = 2.63

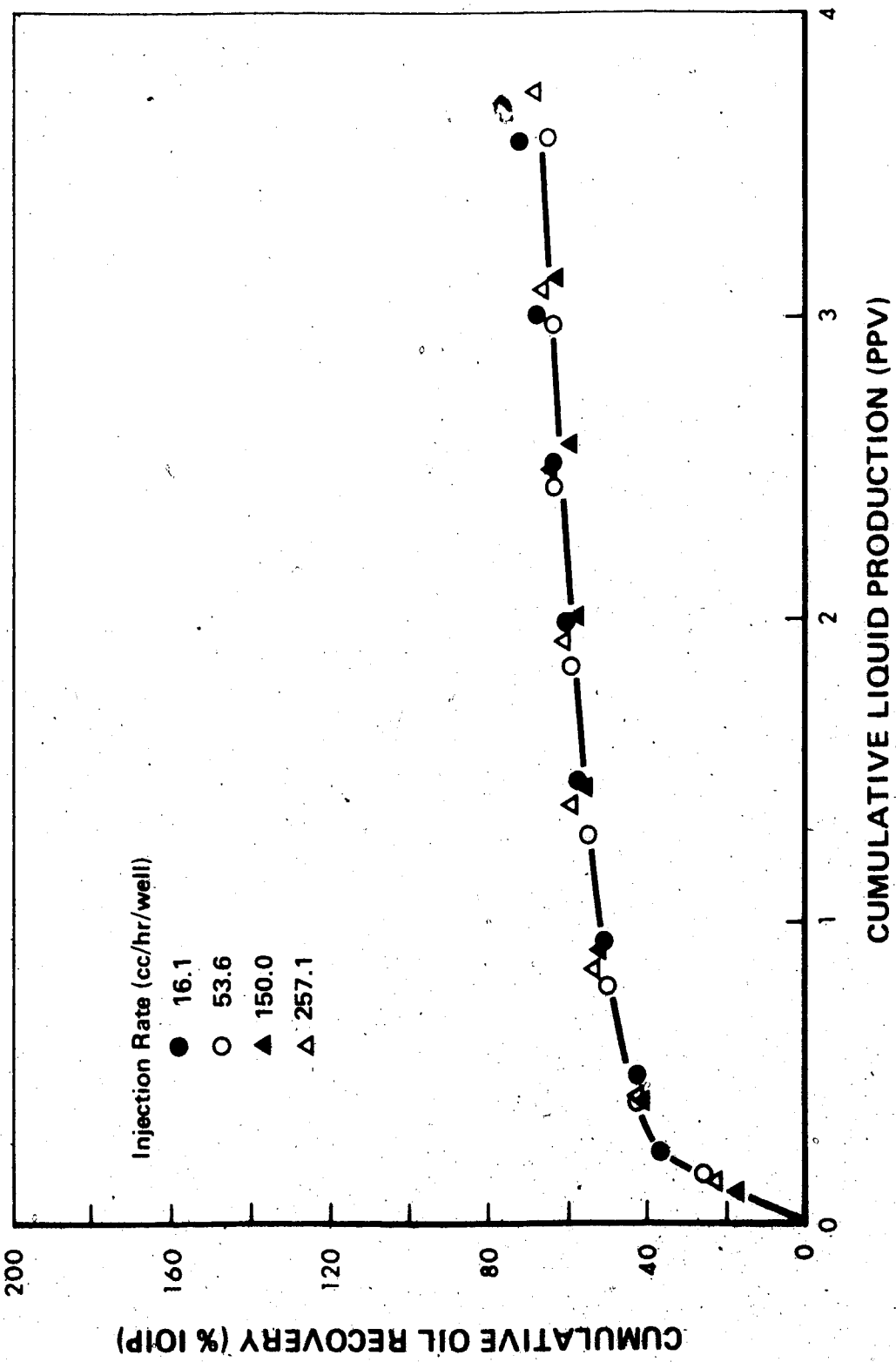


FIGURE 12. Effect of Injection Rate on Oil Recovery from a Modified 9 - Spot Pattern.
 Mobility Ratio = 14.09

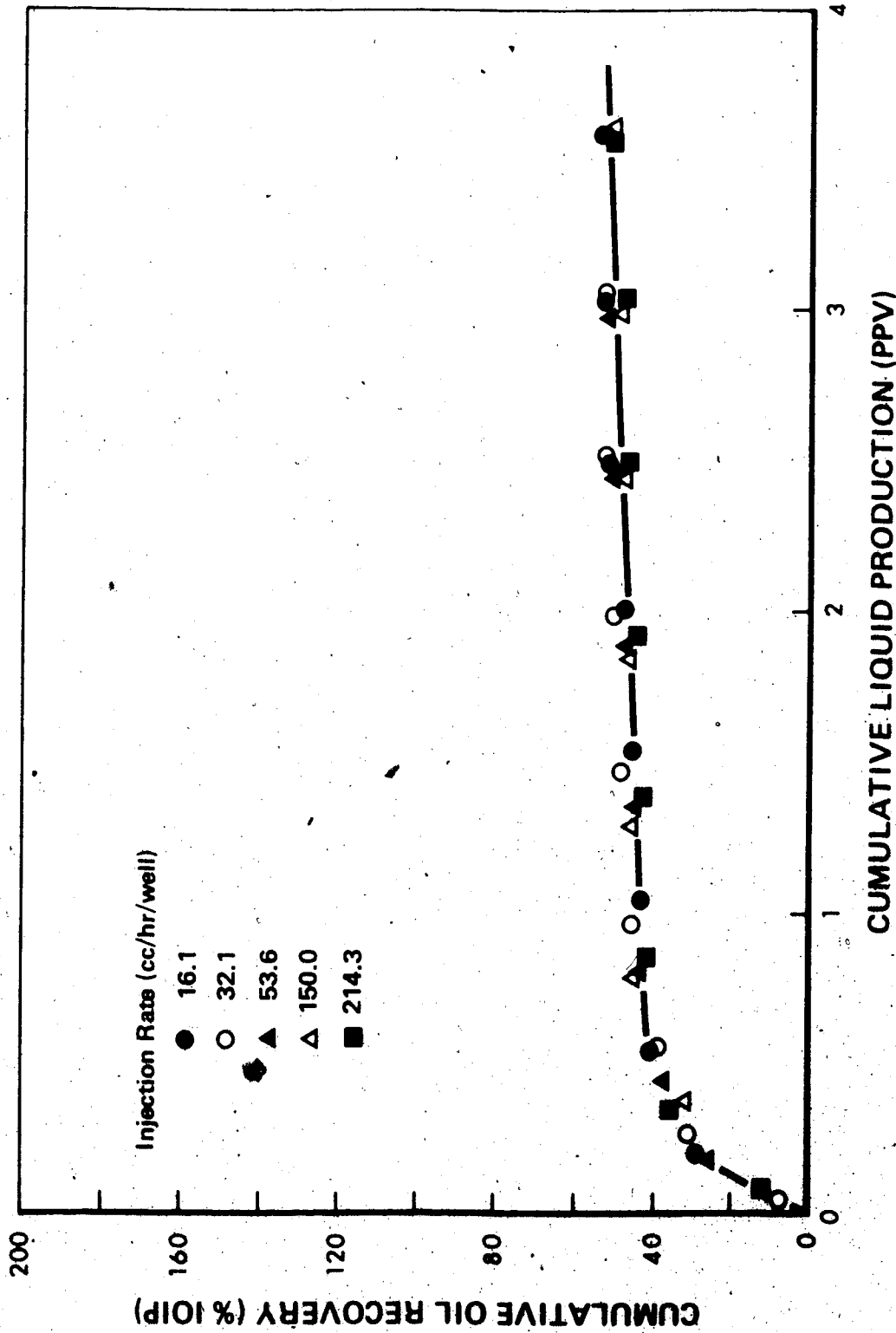
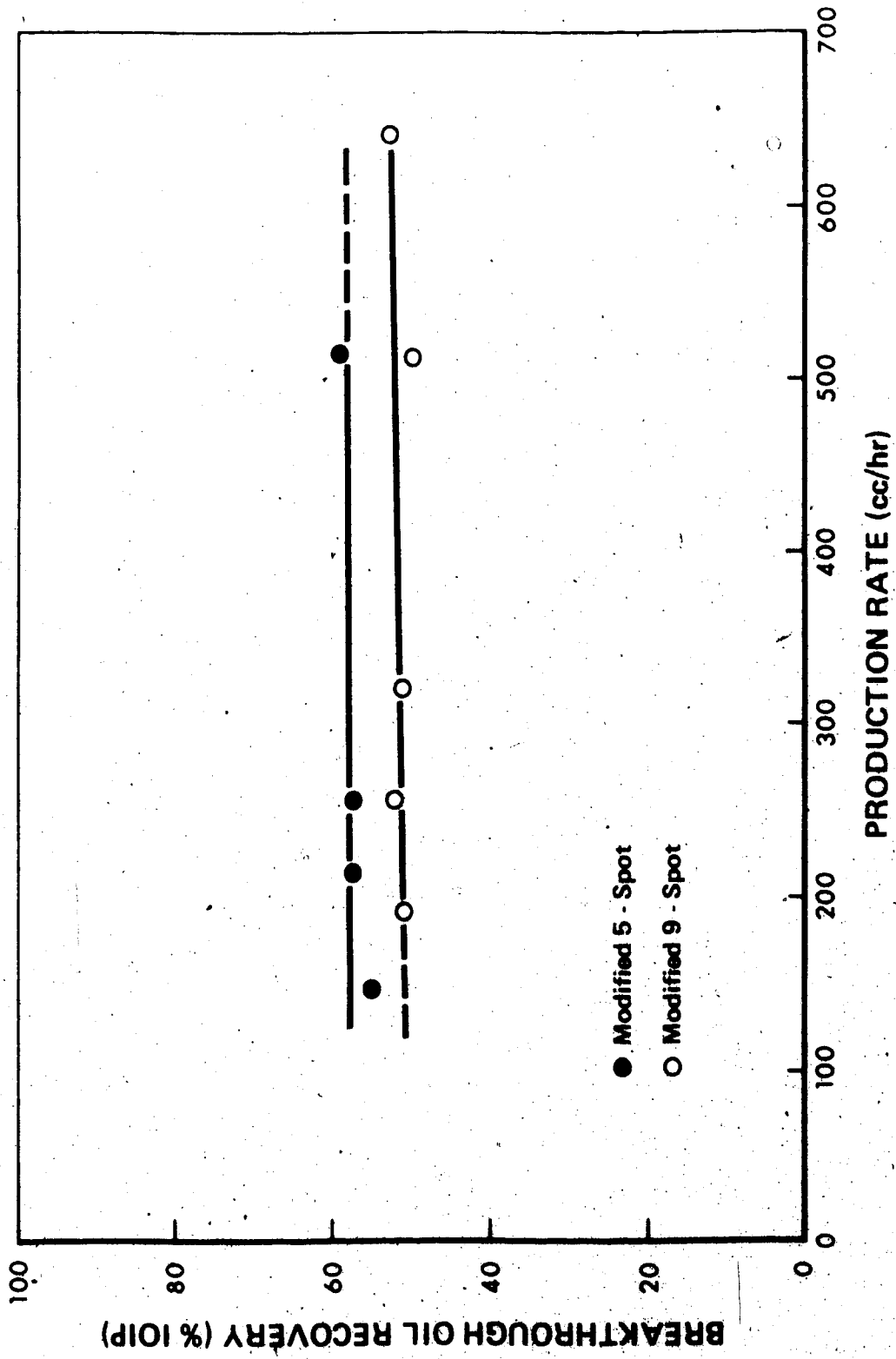


FIGURE 13. Effect of Injection Rate on Oil Recovery from a Modified 9 - Spot Pattern. Mobility Ratio = 20.61



**FIGURE 14. Effect of Rate on Breakthrough Oil Recovery from Modified 5 and 9 - Spot Patterns.
Mobility Ratio = 2.63**

other hand, figures 15 and 16 show that at $M = 14.09$ and 20.61 , the recoveries are rate sensitive especially at low production rates. At these mobility ratios, the breakthrough recoveries decrease rapidly with increasing rate at low rates, but stabilize somewhat at high rates.

Another important observation from figures 14 through 16 is that the five-spot breakthrough recoveries are consistently higher than those of the nine-spot for the range of mobility ratios studied.

Confined Pilot Performance

Figures 17, 18 and 19 show the cross-plots of confined or stabilized five and nine-spot recoveries for the three mobility ratios. In each case, the pilot recoveries for all the stabilized rates were plotted. For example, for $M = 2.63$, recoveries at 342.9, 428.6 and 514.3 cc/hr/well were used to show the confined five-spot recovery profile. The cross-plots show that despite differences in the breakthrough recoveries, the ultimate recoveries from the confined or stabilized five-spot and nine-spot pilots are the same for the three mobility ratios examined.

Figure 20 highlights the effect of mobility ratio on the stabilized five and nine-spot pilot recoveries. This figure was obtained by combining figures 17 through 19. It can be seen that, in general, the stabilized or confined pilot recoveries decrease with increasing mobility ratio.

Pilot Scaling

The calculations of the scaling coefficients (C) for the modified five and nine-spot floods are performed in Appendix D. The

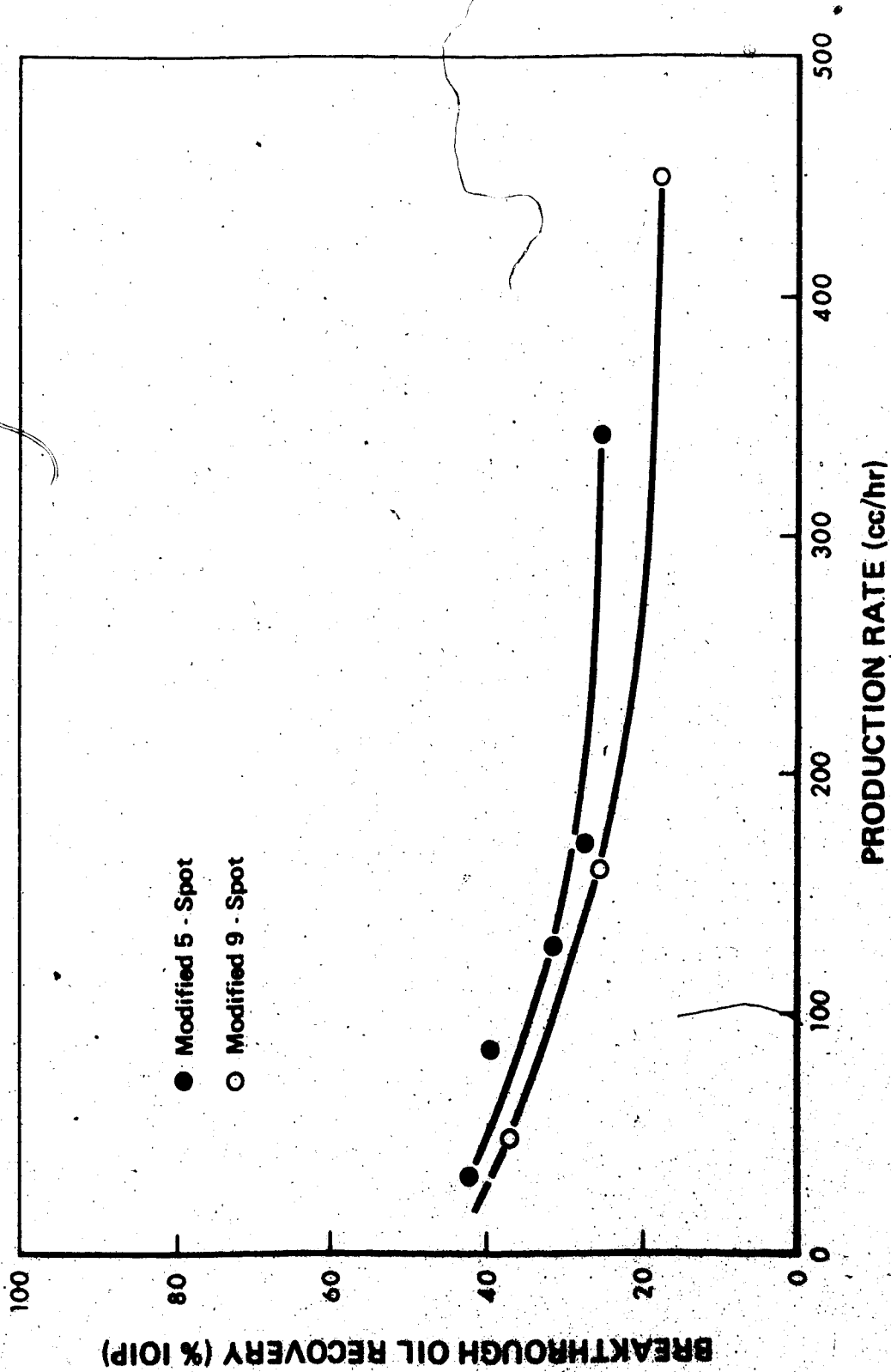


FIGURE 15. Effect of Rate on Breakthrough Oil Recovery from Modified 5 and 9 - Spot Patterns.
Mobility Ratio = 14.09

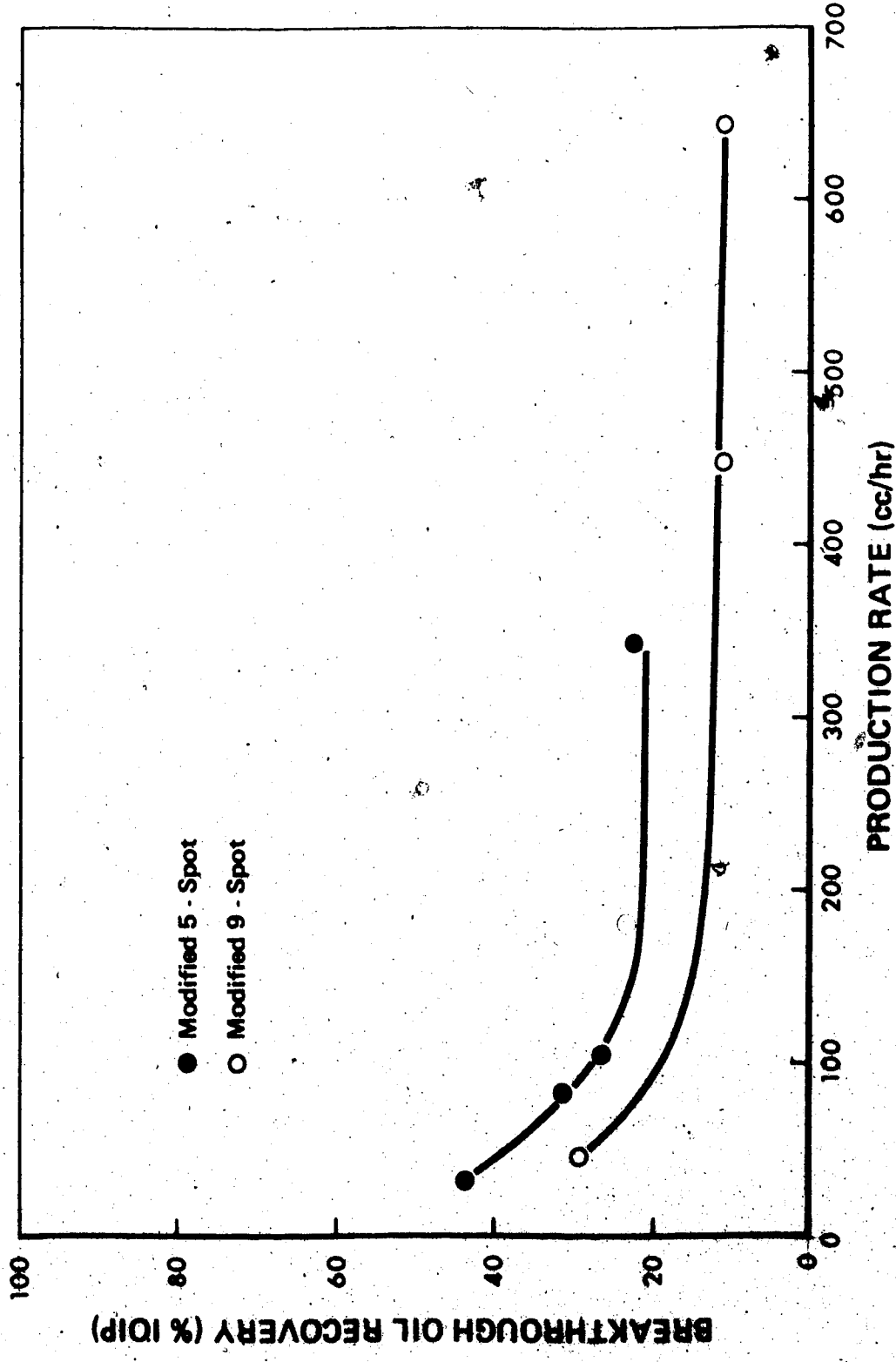


FIGURE 16. Effect of Rate on Breakthrough Oil Recovery from Modified 5 and 9 - Spot Patterns.
Mobility Ratio = 20.61

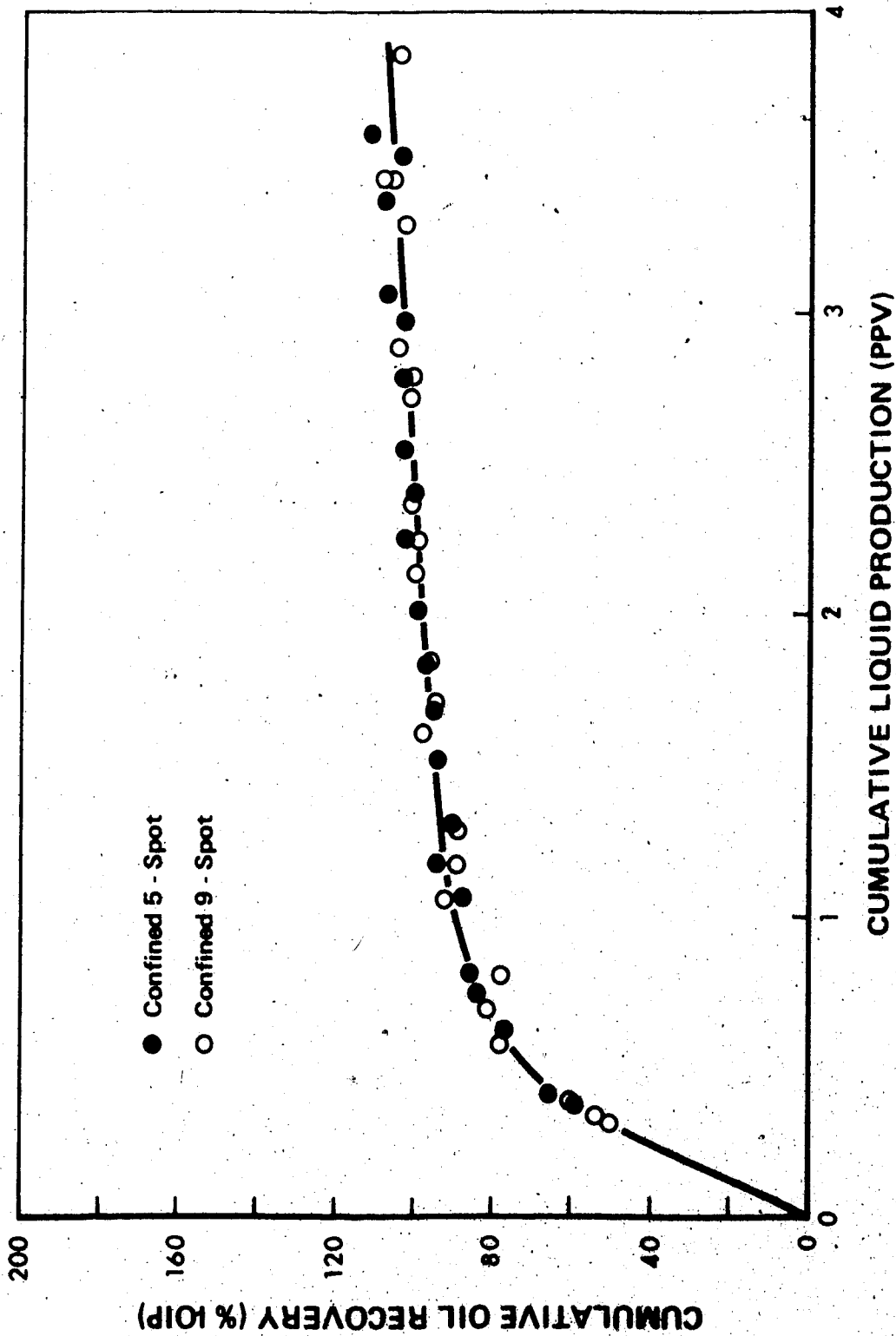


FIGURE 17. Comparison of Stabilized Oil Recovery Profiles from the Modified 5 and 9 - Spot Patterns. Mobility Ratio = 2.63

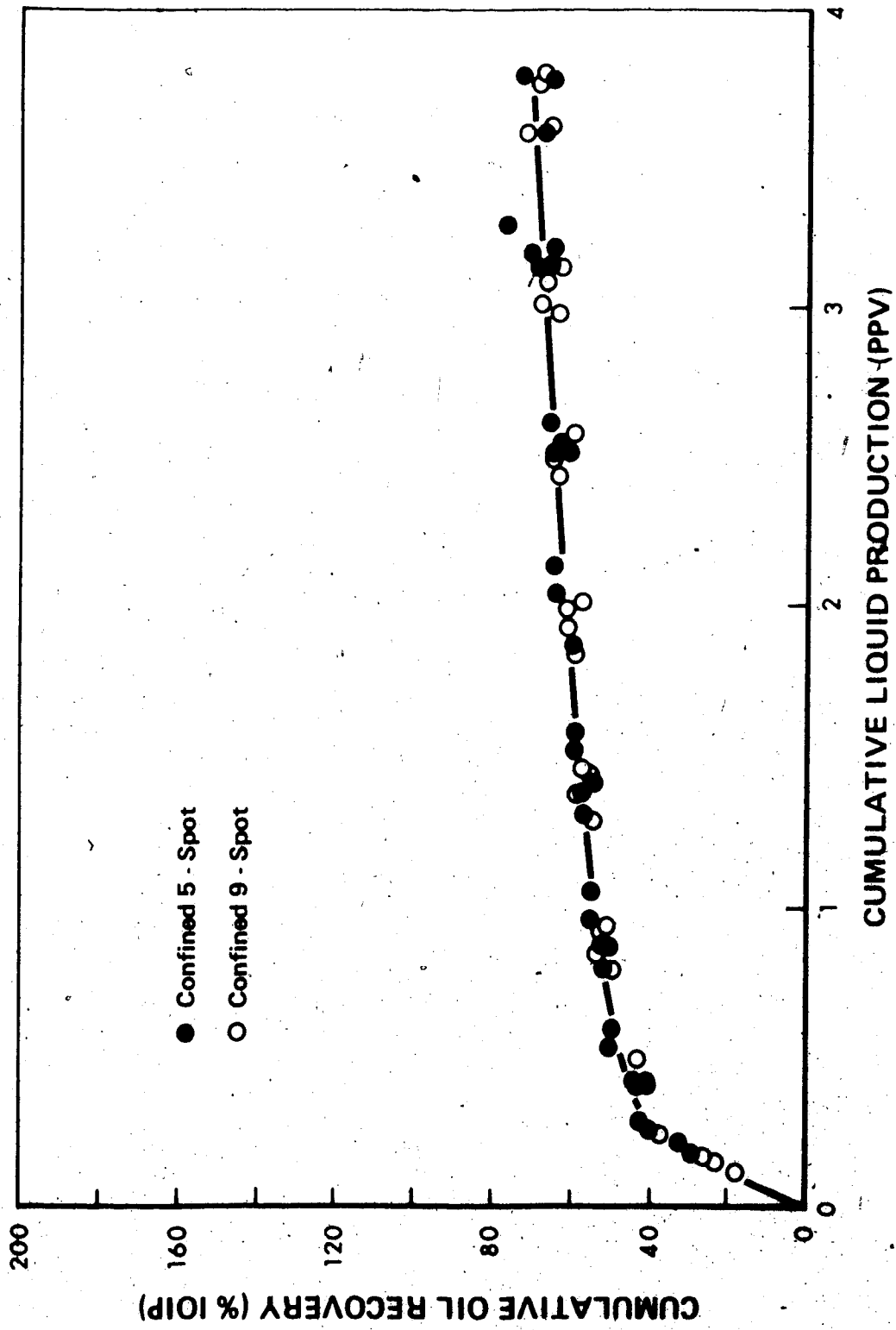


FIGURE 18. Comparison of Stabilized Oil Recovery Profiles from the Modified 5 - Spot Patterns. Mobility Ratio = 14.09

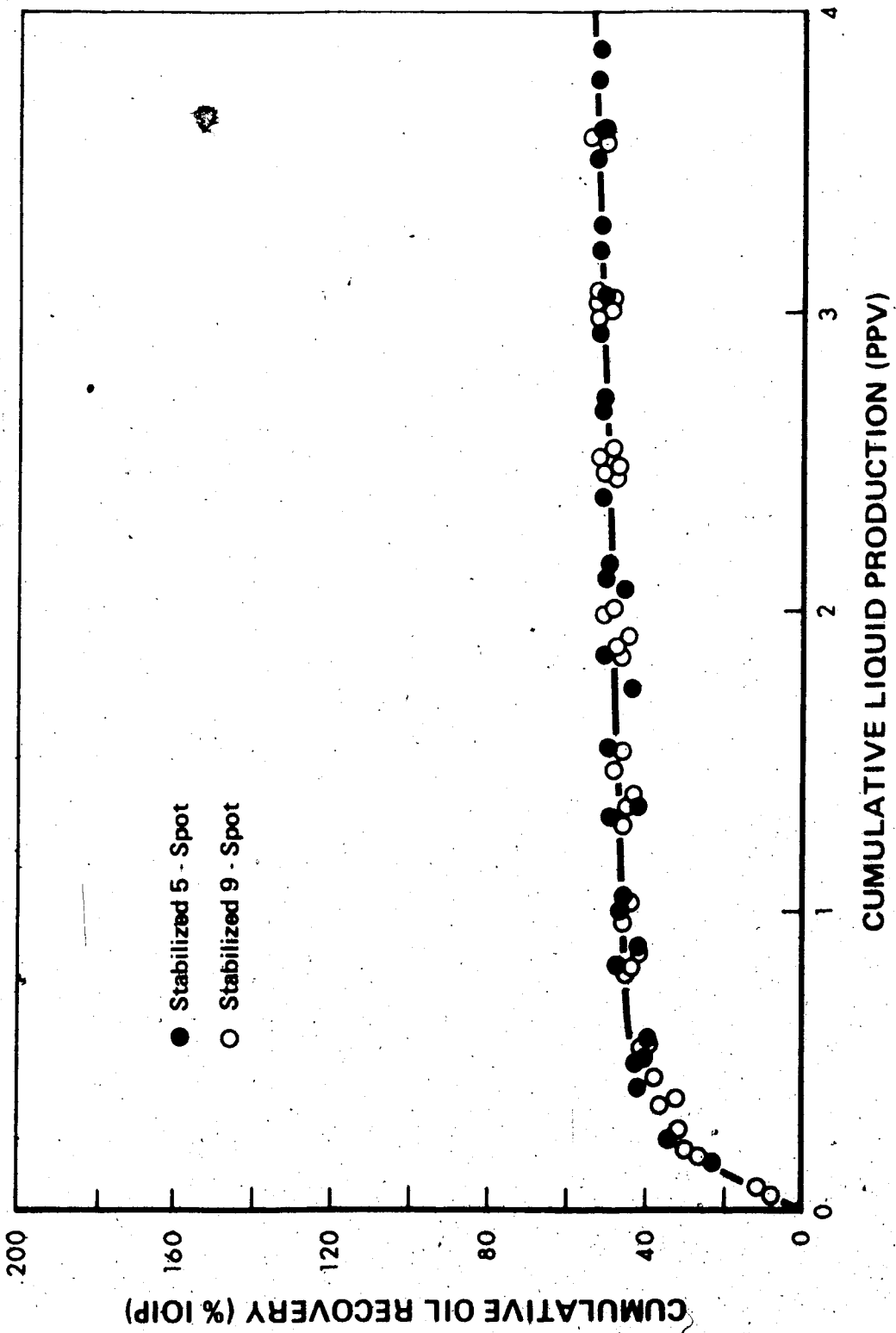


FIGURE 19. Comparison of Stabilized Oil Recovery Profiles from the Modified 5 and 9 - Spot Patterns. Mobility Ratio = 20.61

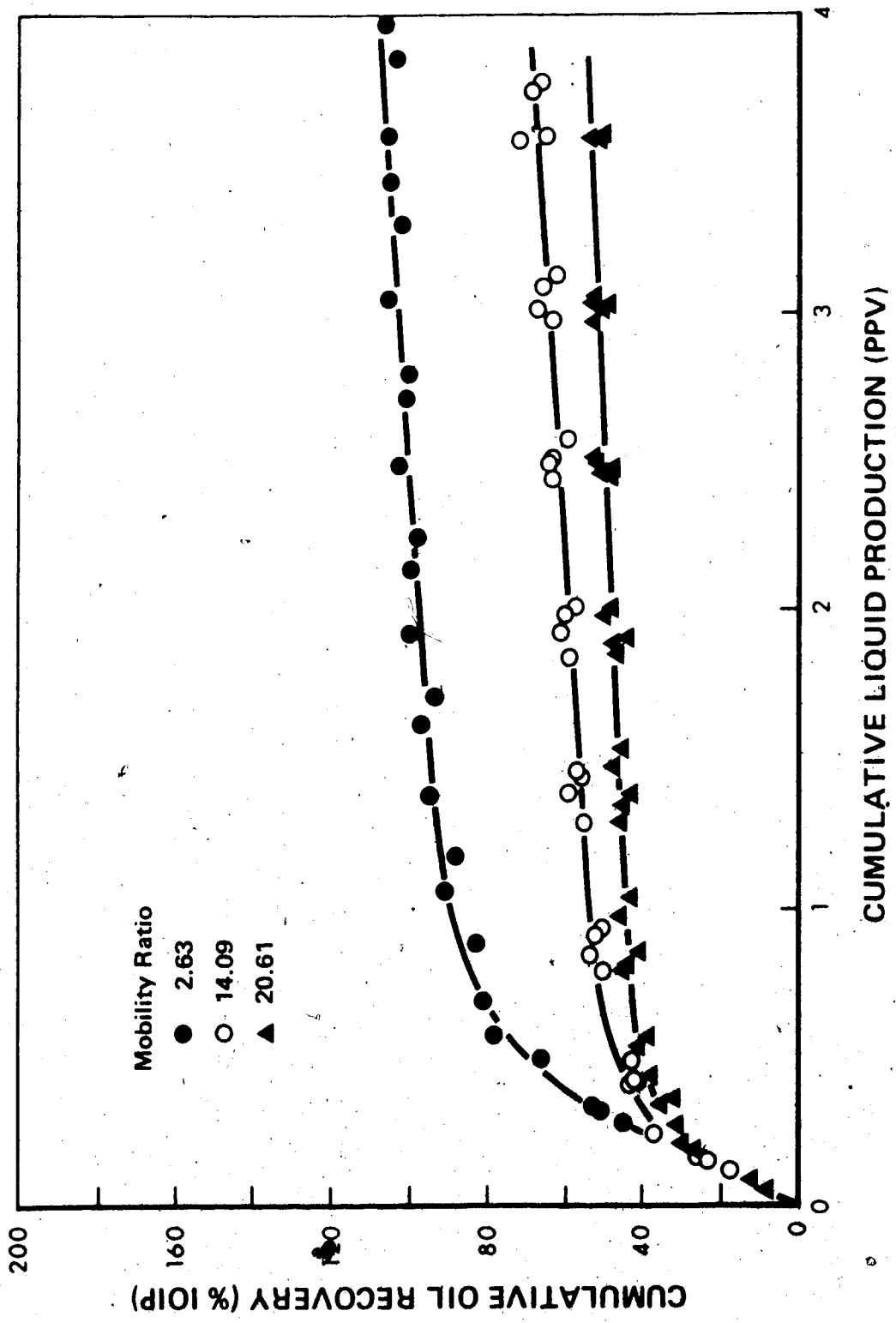


FIGURE 20. Effect of Mobility Ratio on Stabilized Oil Recovery from the Modified 5 and 9 - Spot Patterns.

oil recoveries used to demonstrate the scaling procedure are those obtained after production of 1 and 2 pore volumes of liquid, respectively. The recoveries at these stages of the floods were considered to be steady and no longer subject to the random variations observed in breakthrough recoveries.

Figures 21 and 22 show the variations of recoveries from the modified five and nine-spot pilots after 1 pore volume liquid production, with scaling coefficient (C) at an oil-water viscosity ratio of 1.32. This viscosity ratio corresponds to a mobility ratio of 2.63. It can be seen that for C lower than 2.60×10^{-3} , both the modified five and nine-spot recoveries vary with C , the variation being more pronounced for the nine-spot. For C equal to or greater than 2.60×10^{-3} , the recoveries stabilize and become independent of C . Furthermore, above this critical C , the stabilized or confined five and nine-spot recoveries are identical.

Figures 23 and 24 are the corresponding plots for a viscosity ratio of 8.66 ($M = 14.09$). In this case both pilots are stabilized over the range of scaling coefficients studied. Although the critical value of C does not appear on these plots, it is apparent that at a viscosity ratio of 8.66 ($M = 14.09$), the critical scaling coefficient is lower than that for a viscosity ratio of 1.32 ($M = 2.63$). As observed before, the stabilized five and nine-spot pilot recoveries are identical. The plots for a viscosity ratio of 15.22 ($M = 20.61$) are similar to those just described except that the recoveries at any value of C are lower for the higher viscosity ratio.

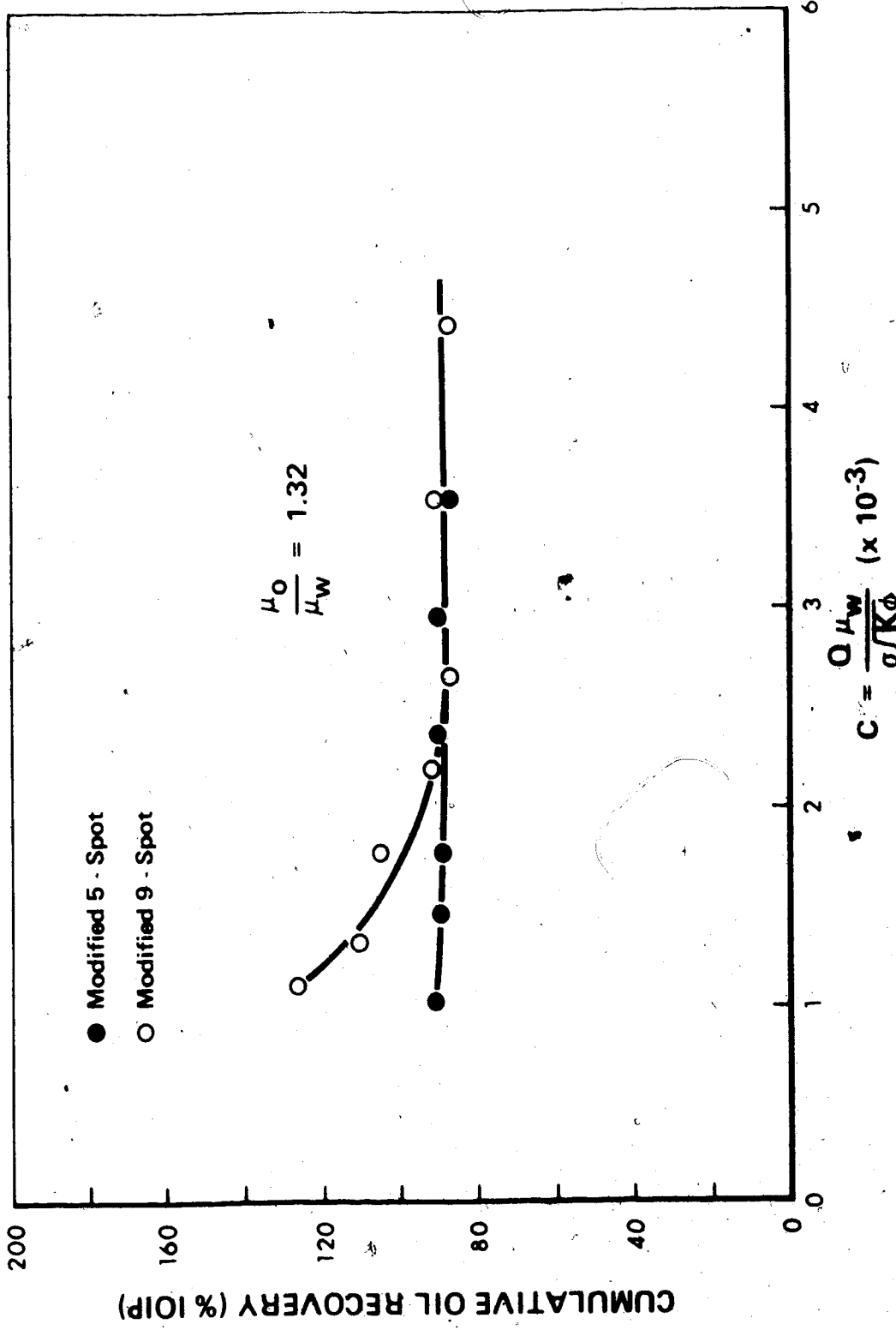


FIGURE 21. Variation of Oil Recovery with Scaling Coefficient at 1 Pore Volume Liquid Production. Mobility Ratio = 2.63

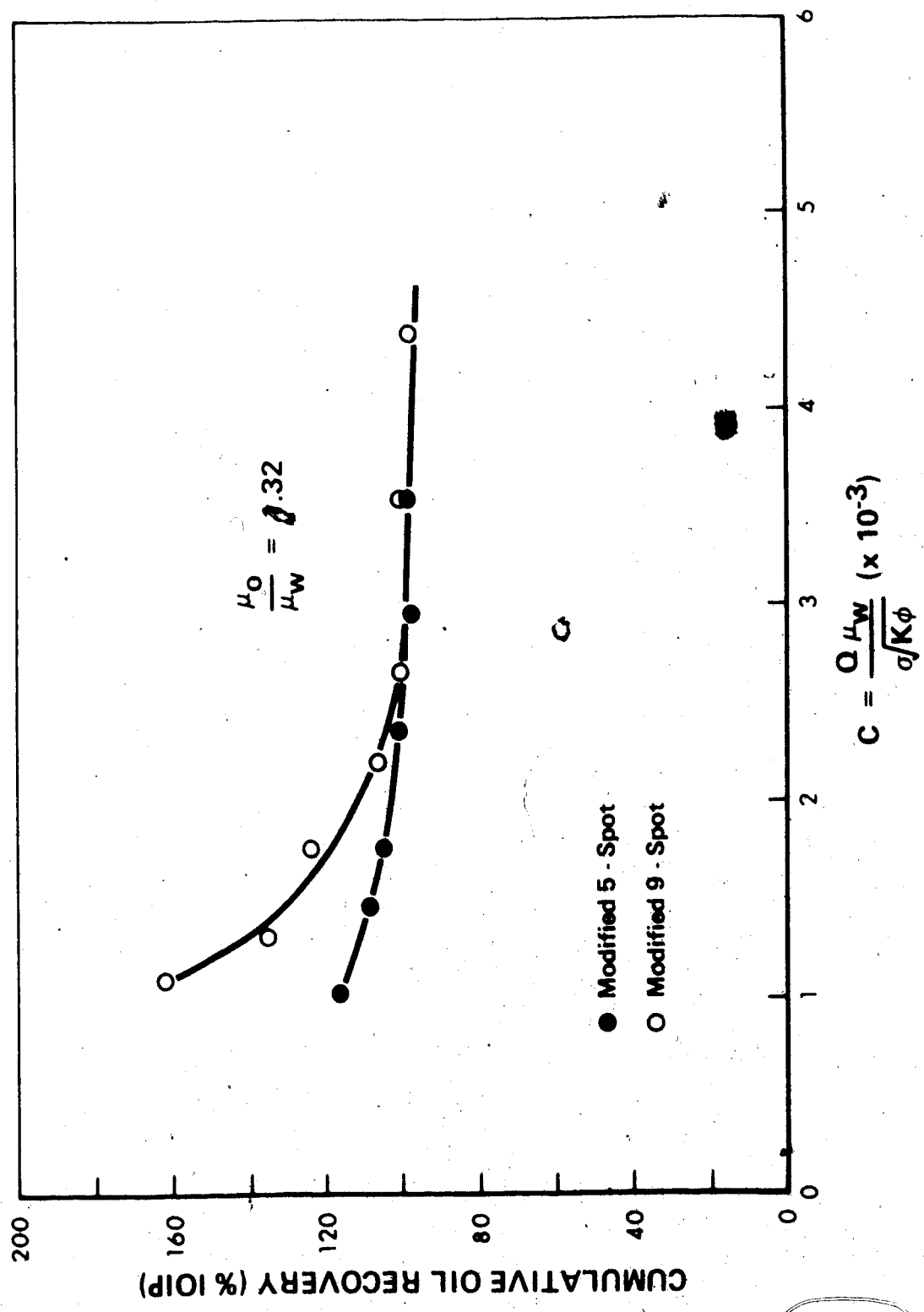


FIGURE 22. Variation of Oil Recovery with Scaling Coefficient at 2 Pore Volumes Liquid Production. Mobility Ratio = 2.63

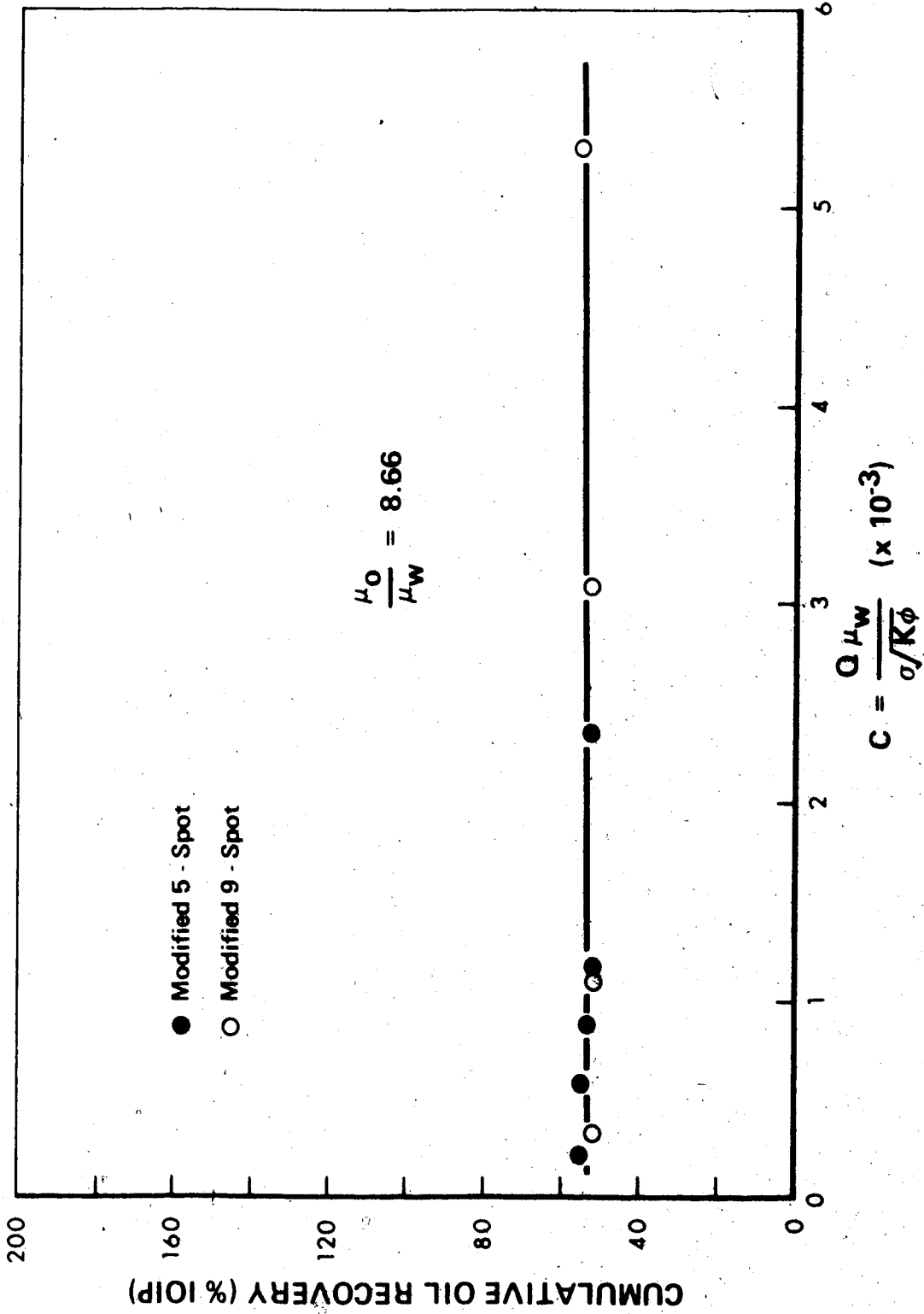


FIGURE 23. Variation of Oil Recovery with Scaling Coefficient at 1 Pore Volume Liquid Production. Mobility Ratio = 14.09

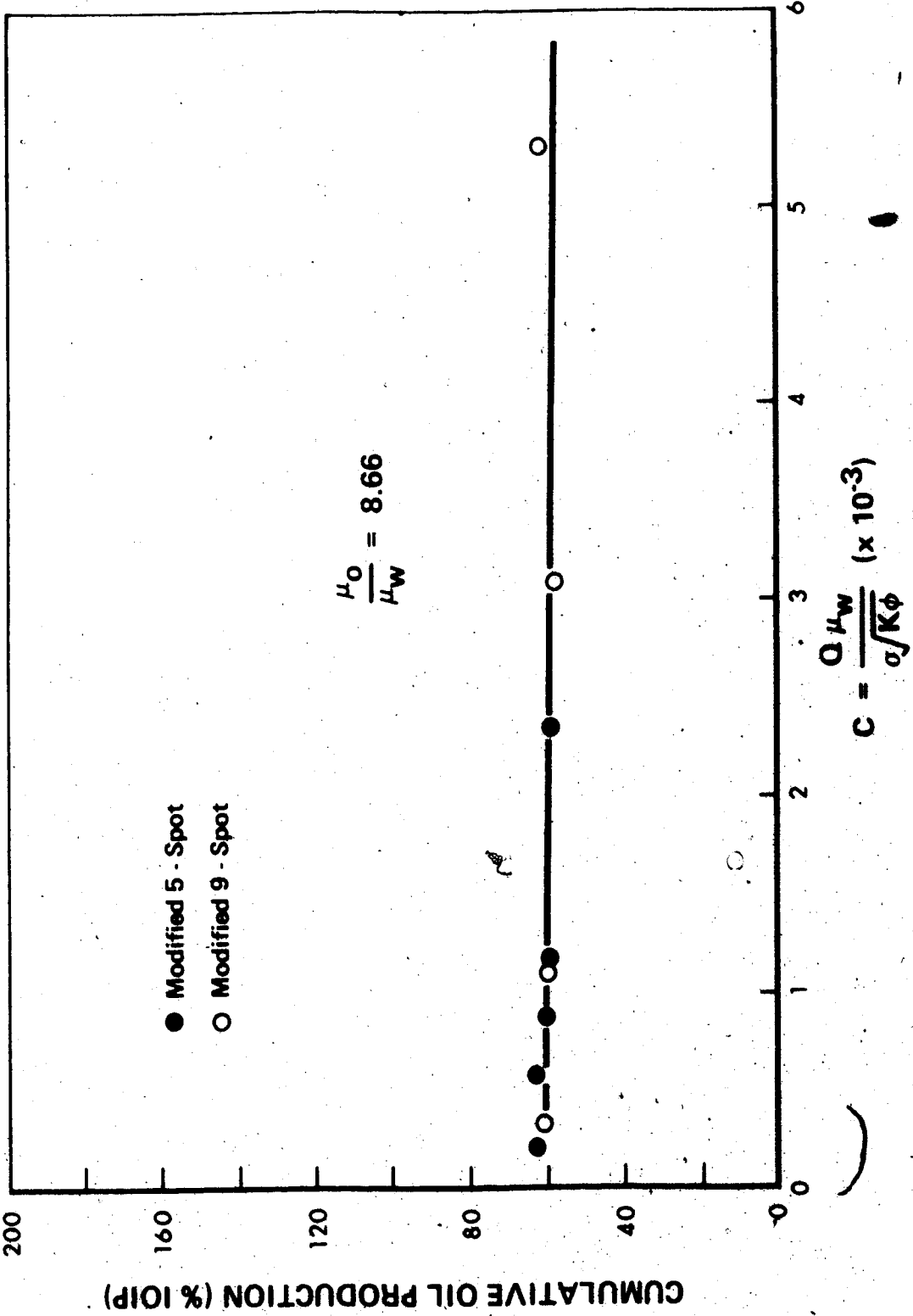


FIGURE 24. Variation of Oil Recovery with Scaling Coefficient at 2 Pore Volumes Liquid Production. Mobility Ratio = 14.09

VI. DISCUSSION OF RESULTS

Isolated Pilot Performances

The performances of the isolated five and nine-spot pilots in this study have demonstrated that pattern confinement cannot be achieved in these floods by rate control only. Consequently, considerable oversweep may be expected whenever isolated pilots are located at the centres of large fields. The practical implication of this observation is that the oil recoveries from such pilots are not representative of what may be expected from large scale floods. They are far too optimistic.

The above observations on isolated pilots disagree with those of Craig (86) who concluded from laboratory studies that the recovery, from a single five-spot may adequately predict large scale flood recovery. The disagreement is due to the differences in the pattern arrangements in both studies. Craig's single five-spot was not truly isolated because it was surrounded by two rings of competing producers which limited the amount of fluid available to the pilot producer. Also, this well arrangement in conjunction with an initial gas saturation gave rise to radial water fronts which provided an effective confining mechanism around the pilot producer.

In the present study, neither competing producers nor initial gas saturation was used with the result that no confining mechanism, such as observed by Craig, was present. Instead, it was observed that the water fronts expanded with continued water injection thereby contacting more and more oil bearing areas beyond the pilot perimeter.

Pattern Confinement

The results presented in figures 8 and 11 indicate that when surrounded by eight like patterns, the five and nine-spot pilots will be effectively confined if the injection rates are sufficiently high to ensure stabilized floods. At injection rates below the critical, the pilots behave as if unconfined, yielding overly optimistic oil recoveries.

At high mobility ratios, pattern confinement may be obtained at lower injection rates than for low mobility ratios. For example, for $M = 14.09$, figures 9 and 12 show that the pilots are virtually confined and their recoveries independent of rate over the entire range of injection rates studied. For $M = 20.61$, however, slight rate sensitivities persist at low rates as may be seen on figures 10 and 13. These rate sensitivities are attributed to errors in the flooding results caused by the formation of emulsions which characterized the displacement process at this mobility ratio.

Mechanism of Oversweep

Visual observations of the movement of the colored injection water gave some insight into the mechanism of oversweep in the isolated and modified pilots.

In the isolated pilots, the injected water continued to expand beyond the original pilot areas contacting fresh oil bearing areas as flooding progressed. As there were no pressure sinks outside of the pilot areas, the injected water was imbibed into the oil bearing areas surrounding the pilots. Water imbibition resulted in a counter-flow of oil toward the pilot producer.

The effectiveness of imbibition as a displacement mechanism is known to increase with time (87). This accounts for the oversweep and hence higher oil recoveries observed at low injection rates as compared to the high rates.

In the case of the modified pilots, the oversweep mechanism was somewhat different. At low injection rates, the flood fronts were generally diffuse with no distinct boundary between the injected water and the displaced oil. Corridors of the pilot areas remained uncontacted by water during the early stages of the flood. These corridors provided the paths through which extraneous oil reached the pilot producer. Also, there was considerable lag between water arrival at the pilot producer and water production. This is the familiar boundary or capillary end effect. This effect led to grossly exaggerated breakthrough oil recoveries. As the flooding progressed, the initially uniform colored water distribution became grossly distorted creating more paths for both injected water and displaced oil from the surrounding patterns to reach the pilot producer.

At high injection rates, the displacement process was remarkably different. The radial water fronts quickly cusped into a squared-off pattern, with much of the pilot area contacted at water breakthrough. The squared-off water fronts provided the confining mechanism in this study much in the same way as did the coalescing radial fronts in Craig's (88). Other distinctive features of the displacement were sharp flood fronts and little or no capillary end effect.

Pilot Scaling

The scaling procedure originally suggested by Rapoport et al (89) for five-spot pilots was extended to nine-spot floods. Use was made of the injection-production well ratios of confined five and nine-spot patterns in determining the rate used to calculate the scaling coefficients, C . The ratios are 1:1 for the five-spot and 3:1 for the nine-spot.

At a viscosity ratio of 1.32 ($M = 2.63$), the scaling results shown in figures 21 and 22 are similar to those of Rapoport et al (90). At scaling coefficients lower than the critical, both studies indicate that oil recoveries are sensitive to C ; but above the critical, the recoveries are stabilized and essentially independent of C . However, Rapoport et al (91) found that oil recovery increased with C at low scaling coefficients, whereas the opposite is true for the present study.

This difference in oil recovery performances may be attributed to the nature of pattern confinement in the two studies. In the present study, dynamic confinement was obtained only at rates above the critical. At low rates, therefore, the pilots were practically unconfined. Thus the high recoveries at low rates were due to pattern oversweep rather than to high displacement efficiency. As injection rates increased toward the critical, the oil recoveries decreased because the floods approached confinement. The system studied by Rapoport et al (92) was mechanically confined; therefore, their floods were not subject to oversweep. The low recoveries obtained at low rates or low scaling coefficients by these authors reflect both the lack of oversweep and the generally recognized inefficiency of slow immiscible displacement.

On the other hand, the increase in recovery with increasing rates or increasing scaling coefficients reflects the higher recovery efficiency usually attributed to high displacement rates.

In this study, the critical C for a viscosity ratio of 1.32 ($M = 2.63$) is 2.60×10^{-3} as compared to 3.50×10^{-3} obtained by Rapoport et al (93) at a viscosity ratio of unity. The agreement in the order of magnitude is remarkable in view of wettability and other differences between the two systems.

Above the critical C , both the five-spot and nine-spot floods stabilize and yield identical oil recoveries. The two floods therefore become equivalent at sufficiently high rates or scaling coefficients.

At a viscosity ratio of 8.66 ($M = 14.09$), the modified five and nine-spot floods are stabilized and identical at much lower values of C than at a viscosity ratio of 1.32 ($M = 2.63$). Thus, as viscosity ratio increases the critical injection rate or critical scaling coefficient decreases. This observation supports the theoretical prediction of Equation 17 which shows that as the viscosity ratio (λ) increases, lower values of C are required to render the rate dependent terms of the flood performance negligible.

Effect of Mobility Ratio

The mobility ratios examined in this study fall within the range usually considered unfavorable to waterflooding. Although the effects of increasingly adverse mobility ratios on pilot recoveries have been pointed out elsewhere in this discussion, a brief summary is in order.

Increasing mobility ratios predictably result in lower oil recoveries from both isolated and confined pilots. As these lower recoveries tend to mask the severity of oversweep in the unconfined pilots, due care should be exercised in interpreting pilot recovery data obtained under adverse mobility ratios.

With regard to pilot scaling, it has been shown that increasing mobility ratios (or viscosity ratios) lead to early flood stabilization and confinement. The agreement between this observation and the predictions of Equation 17 is further evidence of the validity of the theory of immiscible displacement employed in this study.

Generally, the immiscible displacement process at the higher mobility ratios was characterized by low breakthrough sweep efficiencies, diffuse flood fronts, high water-oil ratios after breakthrough and considerable subordinate oil production. These observations agree in a qualitative way with those reported by other investigators.

Five-Spot versus Nine-Spot Performance

As pointed out earlier, the recovery profiles of the isolated five and nine-spot pilots are very similar over the range of the mobility ratios studied.

On the other hand, figures 14 through 16 show that the five-spot breakthrough recoveries are consistently higher than those of the nine-spot. Surprising as these results may be, they are in full accord with the theoretical calculations of Krutter (94) and Muskat (95) which indicate that depending on the rate ratio of the corner to side well, the nine-spot breakthrough efficiency may be lower than that of the five-spot.

Although the sweep efficiencies were not calculated, plates 3 and 4 give a qualitative view of the breakthrough areal coverage for the stabilized or confined five-spot and nine-spot patterns, respectively. Plate 4 shows that the four side wells are responsible for the early water breakthrough observed in the nine-spot pilots. This breakthrough behaviour of the nine-spot floods emphasizes the need for strict rate control of the corner and side wells if the potential benefits of nine-spot floods are to be realized.

Despite the differences in breakthrough recoveries, the cross-plots shown in figures 17 through 19 indicate that the ultimate recoveries from the stabilized or confined five and nine-spot floods are identical. This observation is important from a practical standpoint. If field pilots behave as laboratory pilots, then a limited number of nine-spots, such as presented in this study, may be used to study the feasibility of large scale five-spot floods in situations where the lead time is the overriding factor. On the other hand, if the lead time is unimportant, the observation casts doubt on the wisdom of using nine-spot floods as the same results could indeed be obtained with a limited number of five-spots at a lower cost.

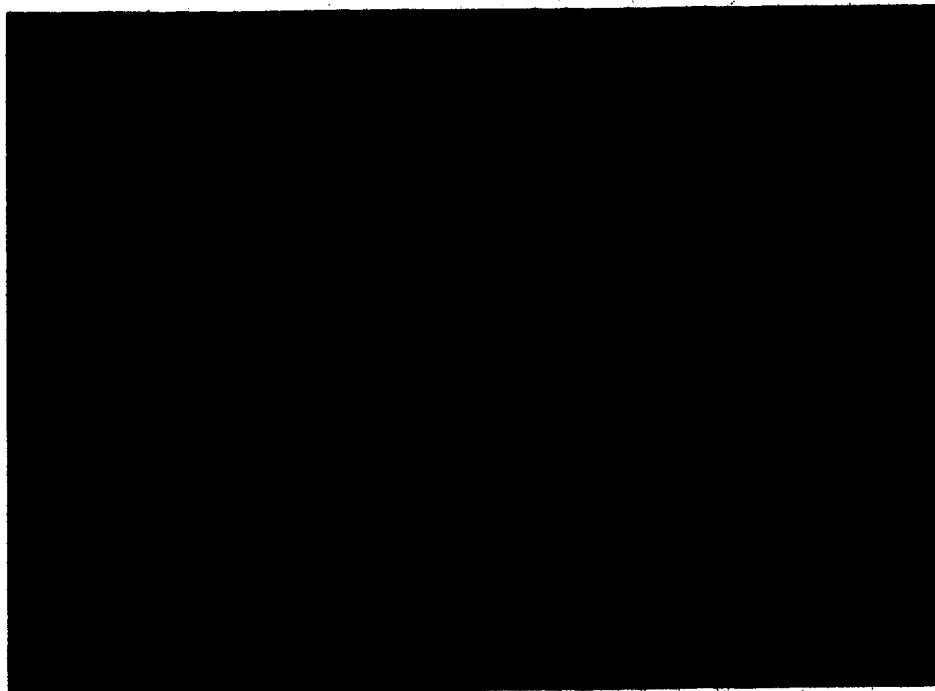


PLATE 3. Breakthrough Areal Coverage for a Confined 5-Spot Pattern

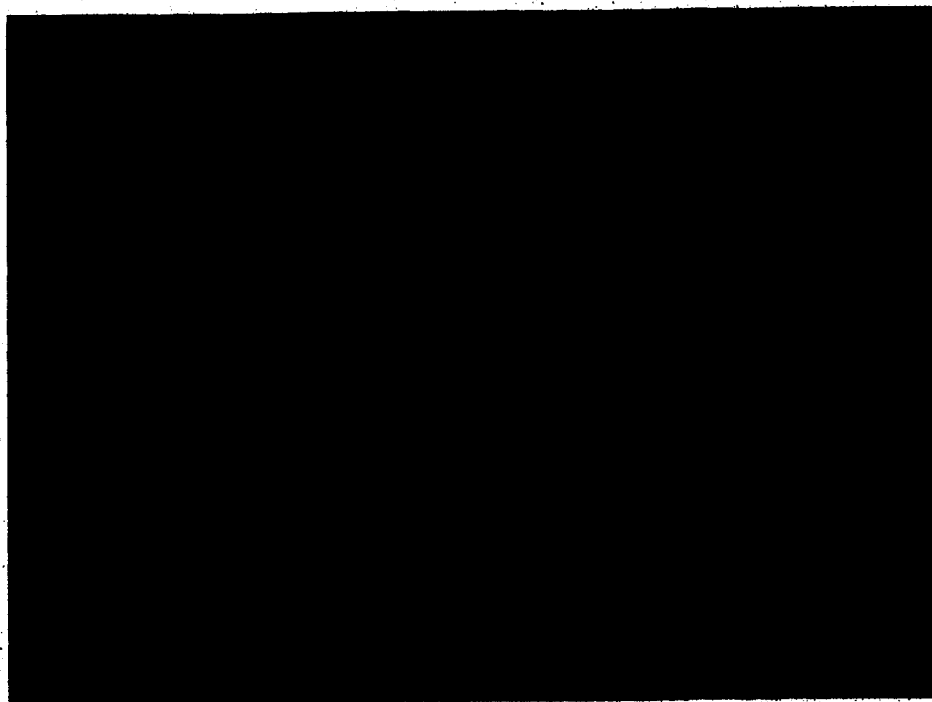


PLATE 4. Breakthrough Areal Coverage for a Confined 9-Spot Pattern

VII. SUMMARY AND CONCLUSIONS

A laboratory study has been conducted on isolated and partially confined five and nine-spot waterflood pilots. The model consisted of an unconsolidated pack of glass beads sandwiched between two transparent lucite plates. Colored injection water permitted direct visual observations of the flood fronts. Three mobility ratios were studied; in every case, initial water saturation was present.

The main conclusions drawn from the results and observations of this study are:

1. Both isolated five and nine-spot pilots continue to oversweep their patterns with continued water injection.
2. Pattern confinement may be achieved by surrounding the five and nine-spot pilots with a single ring of eight similar patterns.
3. Such pattern confinement can only be achieved when the injection rates are sufficiently high to ensure stabilized floods.
4. The higher the mobility ratio, the lower the injection rate required to ensure stabilized floods.
5. Increasing mobility ratios lead to decreasing oil recoveries from both isolated and confined pilots at any given water-oil ratio.
6. The five-spot breakthrough performance is superior to the nine-spot operated at a unit corner to side injection rate ratio.
7. The ultimate recoveries from the five-spot and nine-spot pilots are identical provided the floods are stabilized.

8. The scaling procedure proposed by Rapoport et al (96) for five-spot floods may be successfully extended to nine-spot floods by appropriate choice of injection rates.

Recommendations

The pattern arrangements used in the present study by no means exhaust the possibilities. Preliminary studies on an arrangement consisting of a cluster of sixteen inverted five-spots indicated that pattern oversweep was eliminated over a wide range of injection rates due to the formation of radial water banks similar to those observed by Craig (97). This pattern arrangement merits further investigation.

Also, de Haan (98) and others found that injection rates far in excess of those required to ensure flood stability lead to decreasing oil recoveries. This suggests the existence of plateau in the recovery versus rate or scaling coefficient plot. This rate effect was not examined because of the strength limitation of the lucite model used in the present study. To study the flood behaviour at these high rates, it is recommended that the model be reinforced to withstand higher injection pressures than those encountered in the present study.

Finally, the breakthrough sweep efficiency of the nine-spot pattern should be studied in greater detail. In particular, the efficiency should be examined as a function of the corner to side well injection rate ratio. Such an investigation could serve to establish the range of rate ratios which will ensure optimum operation of nine-spot floods. To accomplish this, the present injection system will have to be modified to permit different injection rates into the corner and side wells.

NOMENCLATURE

A	=	Average area perpendicular to direction of flow
C	=	Scaling coefficient
d	=	Distance between corner well and production well
f	=	Fraction of fluid flowing
g	=	Acceleration due to gravity
h	=	Thickness of porous medium
IOIP	=	Initial oil in place
K	=	Absolute permeability
k_{ocw}	=	Effective permeability to oil at residual water saturation
k_{ro}	=	Relative permeability to oil
k_{rw}	=	Relative permeability to water
k_{wro}	=	Effective permeability to water at residual oil saturation
L	=	Characteristic length of the system
M	=	Mobility ratio
m	=	Slope
P	=	Pressure
P_c	=	Capillary pressure
\bar{P}_c	=	Dimensionless capillary pressure
PPV	=	Pattern pore volume
Q	=	Production rate per unit reservoir thickness
q	=	Injection rate per well
r_w	=	Wellbore radius

- S = Saturation
 \vec{u} = Darcy superficial velocity (flux) vector
 u^* = Characteristic superficial velocity
 Z = Elevation below some reference elevation measured positively in a vertical downward direction
 α = Angle with vertical
 θ = Contact angle between solid and water-oil interface measured through the water phase
 μ_o = Oil viscosity
 μ_w = Water viscosity
 ρ = Density
 $\Delta\rho$ = Water-oil density difference
 σ = Oil-water interfacial tension
 ϕ = Porosity
 ψ = k_{ro} times fractional flow of the displacing fluid
 ψ' = $\frac{d\psi}{dS}$

Vector Notation

$$\vec{u} = \vec{i}u_x + \vec{j}u_y + \vec{k}u_z$$

where \vec{i} , \vec{j} and \vec{k} are unit vectors in the x , y and z directions, respectively.

$$\nabla p = \vec{i} \frac{\partial p}{\partial x} + \vec{j} \frac{\partial p}{\partial y} + \vec{k} \frac{\partial p}{\partial z}$$

$$\begin{aligned} \nabla \cdot \vec{u} &= (\vec{i} \frac{\partial}{\partial x} + \vec{j} \frac{\partial}{\partial y} + \vec{k} \frac{\partial}{\partial z}) \cdot (\vec{i}u_x + \vec{j}u_y + \vec{k}u_z) \\ &= \frac{\partial u_x}{\partial x} + \frac{\partial u_y}{\partial y} + \frac{\partial u_z}{\partial z} \end{aligned}$$

REFERENCES

1. Bernard, W.J. and Caudle, B.H.: "Model Studies of Pilot Water Floods", Trans., AIME (1967), 240, pp.404-410.
2. Caudle, B.H. and Loncaric, I.G.: "Oil Recovery in Five-Spot Pilot Floods", Trans., AIME (1960), 219, pp.132-136.
3. Culham, W.E.: "A Model Study of an Isolated Nine Spot", M.Sc. Thesis, University of Alberta, 1962, p.58.
4. Dranchuk, P.M. and Jain, A.: "The Effect of Pattern Confinement on Oil Recovery for the Five-Spot Pattern", Jour. of Can. Pet. Tech., Vol.9, No.4, 1970, pp.237-241.
5. Pritchard, K.C.G.: "A Model Study of A Sandstone System", M.Sc. Thesis, University of Alberta, 1962, p.45.
6. Craig, F.F., Jr.: "Laboratory Model Study of Single Five-Spot and Single Injection Well Pilot Waterflooding", JPT (Dec 1965), 17, pp.1454-1460.
7. Dalton, R.L., Jr., Rapoport, L.A. and Carpenter, C.W., Jr.: "Laboratory Studies of Pilot Water Floods", Trans., AIME (1960), 219, pp.24-30.
8. Rosenbaum, M.J.F. and Matthews, C.S.: "Studies on Pilot Water Flooding", Trans., AIME (1959), 216, pp.316-323.
9. Bernard, W.J. and Caudle, B.H., loc. cit.
10. Dalton, R.L., Jr., Rapoport, L.A. and Carpenter, C.W., Jr., loc. cit.
11. Bernard, W.J. and Caudle, B.H., loc. cit.
12. Bhatia, S.K.: "A Model Study of Isolated Well Patterns", M.Sc. Thesis, University of Alberta, 1967, p.102.
13. Caudle, B.H. and Loncaric, I.G., loc. cit.
14. Dranchuk, P.M. and Jain, A., op. cit.
15. Neilson, I.D.R. and Flock, D.L.: "The Effect of a Free Gas Saturation on the Sweep Efficiency of an Isolated Five-Spot", CIM Bull. (1962), 55, p.124.
16. Pritchard, K.C.G., loc. cit.
17. Caudle, B.H. and Loncaric, I.G., loc. cit.

18. Ibid.
19. Dranchuk, P.M. and Jain, A., op. cit.
20. Rapoport, L.A., Carpenter, C.W., Jr. and Leas, W.J.: "Laboratory Studies of Five-Spot Water Flood Performance", Trans., AIME (1958), 213, pp.113-120.
21. Dalton, R.L., Jr., Rapoport, L.A. and Carpenter, C.W., Jr., loc. cit.
22. Craig, F.F., Jr., loc. cit.
23. Dalton, R.L., Jr., Rapoport, L.A. and Carpenter, C.W., Jr., loc. cit.
24. Caudle, B.H. and Loncaric, I.G., loc. cit.
25. Dalton, R.L., Jr., Rapoport, L.A. and Carpenter, C.W., Jr., loc. cit.
26. Buckley, S.E. and Leverett, M.C.: "Mechanism of Fluid Displacement in Sands", Trans., AIME (1942), 146, pp.107-116.
27. Richardson, J.G. and Perkins, F.M., Jr.: "A Laboratory Investigation of the Effect of Rate on Recovery of Oil by Water Flooding", Trans., AIME (1957), 210, pp.115-121.
28. Rapoport, L.A., Carpenter, C.W., Jr. and Leas, W.J., loc. cit.
29. Rapoport, L.A. and Leas, W.J.: "Properties of Linear Waterfloods", Trans., AIME (1953), 198, pp.139-148.
30. de Haan, H.J.: "Effect of Capillary Forces in the Water-Drive Process", Proc. Fifth World Petroleum Congress, Sec. II, (1959), p.25.
31. Ibid.
32. Engelberts, W.F. and Klinkenberg, L.J.: "Laboratory Experiments on the Displacement of Oil by Water from Packs of Granular Materials", Proc. Third World Petroleum Congress, Sec. II, (1951), p.544.
33. Rapoport, L.A., Carpenter, C.W., Jr. and Leas, W.J., loc. cit.
34. Rapoport, L.A. and Leas, W.J., loc. cit.
35. Douglas, J., Jr., Blair, P.M. and Wagner, R.J.: "Calculation of Linear Waterflood Behaviour Including the Effects of Capillary Pressure", Trans., AIME (1958), 213, pp.96-102.

36. Ibid.
37. Jones-Parra, J., Stahl, C.D. and Calhoun, J.C.: "A Theoretical and Experimental Study of Constant Rate Displacements in Water Wet Systems", *Prod. Monthly*, (Jan 1954), 18, pp.18-26.
38. Kyte, J.R. and Rapoport, L.A.: "Linear Waterflood Behaviour and End Effects in Water-Wet Porous Media", *Trans., AIME* (1958), 213, pp.423-426.
39. Perkins, F.M., Jr.: "An Investigation of the Role of Capillary Forces in Laboratory Water Floods", *Trans., AIME* (1957), 210, pp.409-411.
40. Leverett, M.C.: "Capillary Behaviour in Porous Solids", *Trans., AIME* (1941), 142, pp.152-168.
41. Aronofsky, J.S. and Ramey, H.J., Jr.: "Mobility Ratio - Its Influence on Injection or Production Histories in Five-Spot Water Flood", *Trans., AIME* (1956), 207, pp.205-210.
42. Dyes, A.B., Caudle, B.H. and Erickson, R.A.: "Oil Production After Breakthrough as Influenced by Mobility Ratio", *Trans., AIME* (1954), 201, pp.81-86.
43. Caudle, B.H., Erickson, R.A. and Slobod, R.L.: "The Encroachment of Fluids Beyond the Normal Well Patterns", *Trans., AIME* (1955), 204, pp.79-83.
44. Fay, C.H. and Prats, M.: "Application of Numerical Methods to Cycling and Flooding Problems", *Proc. Third World Petroleum Congress, Sec.II*, (1951), p.555.
45. Bradley, H.B., Heller, J.P. and Odeh, A.S.: "A Potentiometric Study of the Effects of Mobility Ratio on Reservoir Flow Patterns", *Trans., AIME* (1961), 222, pp.125-129.
46. Ibid.
47. Buckley, S.E. and Leverett, M.C., *loc. cit.*
48. Craig, F.F., Jr., Geffen, T.M. and Morse, R.A.: "Oil Recovery Performance of Pattern Gas or Water Injection Operations from Model Tests", *Trans., AIME* (1955), 204, pp.7-14.
49. Perkins, F.M., Jr. and Collins, R.E.: "Scaling Laws for Laboratory Flow Models of Oil Reservoirs", *Trans., AIME* (1960), 219, pp.383-385.
50. Caudle, B.H. and Loncaric, I.G., *loc. cit.*
51. Dyes, A.B., Caudle, B.H. and Erickson, R.A., *loc. cit.*

52. Caudle, B.H. and Loncaric, I.G., loc. cit.
53. Dyes, A.B., Caudle, B.H. and Erickson, R.A., loc. cit.
54. Aronofsky, J.S. and Ramey, H.J., Jr., loc. cit.
55. Caudle, B.H., Erickson, R.A. and Slobod, R.L., loc. cit.
56. Cheek, R.E. and Menzie, D.E.: "Fluid Mapper Model Studies of Mobility Ratio", Trans., AIME (1955), 204, pp.278-281.
57. Dyes, A.B., Caudle, B.H. and Erickson, R.A., loc. cit.
58. Bradley, H.B., Heller, J.P. and Odeh, A.S., loc. cit.
59. Ibid.
60. Krutter, H.: "Nine-Spot Flooding Program", O&GJ, (Aug 17, 1939), 38, pp.50-52.
61. Muskat, M.: "The Theory of Nine-Spot Flooding Networks", Prod. Monthly, (March 1948), 12, p.14.
62. Crawford, P.B.: "Laboratory Factors Affecting Water Flood Pattern Performance and Selection", JPT (Dec 1960), 12, pp.11-15.
63. Dranchuk, P.M. and Jain, A., op. cit.
64. Caudle, B.H. and Loncaric, I.G., loc. cit.
65. Geertsma, J., Croes, G.A. and Schwarz, N.: "Theory of Dimensionally Scaled Models of Petroleum Reservoirs", Trans., AIME (1956), 207, pp.118-127.
66. Leverett, M.C., Lewis, W.B. and True, M.E.: "Dimensional Model Studies of Oilfield Behaviour", Trans., AIME (1942), 146, pp.175-192.
67. Engelberts, W.F. and Klinkenberg, L.J., loc. cit.
68. Rapoport, L.A.: "Scaling Laws for Use in Design and Operation of Water-Oil Flow Models", Trans., AIME (1955), 204, pp.143-150.
69. Rapoport, L.A. and Leas, W.J., loc. cit.
70. Geertsma, J., Croes, G.A. and Schwarz, N., loc. cit.
71. Spivak, A.: "Gravity Segregation in Two-Phase Displacement Processes", Trans., AIME (1974), 257, pp.619-632.
72. Buckley, S.E. and Leverett, M.C., loc. cit.

73. Rapoport, L.A. and Leas, W.J., loc. cit.
74. Ibid.
75. Perkins, F.M., Jr. and Collins, R.E., loc. cit.
76. van Meurs, P. and van der Poel, C.: "A Theoretical Description of Water-Drive Processes Involving Viscous Fingering", Trans., AIME (1958), 213, pp.103-112.
77. Chuoke, R.L., van Meurs, P. and van der Poel, C.: "The Instability of Slow, Immiscible, Viscous Liquid-Liquid Displacement in Permeable Media", Trans., AIME (1959), 216, pp.188-194.
78. Rachford, H.H., Jr.: "Instability in Water Flooding Oil From Water-Wet Porous Media Containing Connate Water", Trans., AIME (1964), 231, pp.133-148.
79. Ibid.
80. Rapoport, L.A. and Leas, W.J., loc. cit.
81. Rapoport, L.A., Carpenter, C.W., Jr. and Leas, W.J., loc. cit.
82. Ibid.
83. Ibid.
84. Jain, A., op. cit.
85. Perkins, F.M., Jr. and Collins, R.E., loc. cit.
86. Craig, F.F., Jr., loc. cit.
87. Clark, N.J.: "Elements of Petroleum Reservoirs", AIME Publication, p.119.
88. Craig, F.F., Jr., loc. cit.
89. Rapoport, L.A., Carpenter, C.W., Jr. and Leas, W.J., loc. cit.
90. Ibid.
91. Ibid.
92. Ibid.
93. Ibid.
94. Krutter, H., loc. cit.
95. Muskat, M., loc. cit.

96. Rapoport, L.A., Carpenter, C.W., Jr. and Leas, W.J., loc. cit.
97. Craig, F.F., Jr., loc. cit.
98. de Haan, H.J., loc. cit.
99. Perkins, F.M., Jr. and Collins, R.E., loc. cit.

BIBLIOGRAPHY

1. Aronofsky, J.S.: "Mobility Ratio-Its Influence on Flood Patterns During Water Encroachment", Trans., AIME (1952), 195, pp.15-23.
2. Bentsen, R.G.: "Advantages of A Consistent Definition For Mobility Ratio", Paper presented at the 26th Annual Tech. Meeting of the Pet. Soc. of CIM in Banff, June 11, 1975.
3. Burton, M.E. and Crawford, P.B.: "Application of the Gelatin Model for Studying Mobility Ratio Effects", Trans., AIME (1955), 204, p.79.
4. Caudle, B.H. and Witte, M.D.: "Production Changes During Sweepout in a Five-Spot System", Trans., AIME (1959), 216, pp.446-448.
5. Cotman, N.T., Still, G.R. and Crawford, P.B.: "Laboratory Comparison of Oil Recovery in Five-Spot and Nine-Spot Waterflood Patterns", Prod. Monthly, (Dec 1962), 26, pp.10-13.
6. Croes, G.A. and Schwarz, N.: "Dimensionally Scaled Experiments and the Theories on the Water-Drive Process", Trans., AIME (1955), 204, pp.35-42.
7. Deppe, J.C.: "Injection Rates - The Effect of Mobility Ratio, Area Swept and Pattern", Trans., AIME (1961), 222, pp.81-91.
8. Douglas, J., Jr., Peaceman, D.W. and Rachford, H.H., Jr.: "A Method for Calculating Multi-Dimensional Immiscible Displacement", Trans., AIME (1959), 216, pp.297-308.
9. Dranchuk, P.M. and Peters, E.J.: "Pattern Oversweep in Nine-Spot Waterflood Pilots", Paper presented at the 26th Annual Tech. Meeting of Pet. Soc. of CIM in Banff, June 11, 1975.
10. Earlougher, R.C.: "Relationship Between Velocity, Oil Saturation, and Flooding Efficiency", Trans., AIME (1943), 151, pp.125-137.
11. Fayers, F.J. and Sheldon, J.W.: "The Effect of Capillary Pressure and Gravity on Two-Phase Fluid Flow in a Porous Medium", Trans., AIME (1959), 216, pp.147-155.
12. Fischer-Rosenbaum, M.J. and Mathews, C.S.: "Studies on Pilot Water Flooding", Trans., AIME (1959), 216, pp.316-323.
13. Gaucher, D.H. and Lindley, D.C.: "Waterflood Performance in a Stratified, Five-Spot Reservoir - A Scaled Model Study", Trans., AIME (1960), 219, pp.208-215.

14. Habermann, B.: "The Efficiency of Miscible Displacement as a Function of Mobility Ratio", Trans., AIME (1960), 219, pp.264-271.
15. Hawthorne, R.G.: "Two-Phase Flow in Two-Dimensional Systems - Effects of Rate, Viscosity and Density on Fluid Displacement in Porous Media", Trans., AIME (1960), 219, pp.81-87.
16. Jordan, J.K., McCardell, W.M. and Hocott, C.R.: "Effect of Rate on Oil Recovery by Water Flooding", O&GJ, (May 13, 1957), 55, pp.98-130.
17. Levine, J.S.: "Displacement Experiments in a Consolidated Porous System", Trans., AIME (1954), 201, pp.57-66.
18. Matthews, C.S. and Fischer, M.J.: "Effect of Dip on Five-Spot Sweep Pattern", Trans., AIME (1956), 207, pp.111-117.
19. Moore, T.F. and Slobod, R.L.: "The Effect of Viscosity and Capillarity on the Displacement of Oil by Water", Prod. Monthly, (Aug 1956), 20, pp.20-30.
20. Morel-Seytoux, H.J.: "unit Mobility Ratio Displacement Calculations for Pattern Floods in Homogeneous Medium", Trans., AIME (1966), 237, pp.217-227.
21. Nielsen, R.L. and Tek, M.R.: "Evaluation of Scale-Up Laws for Two-Phase Flow Through Porous Media", Trans., AIME (1963), 228, pp.164-176.
22. Newcombe, J., McGhee, J. and Rzasa, M.J.: "Wettability versus Displacement in Water Flooding in Unconsolidated Sand Columns", Trans., AIME (1955), 204, pp.227-232.
23. Nobles, M.A. and Janzen, H.B.: "Application of a Resistance Network for Studying Mobility Ratio Effects", Trans., AIME (1958), 213, pp.356-358.
24. Prats, M, Hazebroek, P. and Allen, E.E.: "Effect of Off-Pattern Wells on the Behaviour of a Five-Spot Flood", Trans., AIME (1962), 225, pp.173-178.
25. Prats, M., Strickler, W.R. and Matthews, C.S.: "Single Fluid Five-Spot Floods in Dipping Reservoirs", Trans., AIME (1955), 204, pp.160-174.
26. Prats, M., Matthews, C.S., Jewett, R.L. and Baker, J.D.: "Prediction of Injection Rate and Production History for Multi-Fluid Five-Spot Floods", Trans., AIME (1959), 216, pp.98-105.
27. van Meurs, P.: "The Use of Transparent Three-Dimensional Models for Studying the Mechanism of Flow Processes in Oil Reservoirs", Trans., AIME (1957), 210, pp.295-301.

APPENDIX A

Determination of the Permeability and Porosity of the Model

The absolute permeability of the model was determined using Muskat's equation for the five-spot pattern:

$$q_1 = \frac{0.00354 Kh}{\mu_w \left(\ln \frac{d}{r_w} - 0.619 \right)} \Delta P$$

where

K = absolute permeability to water, mds

q_1 = total injection rate, bbls/day

μ_w = water viscosity, cp

d = distance between injection well and production well, ft

r_w = wellbore radius, ft

ΔP = pressure differential, psi

h = formation thickness, ft

Rearranging,

$$\Delta P = \frac{\mu_w \left(\ln \frac{d}{r_w} - 0.619 \right)}{0.003541 Kh} q$$

Thus a graph of ΔP versus q is linear with a slope given by

$$m = \frac{\mu_w \left(\ln \frac{d}{r_w} - 0.619 \right)}{0.003541 Kh}$$

A five-spot pattern was set up with the model fully saturated with distilled water. Water was injected into the pattern at various

rates and the corresponding pressure differentials measured. The results were as follows:

q_1 bbls/day	ΔP psi
0.0000	0.0000
0.0967	1.2863
0.1450	1.8181
0.1934	2.5580
0.2417	3.1720

Other pertinent data were as follows:

$$\begin{aligned} \mu_w &= 0.9907 \text{ c} \\ h &= 0.01482 \text{ ft} \\ r_w &= 0.00404 \text{ ft} \\ d &= 0.6670 \text{ ft} \\ \ln(d/r_w) &= 5.230 \text{ ft} \end{aligned}$$

The plot of ΔP versus q , shown in figure 25, had a slope of 13.17.

Therefore,

$$13.17 = \frac{0.9907 (5.23 - 0.619)}{0.003541 \times 0.01482 \times K}$$

from which

$$K = 6.60 \text{ darcys}$$

The porosity was obtained by a material balance calculation. Before packing, the model was filled with distilled water to determine the bulk volume. After packing, it was completely saturated with distilled water to determine the pore volume. The following results were obtained:

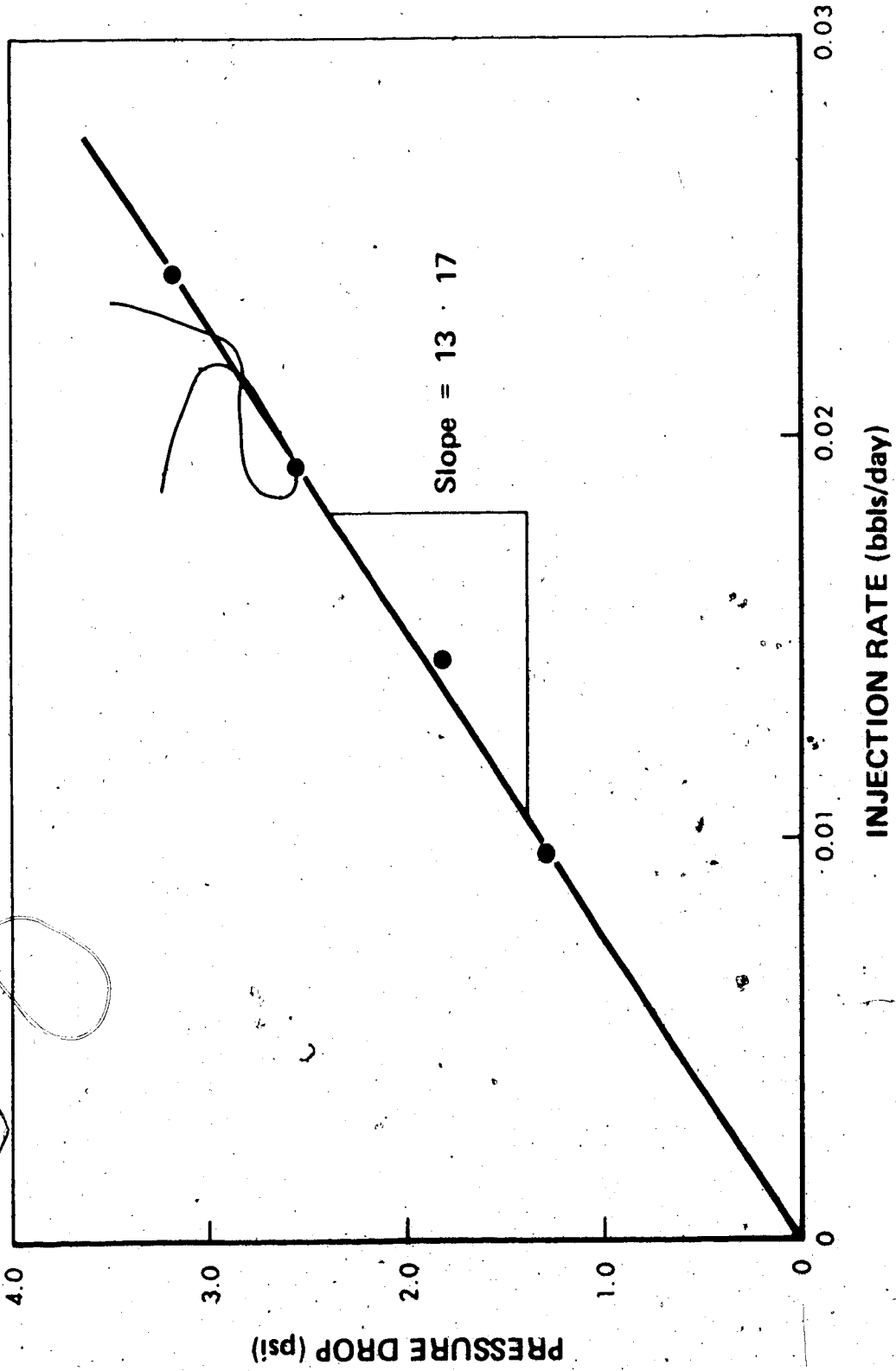


FIGURE 25. Variation of Pressure Drop with Injection Rate into a 5 - Spot Pattern.

Bulk volume = 5711.0 cc

Pore volume = 2080.0 cc

Porosity = 36.42%

APPENDIX B

Flooding Results

ISOLATED 5-SPOT PATTERN
 OIL TYPE KEROSENE CONNATE WATER (%) = 36.0

RUN NO 1 INJECTION RATE/WELL (CC/HR) = 42.9

OBSERVED PRODUCTION DATA

INCREMENTAL PRODUCTION			CUMULATIVE PRODUCTION			
GROSS (CC)	WATER (CC)	OIL (CC)	GROSS (CC)	(PV)	OIL (CC)	(%OIP)
0.0	0.0	0.0	0.0	0.000	0.0	0.00
24.9	0.0	24.9	24.9	0.654	24.9	102.38
10.5	2.5	8.0	35.4	0.930	32.9	135.28
12.7	5.5	7.1	48.0	1.264	40.0	164.88
16.0	9.9	6.1	64.1	1.685	46.2	189.96
18.5	12.7	5.8	82.6	2.171	52.0	213.81
19.5	13.7	5.8	102.1	2.684	57.8	237.66
19.8	13.6	6.2	121.9	3.205	63.9	263.15
20.9	14.6	6.3	142.8	3.754	70.3	289.06

RUN NO 2 INJECTION RATE/WELL (CC/HR) = 150.0

OBSERVED PRODUCTION DATA

INCREMENTAL PRODUCTION			CUMULATIVE PRODUCTION			
GROSS (CC)	WATER (CC)	OIL (CC)	GROSS (CC)	(PV)	OIL (CC)	(%OIP)
0.0	0.0	0.0	0.0	0.000	0.0	0.00
21.2	0.0	21.2	21.2	0.557	21.2	87.17
10.6	3.7	6.9	31.7	0.836	28.1	115.54
11.5	6.9	4.6	43.3	1.138	32.7	134.45
16.3	10.7	5.6	59.5	1.567	38.2	157.48
19.6	14.2	5.4	79.1	2.082	43.7	179.68
20.8	15.8	5.0	99.9	2.629	48.7	200.24
22.0	17.0	5.0	121.9	3.207	53.7	220.80
19.9	16.0	3.8	141.8	3.730	57.5	236.84

ISOLATED 5-SPOT PATTERN
 OIL TYPE KEROSENE CONNATE WATER (%) = 36.0

RUN NO 3 INJECTION RATE/WELL (CC/HR) = 514.3

OBSERVED PRODUCTION DATA

INCREMENTAL PRODUCTION			CUMULATIVE PRODUCTION			
GROSS (CC)	WATER (CC)	OIL (CC)	GROSS (CC)	(PV)	OIL (CC)	(%OIP)
0.0	0.0	0.0	0.0	0.000	0.0	0.00
19.3	0.0	19.3	19.3	0.507	19.3	79.35
11.4	5.2	6.2	30.7	0.807	25.5	104.85
13.3	9.0	4.3	44.0	1.156	29.8	122.53
15.9	11.8	4.1	59.8	1.574	33.9	139.39
20.4	16.0	4.3	80.2	2.111	38.2	157.48
20.5	17.4	3.1	100.7	2.650	41.3	170.23
22.5	18.0	4.5	123.2	3.241	45.8	188.73
22.4	18.9	3.5	145.6	3.830	49.3	203.12

ISOLATED 9-SPOT PATTERN

OIL TYPE KEROSENE

CONNATE WATER (%) = 36.0

RUN NO 4

INJECTION RATE/WELL (CC/HR) = 21.4

OBSERVED PRODUCTION DATA

INCREMENTAL PRODUCTION			CUMULATIVE PRODUCTION			
GROSS (CC)	WATER (CC)	OIL (CC)	GROSS (CC)	(PV)	OIL (CC)	(%IOIP)
0.0	0.0	0.0	0.0	0.000	0.0	0.00
18.5	0.0	18.5	18.5	0.486	18.5	76.06
10.7	3.0	7.6	29.2	0.767	26.2	107.73
13.5	8.0	5.5	42.7	1.122	31.7	130.34
19.4	11.8	7.5	62.0	1.632	39.3	161.59
19.0	13.0	6.0	81.1	2.132	45.3	186.26
20.4	14.2	6.2	101.5	2.668	51.5	211.76
27.1	18.6	8.5	128.6	3.381	60.0	246.71
21.0	15.2	5.8	149.6	3.933	65.8	270.56

RUN NO 5

INJECTION RATE/WELL (CC/HR) = 53.6

OBSERVED PRODUCTION DATA

INCREMENTAL PRODUCTION			CUMULATIVE PRODUCTION			
GROSS (CC)	WATER (CC)	OIL (CC)	GROSS (CC)	(PV)	OIL (CC)	(%IOIP)
0.0	0.0	0.0	0.0	0.000	0.0	0.00
16.0	0.0	16.0	16.0	0.420	16.0	65.78
11.5	3.4	8.1	27.5	0.723	24.1	99.09
13.5	7.9	5.6	41.0	1.077	29.7	122.12
17.0	11.7	5.3	58.0	1.524	35.0	143.91
19.5	14.1	5.4	77.5	2.037	40.4	166.11
18.2	13.5	4.6	95.7	2.516	45.1	185.44
19.0	14.5	4.5	114.7	3.015	49.6	203.94
20.3	15.9	4.4	135.0	3.549	54.0	222.04

ISOLATED 9-SPOT PATTERN

OIL TYPE KEROSENE CONNATE WATER (%) = 36.0

RUN NO 6 INJECTION RATE/WELL (CC/HR) = 85.7

OBSERVED PRODUCTION DATA

INCREMENTAL PRODUCTION			CUMULATIVE PRODUCTION			
GROSS (CC)	WATER (CC)	OIL (CC)	GROSS (CC)	(PV)	OIL (CC)	(%OIP)
0.0	0.0	0.0	0.0	0.000	0.0	0.00
20.5	0.0	20.5	20.5	0.538	20.5	84.29
10.5	5.0	5.5	31.0	0.815	26.0	106.90
16.5	11.9	4.6	47.5	1.248	30.6	125.82
20.8	16.4	4.4	68.3	1.795	35.0	143.91
21.5	18.3	3.2	89.8	2.361	38.2	157.07
21.0	18.0	3.0	110.8	2.913	41.2	169.40
22.0	18.9	3.1	132.8	3.491	44.3	182.15

RUN NO 7 INJECTION RATE/WELL (CC/HR) = 128.6

OBSERVED PRODUCTION DATA

INCREMENTAL PRODUCTION			CUMULATIVE PRODUCTION			
GROSS (CC)	WATER (CC)	OIL (CC)	GROSS (CC)	(PV)	OIL (CC)	(%OIP)
0.0	0.0	0.0	0.0	0.000	0.0	0.00
15.6	0.0	15.6	15.6	0.410	15.6	64.14
10.5	5.8	4.7	26.1	0.686	20.3	83.47
16.4	12.0	4.3	42.5	1.117	24.7	101.56
20.1	16.0	4.0	62.5	1.645	28.7	118.42
20.5	17.3	3.2	83.1	2.184	31.9	131.57
22.2	19.0	3.1	105.3	2.768	35.2	144.73
21.0	18.0	3.0	126.3	3.320	38.2	157.07
22.2	19.8	2.3	148.5	3.904	40.5	166.94

ISOLATED 9-SPOT PATTERN

OIL TYPE KEROSENE CONNATE WATER (%) = 36.0

RUN NO 8 INJECTION RATE/WELL (CC/HR) = 257.1

OBSERVED PRODUCTION DATA

INCREMENTAL PRODUCTION			CUMULATIVE PRODUCTION			
GROSS (CC)	WATER (CC)	OIL (CC)	GROSS (CC)	(PV)	OIL (CC)	(%IOP)
0.0	0.0	0.0	0.0	0.000	0.0	0.00
14.6	0.0	14.6	14.6	0.383	14.6	60.03
14.0	7.7	6.3	28.6	0.751	20.9	85.93
17.9	14.9	3.0	46.5	1.222	23.9	98.27
20.8	18.0	2.7	67.3	1.769	26.7	109.78
21.8	18.4	3.4	89.0	2.342	30.1	123.76
22.0	19.3	2.7	111.0	2.921	32.8	134.86
22.2	19.7	2.5	133.3	3.504	35.3	145.14

MODIFIED 5-SPOT PATTERN

OIL TYPE KERQSENF CONNATE WATER (%) = 36.0

RUN NO 9 INJECTION RATE/WELL (CC/HR) = 150.0

OBSERVED PRODUCTION DATA

INCREMENTAL PRODUCTION			CUMULATIVE PRODUCTION			
GROSS (CC)	WATER (CC)	OIL (CC)	GROSS (CC)	(PV)	OIL (CC)	(%OIP)
0.0	0.0	0.0	0.0	0.000	0.0	0.00
13.4	0.0	13.4	13.4	0.352	13.4	55.09
10.0	4.9	5.1	23.4	0.615	18.5	76.06
14.0	10.5	3.5	37.4	0.973	22.0	90.46
17.3	14.2	3.1	54.7	1.438	25.1	103.20
18.8	16.0	2.7	73.5	1.932	27.9	114.72
19.0	16.5	2.5	92.5	2.432	30.4	125.00
18.6	16.8	1.7	111.0	2.921	32.2	132.40

RUN NO 10 INJECTION RATE/WELL (CC/HR) = 214.3

OBSERVED PRODUCTION DATA

INCREMENTAL PRODUCTION			CUMULATIVE PRODUCTION			
GROSS (CC)	WATER (CC)	OIL (CC)	GROSS (CC)	(PV)	OIL (CC)	(%OIP)
0.0	0.0	0.0	0.0	0.000	0.0	0.00
14.0	0.0	14.0	14.0	0.368	14.0	57.56
12.6	7.3	5.3	26.6	0.699	19.3	79.35
16.5	13.1	3.4	43.1	1.133	22.7	93.33
20.7	18.0	2.6	63.8	1.677	25.4	104.44
20.2	18.6	1.5	84.0	2.208	27.0	111.02
19.5	17.7	1.8	103.5	2.721	28.8	118.42
21.0	19.5	1.5	124.5	3.273	30.3	124.58
21.3	19.0	2.2	145.8	3.833	32.6	134.04

MODIFIED 5-SPOT PATTERN

OIL TYPE KEROSENE CONNATE WATER (%) = 36.0

RUN NO 11 INJECTION RATE/WELL (CC/HR) = 257.1

OBSERVED PRODUCTION DATA

INCREMENTAL PRODUCTION			CUMULATIVE PRODUCTION			
GROSS (CC)	WATER (CC)	OIL (CC)	GROSS (CC)	(PV)	OIL (CC)	(%OIP)
0.0	0.0	0.0	0.0	0.000	0.0	0.00
14.0	0.0	14.0	14.0	0.368	14.0	57.56
11.5	6.1	5.4	25.5	0.670	19.4	79.77
18.0	15.0	3.0	43.5	1.143	22.4	92.10
18.7	16.5	2.1	62.2	1.635	24.6	101.15
19.5	17.9	1.6	81.7	2.148	26.2	107.73
20.4	19.5	0.8	102.1	2.684	27.1	111.43
19.0	18.0	1.0	121.1	3.183	28.1	115.54

RUN NO 12 INJECTION RATE/WELL (CC/HR) = 342.9

OBSERVED PRODUCTION DATA

INCREMENTAL PRODUCTION			CUMULATIVE PRODUCTION			
GROSS (CC)	WATER (CC)	OIL (CC)	GROSS (CC)	(PV)	OIL (CC)	(%OIP)
0.0	0.0	0.0	0.0	0.000	0.0	0.00
16.0	0.0	16.0	16.0	0.420	16.0	65.78
12.5	8.0	5.5	28.5	0.749	20.5	84.29
16.5	14.0	2.5	45.0	1.183	23.0	94.57
19.4	19.3	0.0	64.4	1.693	23.1	94.98
21.3	19.5	1.7	85.6	2.253	24.9	102.38
20.5	20.4	0.1	106.1	2.792	25.0	102.79
22.2	21.0	1.1	128.3	3.375	26.2	107.73

MODIFIED 5-SPOT PATTERN

OIL TYPE KEROSENE CONNATE WATER (%) = 36.0

RUN NO 13 INJECTION RATE/WELL (CC/HR) = 428.6

OBSERVED PRODUCTION DATA

INCREMENTAL PRODUCTION			CUMULATIVE PRODUCTION			
GROSS (CC)	WATER (CC)	OIL (CC)	GROSS (CC)	(PV)	OIL (CC)	(%INIP)
0.0	0.0	0.0	0.0	0.000	0.0	0.00
16.0	0.0	16.0	16.0	0.420	16.0	65.78
15.1	10.1	5.0	31.1	0.817	21.0	86.34
18.6	17.8	0.7	49.7	1.306	21.8	89.63
20.3	18.5	1.7	70.0	1.840	23.6	97.04
21.5	20.7	0.8	91.5	2.405	24.4	100.32
21.8	21.2	0.6	113.2	2.978	25.0	102.79
20.7	20.5	0.1	134.0	3.523	25.2	103.61

RUN NO 14 INJECTION RATE/WELL (CC/HR) = 514.3

OBSERVED PRODUCTION DATA

INCREMENTAL PRODUCTION			CUMULATIVE PRODUCTION			
GROSS (CC)	WATER (CC)	OIL (CC)	GROSS (CC)	(PV)	OIL (CC)	(%INIP)
0.0	0.0	0.0	0.0	0.000	0.0	0.00
14.5	0.0	14.5	14.5	0.381	14.5	59.62
9.3	5.0	4.3	23.8	0.625	18.8	77.30
16.6	14.2	2.4	40.4	1.062	21.2	87.17
17.5	15.9	1.6	57.9	1.522	22.8	93.75
19.0	17.7	1.3	76.9	2.021	24.1	99.09
20.3	19.3	1.0	97.1	2.555	25.1	103.20
19.5	18.5	1.0	116.6	3.068	26.1	107.31
20.0	19.0	1.0	136.7	3.594	27.1	111.43

MODIFIED 9-SPOT PATTERN

OIL TYPE KEROSENE

CONNATE WATER (%) = 36.0

RUN NO 15

INJECTION RATE/WELL (CC/HR) = 53.6

OBSERVED PRODUCTION DATA

INCREMENTAL PRODUCTION			CUMULATIVE PRODUCTION			
GROSS (CC)	WATER (CC)	OIL (CC)	GROSS (CC)	(PV)	OIL (CC)	(%INIP)
0.0	0.0	0.0	0.0	0.000	0.0	0.00
14.0	0.0	14.0	14.0	0.368	14.0	57.56
12.0	0.9	11.1	26.0	0.683	25.1	103.20
10.5	5.2	5.3	36.5	0.959	30.4	125.00
17.5	13.0	4.5	54.0	1.419	34.9	143.50
19.6	15.9	3.7	73.6	1.935	38.5	158.71
21.5	17.5	4.0	95.1	2.500	42.5	175.16
22.4	20.0	2.3	117.5	3.089	44.9	185.03
22.5	20.7	1.8	140.0	3.680	46.7	192.43

RUN NO 16

INJECTION RATE/WELL (CC/HR) = 64.3

OBSERVED PRODUCTION DATA

INCREMENTAL PRODUCTION			CUMULATIVE PRODUCTION			
GROSS (CC)	WATER (CC)	OIL (CC)	GROSS (CC)	(PV)	OIL (CC)	(%INIP)
0.0	0.0	0.0	0.0	0.000	0.0	0.00
12.4	0.0	12.4	12.4	0.326	12.4	50.98
10.9	2.0	8.9	23.3	0.612	21.3	87.58
11.5	7.0	4.5	34.8	0.914	25.8	106.08
16.0	12.3	3.7	50.8	1.335	29.5	121.30
19.7	17.0	2.6	70.5	1.853	32.2	132.40
21.0	18.6	2.4	91.5	2.405	34.6	142.27
20.4	18.6	1.7	111.9	2.942	36.4	149.87
20.8	19.5	1.2	132.6	3.488	37.7	155.01

MODIFIED 9-SPOT PATTERN

OIL TYPE KEROSENE CONNATE WATER (%) = 36.0

RUN NO 17 INJECTION RATE/WELL (CC/HR) = 85.7

OBSERVED PRODUCTION DATA

INCREMENTAL PRODUCTION			CUMULATIVE PRODUCTION			
GROSS (CC)	WATER (CC)	OIL (CC)	GROSS (CC)	(PV)	OIL (CC)	(%INIP)
0.0	0.0	0.0	0.0	0.000	0.0	0.00
12.8	0.0	12.8	12.8	0.336	12.8	52.63
11.4	2.0	9.4	24.2	0.636	22.2	91.28
13.5	10.3	3.2	37.7	0.991	25.4	104.44
17.0	14.5	2.5	54.7	1.438	27.9	114.72
18.7	16.4	2.2	73.4	1.929	30.2	124.17
20.8	19.7	1.1	94.1	2.476	31.3	128.70
20.8	19.6	1.2	114.9	3.023	32.5	133.63
20.7	19.2	1.5	135.6	3.567	34.0	139.80

RUN NO 18 INJECTION RATE/WELL (CC/HR) = 107.1

OBSERVED PRODUCTION DATA

INCREMENTAL PRODUCTION			CUMULATIVE PRODUCTION			
GROSS (CC)	WATER (CC)	OIL (CC)	GROSS (CC)	(PV)	OIL (CC)	(%INIP)
0.0	0.0	0.0	0.0	0.000	0.0	0.00
12.5	0.0	12.5	12.5	0.328	12.5	51.39
11.3	4.5	6.8	23.8	0.625	19.3	79.35
14.0	11.0	3.0	37.8	0.993	22.3	91.69
19.0	16.6	2.4	56.8	1.493	24.7	101.56
20.6	19.3	1.2	77.4	2.035	26.0	106.90
20.6	19.8	0.7	98.0	2.576	26.8	110.19
21.7	21.5	0.1	119.6	3.147	27.0	111.02
22.7	21.7	1.0	142.3	3.744	28.0	115.13

MODIFIED 9-SPOT PATTERN

OIL TYPE KEROSENE CONNATE WATER (%) = 36.0

RUN NO 19 INJECTION RATE/WELL (CC/HR) = 128.6

OBSERVED PRODUCTION DATA

INCREMENTAL PRODUCTION			CUMULATIVE PRODUCTION			
GROSS (CC)	WATER (CC)	OIL (CC)	GROSS (CC)	(PV)	OIL (CC)	(%OIP)
0.0	0.0	0.0	0.0	0.000	0.0	0.00
11.0	0.0	11.0	11.0	0.289	11.0	45.23
8.0	2.8	5.2	19.0	0.499	16.2	66.61
15.0	10.8	4.2	34.0	0.893	20.4	83.88
18.7	16.0	2.6	52.7	1.385	23.1	94.98
20.7	19.5	1.1	73.4	1.929	24.2	99.91
21.2	20.3	0.8	94.6	2.487	25.1	103.61
21.5	21.0	0.5	116.1	3.052	25.6	105.67
20.6	20.5	0.0	136.7	3.594	25.7	106.08

RUN NO 20 INJECTION RATE/WELL (CC/HR) = 171.4

OBSERVED PRODUCTION DATA

INCREMENTAL PRODUCTION			CUMULATIVE PRODUCTION			
GROSS (CC)	WATER (CC)	OIL (CC)	GROSS (CC)	(PV)	OIL (CC)	(%OIP)
0.0	0.0	0.0	0.0	0.000	0.0	0.00
12.2	0.0	12.2	12.2	0.320	12.2	50.16
9.8	3.0	6.8	22.0	0.578	19.0	78.12
18.5	15.1	3.4	40.5	1.064	22.4	92.10
20.9	19.5	1.3	61.3	1.614	23.7	97.86
20.0	19.5	0.5	81.4	2.140	24.2	99.91
22.2	21.9	0.2	103.5	2.723	24.6	101.15
21.9	21.5	0.3	125.4	3.299	24.9	102.79
21.3	21.0	0.2	146.8	3.859	25.2	104.03

MODIFIED 9-SPOT PATTERN

OIL TYPE KEROSENE

CONNATE WATER (%) = 36.0

RUN NO 21 J

INJECTION RATE/WELL (CC/HR) = 214.3

OBSERVED PRODUCTION DATA

INCREMENTAL PRODUCTION			CUMULATIVE PRODUCTION			
GRASS (CC)	WATER (CC)	OIL (CC)	GRASS (CC)	(PV)	OIL (CC)	(%OIP)
0.0	0.0	0.0	0.0	0.000	0.0	0.00
13.0	0.0	13.0	13.0	0.341	13.0	53.45
13.0	6.7	6.8	26.5	0.696	19.8	81.41
18.3	16.4	1.9	44.8	1.177	21.7	89.22
20.5	19.3	1.2	65.3	1.716	22.9	94.16
20.4	19.2	1.2	85.6	2.253	24.1	99.09
20.7	20.3	0.3	106.4	2.797	24.5	100.74
24.7	23.6	1.0	131.1	3.446	25.6	105.26
20.0	19.7	0.3	151.1	3.972	25.9	106.49

ISOLATED 5-SPOT PATTERN

OIL TYPE, HGO CONNATE WATER (%) = 33.6

RUN NO 22 INJECTION RATE/WELL (CC/HR) = 16.1

OBSERVED PRODUCTION DATA

INCREMENTAL PRODUCTION			CUMULATIVE PRODUCTION			
GROSS (CC)	WATER (CC)	OIL (CC)	GROSS (CC)	(PV)	OIL (CC)	(%OIP)
0.0	0.0	0.0	0.0	0.000	0.0	0.00
17.4	0.0	17.4	17.4	0.457	17.4	68.95
10.3	7.5	2.7	27.7	0.728	20.2	80.05
15.5	13.2	2.3	43.2	1.135	22.5	89.16
20.0	18.2	1.8	63.2	1.661	24.3	96.29
20.5	18.9	1.6	83.7	2.200	25.9	102.63
18.1	17.0	1.0	101.8	2.676	27.0	106.99
19.9	18.6	1.2	121.6	3.199	28.3	112.14

RUN NO 23 INJECTION RATE/WELL (CC/HR) = 428.6

OBSERVED PRODUCTION DATA

INCREMENTAL PRODUCTION			CUMULATIVE PRODUCTION			
GROSS (CC)	WATER (CC)	OIL (CC)	GROSS (CC)	(PV)	OIL (CC)	(%OIP)
0.0	0.0	0.0	0.0	0.000	0.0	0.00
9.9	0.0	9.9	9.9	0.260	9.9	39.23
10.5	4.9	5.6	20.4	0.536	15.5	61.42
19.5	14.8	4.7	39.9	1.049	20.2	80.05
22.3	19.0	3.2	62.2	1.635	23.5	93.12
20.4	18.4	2.0	82.5	2.171	25.5	101.05
21.6	19.3	2.2	104.1	2.739	27.8	110.16
22.0	19.8	2.2	126.1	3.318	30.0	118.88
23.6	21.5	2.0	149.8	3.938	32.1	127.20

ISOLATED 5-SPOT PATTERN

OIL TYPE HGO

CONNATE WATER (%) = 33.6

RUN NO 24

INJECTION RATE/WELL (CC/HR) = 514.3

OBSERVED PRODUCTION DATA

INCREMENTAL PRODUCTION			CUMULATIVE PRODUCTION			
GROSS (CC)	WATER (CC)	OIL (CC)	GROSS (CC)	(PV)	OIL (CC)	(%OIP)
0.0	0.0	0.0	0.0	0.000	0.0	0.00
7.5	0.0	7.5	7.5	0.197	7.5	29.72
12.3	6.5	5.8	19.8	0.520	13.3	52.70
21.0	16.5	4.5	40.8	1.072	17.8	70.53
21.4	18.1	3.2	62.2	1.635	21.1	83.61
18.9	16.8	2.0	81.0	2.132	23.2	91.93
21.6	19.6	2.0	102.6	2.700	25.2	99.86
23.3	21.4	1.9	125.9	3.312	27.1	107.39
23.8	22.0	1.7	149.7	3.938	28.9	114.52

ISOLATED 9-SPOT PATTERN

OIL TYPE HGD

CONNATE WATER (%) = 33.6

RUN NO 25

INJECTION RATE/WELL (CC/HR) = 21.4

OBSERVED PRODUCTION DATA

INCREMENTAL PRODUCTION			CUMULATIVE PRODUCTION			
GROSS (CC)	WATER (CC)	OIL (CC)	GROSS (CC)	(PV)	OIL (CC)	(%OIP)
0.0	0.0	0.0	0.0	0.000	0.0	0.00
11.0	0.0	11.0	11.0	0.289	11.0	43.59
8.9	2.5	6.4	19.9	0.523	17.4	68.95
14.4	11.1	3.3	34.3	0.901	20.7	82.03
18.5	15.5	3.0	52.8	1.388	23.7	93.92
22.2	20.2	2.0	75.0	1.971	25.7	101.84
20.3	19.4	0.9	95.2	2.505	26.6	105.41
20.0	18.5	1.5	115.2	3.031	28.1	111.35
20.0	18.5	1.5	135.3	3.557	29.6	117.30

RUN NO 26

INJECTION RATE/WELL (CC/HR) = 214.3

OBSERVED PRODUCTION DATA

INCREMENTAL PRODUCTION			CUMULATIVE PRODUCTION			
GROSS (CC)	WATER (CC)	OIL (CC)	GROSS (CC)	(PV)	OIL (CC)	(%OIP)
0.0	0.0	0.0	0.0	0.000	0.0	0.00
4.8	0.0	4.8	4.8	0.126	4.8	19.02
13.7	6.0	7.6	18.5	0.486	12.5	49.53
20.4	14.9	5.5	38.9	1.022	18.0	71.33
21.9	18.8	3.0	60.7	1.598	21.1	83.61
21.0	18.7	2.3	81.8	2.150	23.4	92.73
26.6	24.0	2.5	108.4	2.850	26.0	103.03
21.8	20.3	1.5	130.1	3.423	27.5	108.97
22.5	21.0	1.5	152.6	4.014	29.0	114.92

ISOLATED 9-SPOT PATTERN

OIL TYPE HGO. CONNATE WATER (%) = 33.6

RUN NO 27 INJECTION RATE/WELL (CC/HR) = 342.9

OBSERVED PRODUCTION DATA

INCREMENTAL PRODUCTION			CUMULATIVE PRODUCTION			
GROSS (CC)	WATER (CC)	OIL (CC)	GROSS (CC)	(PV)	OIL (CC)	(%OIP)
0.0	0.0	0.0	0.0	0.000	0.0	0.00
5.3	0.0	5.3	5.3	0.139	5.3	21.00
11.8	5.7	6.1	17.1	0.449	11.4	45.17
21.7	16.2	5.5	38.8	1.020	16.9	66.97
21.7	19.0	2.6	60.4	1.590	19.6	77.67
22.0	19.9	2.1	82.4	2.169	21.7	85.99
20.9	19.3	1.5	103.4	2.718	23.2	92.33
22.0	20.5	1.5	125.4	3.297	24.7	98.27
22.9	22.3	0.5	148.3	3.899	25.3	100.65

MODIFIED 5-SPOT PATTERN

OIL TYPE HGO

CONNATE WATER (%) = 33.6

RUN NO 30

INJECTION RATE/WELL (CC/HR) = 128.6

OBSERVED PRODUCTION DATA

INCREMENTAL PRODUCTION			CUMULATIVE PRODUCTION			
GROSS (CC)	WATER (CC)	OIL (CC)	GROSS (CC)	(PV)	OIL (CC)	(%INIP)
0.0	0.0	0.0	0.0	0.000	0.0	0.00
8.0	0.0	8.0	8.0	0.210	8.0	31.70
7.8	5.5	2.2	15.8	0.415	10.3	40.81
14.5	11.9	2.6	30.3	0.796	12.9	51.12
19.5	18.0	1.5	49.8	1.309	14.4	57.06
21.5	20.9	0.6	71.3	1.874	15.0	59.44
24.0	22.9	1.1	95.3	2.405	16.1	63.80
24.0	22.8	1.2	119.3	3.136	17.3	68.55
24.0	23.0	1.0	143.3	3.767	18.3	72.52

RUN NO 31

INJECTION RATE/WELL (CC/HR) = 171.4

OBSERVED PRODUCTION DATA

INCREMENTAL PRODUCTION			CUMULATIVE PRODUCTION			
GROSS (CC)	WATER (CC)	OIL (CC)	GROSS (CC)	(PV)	OIL (CC)	(%INIP)
0.0	0.0	0.0	0.0	0.000	0.0	0.00
7.0	0.0	7.0	7.0	0.184	7.0	27.74
9.0	5.0	4.0	16.0	0.420	11.0	43.59
17.1	15.3	1.7	33.1	0.870	12.8	50.72
21.0	19.9	1.1	54.1	1.422	13.9	55.08
20.9	19.8	1.0	75.0	1.971	15.0	59.44
21.5	20.6	0.9	96.5	2.537	15.9	63.00
22.8	22.0	0.7	119.2	3.136	16.7	66.18
17.0	17.0	0.0	136.3	3.583	16.7	66.18

MODIFIED 5-SPOT PATTERN

OIL TYPE HGO CONNATE WATER (%) = 33.6

RUN NO 32 INJECTION RATE/WELL (CC/HR) = 342.9

OBSERVED PRODUCTION DATA

INCREMENTAL PRODUCTION			CUMULATIVE PRODUCTION			
GROSS (CC)	WATER (CC)	OIL (CC)	GROSS (CC)	(PV)	OIL (CC)	(%INIP)
0.0	0.0	0.0	0.0	0.000	0.0	0.00
6.5	0.0	6.5	6.5	0.170	6.5	25.75
9.7	5.0	4.6	16.2	0.425	11.2	44.38
17.0	15.0	2.0	33.2	0.872	13.2	52.31
19.5	18.1	1.4	52.7	1.385	14.6	57.85
22.4	22.0	0.3	75.1	1.974	15.0	59.44
21.0	20.6	0.4	96.1	2.526	15.4	61.02
25.5	24.5	1.0	121.6	3.197	16.4	64.99
21.5	21.5	0.0	143.1	3.762	16.4	64.99

MODIFIED 9-SPOT PATTERN

OIL TYPE HGO

CONNATE WATER (%) = 33.6

RUN NO 33

INJECTION RATE/WELL (CC/HR) = 16.1

OBSERVED PRODUCTION DATA

INCREMENTAL PRODUCTION			CUMULATIVE PRODUCTION			
GROSS (CC)	WATER (CC)	OIL (CC)	GROSS (CC)	(PV)	OIL (CC)	(%OIP)
0.0	0.0	0.0	0.0	0.000	0.0	0.00
9.4	0.0	9.4	9.4	0.247	9.4	37.25
9.5	8.1	1.4	18.9	0.496	10.8	42.79
16.9	14.8	2.0	35.8	0.941	12.9	51.12
19.9	18.3	1.5	55.7	1.464	14.5	57.46
20.1	19.4	0.7	75.8	1.992	15.2	60.23
19.9	19.0	0.8	95.6	2.516	16.1	63.80
19.0	18.0	1.0	114.6	3.015	17.1	67.76
21.5	20.5	1.0	136.2	3.581	18.1	71.72

RUN NO 34

INJECTION RATE/WELL (CC/HR) = 53.6

OBSERVED PRODUCTION DATA

INCREMENTAL PRODUCTION			CUMULATIVE PRODUCTION			
GROSS (CC)	WATER (CC)	OIL (CC)	GROSS (CC)	(PV)	OIL (CC)	(%OIP)
0.0	0.0	0.0	0.0	0.000	0.0	0.00
6.5	0.0	6.5	6.5	0.170	6.5	25.75
9.0	4.6	4.4	15.5	0.407	10.9	43.19
14.8	13.1	1.7	30.3	0.796	12.6	49.93
18.9	17.6	1.2	49.2	1.293	13.9	55.08
21.0	20.0	1.0	70.2	1.845	14.9	59.04
22.7	21.6	1.0	92.9	2.442	16.0	63.40
20.5	20.5	0.0	113.4	2.981	16.0	63.40
23.4	23.0	0.3	136.8	3.596	16.4	64.99

MODIFIED 9-SPOT PATTERN

OIL TYPE HGO CONNATE WATER (%) = 33.6

RUN NO 35 INJECTION RATE/WELL (CC/HR) = 150.0

OBSERVED PRODUCTION DATA

INCREMENTAL PRODUCTION			CUMULATIVE PRODUCTION			
GROSS (CC)	WATER (CC)	OIL (CC)	GROSS (CC)	(PV)	OIL (CC)	(%OIP)
0.0	0.0	0.0	0.0	0.000	0.0	0.00
4.5	0.0	4.5	4.5	0.118	4.5	17.83
11.4	5.5	5.9	15.9	0.418	10.4	41.21
18.9	16.2	2.7	34.8	0.914	13.1	51.91
20.5	19.5	1.0	55.3	1.453	14.1	55.87
21.3	20.9	0.4	76.6	2.013	14.5	57.46
21.5	21.0	0.5	98.1	2.579	15.0	59.44
21.1	20.3	0.7	119.1	3.134	15.8	62.61
24.3	23.3	1.0	143.5	3.772	16.8	66.57

RUN NO 36 INJECTION RATE/WELL (CC/HR) = 257.1

OBSERVED PRODUCTION DATA

INCREMENTAL PRODUCTION			CUMULATIVE PRODUCTION			
GROSS (CC)	WATER (CC)	OIL (CC)	GROSS (CC)	(PV)	OIL (CC)	(%OIP)
0.0	0.0	0.0	0.0	0.000	0.0	0.00
5.8	0.0	5.8	5.8	0.152	5.8	22.98
10.3	5.3	5.0	16.1	0.423	10.8	42.79
16.2	13.5	2.6	32.3	0.849	13.4	53.49
20.6	19.2	1.4	52.9	1.390	14.8	59.04
20.5	20.0	0.5	73.4	1.929	15.3	61.02
21.7	20.9	0.7	95.1	2.500	16.2	64.19
22.5	22.0	0.5	117.6	3.091	16.7	66.18
25.0	24.5	0.5	142.6	3.749	17.2	68.16

ISOLATED 5-SPOT PATTERN

OIL TYPE (CWD)

CONNATE WATER (%) = 30.2

RUN NO 37

INJECTION RATE/WELL (CC/HR) = 16.1

OBSERVED PRODUCTION DATA

INCREMENTAL PRODUCTION			CUMULATIVE PRODUCTION			
GROSS (CC)	WATER (CC)	OIL (CC)	GROSS (CC)	(PV)	OIL (CC)	(%IPIP)
0.0	0.0	0.0	0.0	0.000	0.0	0.00
13.3	0.0	13.3	13.3	0.349	13.3	50.16
9.2	5.9	3.2	22.5	0.591	16.6	62.60
16.8	14.4	2.4	39.3	1.033	19.0	71.66
19.0	16.4	2.6	58.3	1.532	21.6	81.46
19.0	16.5	2.5	77.3	2.032	24.1	90.89
20.0	18.0	2.0	97.3	2.558	26.1	98.43
20.4	18.7	1.7	117.6	3.094	27.8	104.84
19.4	18.1	1.2	137.1	3.604	29.1	109.75

RUN NO 38

INJECTION RATE/WELL (CC/HR) = 428.6

OBSERVED PRODUCTION DATA

INCREMENTAL PRODUCTION			CUMULATIVE PRODUCTION			
GROSS (CC)	WATER (CC)	OIL (CC)	GROSS (CC)	(PV)	OIL (CC)	(%IPIP)
0.0	0.0	0.0	0.0	0.000	0.0	0.00
8.0	0.0	8.0	8.0	0.210	8.0	30.17
13.3	9.0	4.3	21.3	0.560	12.3	46.39
16.5	13.3	3.2	37.8	0.993	15.5	58.45
20.0	17.0	3.0	57.8	1.519	18.5	69.77
20.5	18.4	2.1	78.3	2.058	20.6	77.69
21.0	19.0	2.0	99.3	2.610	22.6	85.23
19.3	17.5	1.7	118.5	3.118	24.4	92.02
20.9	19.4	1.5	139.5	3.667	25.9	97.68

ISOLATED 5-SPOT PATTERN

OIL TYPE CWD

CONNATE WATER (%) = 30.2

RUN NO. 39

INJECTION RATE/WELL (CC/HR) = 514.3

OBSERVED PRODUCTION DATA

INCREMENTAL PRODUCTION			CUMULATIVE PRODUCTION			
GROSS WATER (CC)	OIL (CC)	GROSS (CC)	GROSS (CC)	(PV)	OIL (CC)	(%OIP)
0.0	0.0	0.0	0.0	0.000	0.0	0.00
5.1	0.0	5.1	5.1	0.134	5.1	19.23
12.0	7.1	4.9	17.1	0.449	10.0	37.71
18.2	14.8	3.3	35.3	0.928	13.3	50.53
19.8	17.0	2.7	55.0	1.448	16.2	61.09
20.5	18.4	2.1	75.6	1.987	18.3	69.01
19.5	17.7	1.8	95.1	2.500	20.1	75.80
20.4	18.5	1.8	115.5	3.036	22.0	82.97
19.1	17.7	1.4	134.6	3.538	23.4	88.25

ISOLATED SPOT PATTERN

OIL TYPE CWD CONNATE WATER (%) = 30.2

RUN NO 40 INJECTION RATE/WELL (CC/HR) = 21.4

OBSERVED PRODUCTION DATA

INCREMENTAL PRODUCTION			CUMULATIVE PRODUCTION			
GROSS (CC)	WATER (CC)	OIL (CC)	GROSS (CC)	(PV)	OIL (CC)	(%OIP)
0.0	0.0	0.0	0.0	0.000	0.0	0.00
11.0	0.0	11.0	11.0	0.289	11.0	41.48
12.5	8.1	4.4	23.5	0.617	15.4	58.08
17.5	14.8	2.7	41.0	1.077	18.1	68.26
19.0	17.0	2.0	60.0	1.577	20.1	75.80
19.4	18.0	1.3	79.4	2.087	21.5	81.08
20.6	19.9	0.7	100.0	2.629	22.2	83.72
22.4	21.6	0.7	122.4	3.218	23.0	86.74
19.6	19.6	0.0	142.0	3.733	23.0	86.74

RUN NO 41 INJECTION RATE/WELL (CC/HR) = 85.7

OBSERVED PRODUCTION DATA

INCREMENTAL PRODUCTION			CUMULATIVE PRODUCTION			
GROSS (CC)	WATER (CC)	OIL (CC)	GROSS (CC)	(PV)	OIL (CC)	(%OIP)
0.0	0.0	0.0	0.0	0.000	0.0	0.00
4.5	0.0	4.5	4.5	0.118	4.5	16.97
10.3	4.5	5.8	14.8	0.389	10.3	38.84
18.2	14.5	3.6	33.0	0.867	13.9	52.80
21.1	19.5	1.5	54.0	1.422	15.5	58.83
22.0	20.4	1.6	76.1	2.000	17.2	64.87
21.5	19.9	1.6	97.6	2.566	18.8	70.90
21.6	20.1	1.5	119.1	3.134	20.3	76.56
21.6	20.1	1.5	140.8	3.701	21.8	82.22

ISOLATED 9-SPOT PATTERN

OIL TYPE CWD CONNATE WATER (%) = 30.2

RUN NO 42 INJECTION RATE/WELL (CC/HR) = 342.9

OBSERVED PRODUCTION DATA

INCREMENTAL PRODUCTION			CUMULATIVE PRODUCTION			
GROSS (CC)	WATER (CC)	OIL (CC)	GROSS (CC)	(PV)	OIL (CC)	(%INIP)
0.0	0.0	0.0	0.0	0.000	0.0	0.00
3.5	0.0	3.5	3.5	0.092	3.5	13.20
12.3	7.2	5.1	15.8	0.415	8.6	32.43
20.4	16.8	3.5	36.2	0.951	12.2	46.01
20.9	18.5	2.3	57.0	1.501	14.5	55.06
21.0	19.5	1.5	78.1	2.053	16.1	60.72
21.8	20.5	1.2	99.9	2.626	17.3	65.62
21.5	20.5	1.0	121.4	3.191	18.3	69.39
22.0	21.0	1.0	143.3	3.770	19.3	73.16

MODIFIED 5-SPOT PATTERN

OIL TYPE (CWO)

CONNATE WATER (%) = 30.2

RUN NO 43

INJECTION RATE/WELL (CC/HR) = 32.1

OBSERVED PRODUCTION DATA

INCREMENTAL PRODUCTION			CUMULATIVE PRODUCTION			
GROSS (CC)	WATER (CC)	OIL (CC)	GROSS (CC)	(PV)	OIL (CC)	(%OIP)
	0.0	0.0	0.0	0.000	0.0	0.00
9.0	0.0	9.0	9.0	0.236	9.0	33.94
10.3	8.4	1.8	19.3	0.507	10.9	41.11
14.5	14.3	0.2	33.8	0.888	11.1	41.86
17.7	17.5	0.1	51.5	1.354	11.3	42.61
14.6	14.3	0.2	66.1	1.737	11.5	43.75
12.7	12.1	0.6	78.8	2.071	12.1	46.01
18.1	17.4	0.7	96.9	2.547	12.8	48.65
18.4	17.6	0.7	115.2	3.031	13.6	51.67
21.8	21.6	0.2	137.0	3.604	13.8	52.42

RUN NO 44

INJECTION RATE/WELL (CC/HR) = 85.7

OBSERVED PRODUCTION DATA

INCREMENTAL PRODUCTION			CUMULATIVE PRODUCTION			
GROSS (CC)	WATER (CC)	OIL (CC)	GROSS (CC)	(PV)	OIL (CC)	(%OIP)
0.0	0.0	0.0	0.0	0.000	0.0	0.00
8.3	0.0	8.3	8.3	0.218	8.3	31.30
10.5	7.5	3.0	18.8	0.494	11.3	42.61
19.5	18.4	1.1	38.3	1.006	12.4	46.76
20.6	19.9	0.7	58.9	1.548	13.1	49.40
23.0	22.9	0.1	81.9	2.153	13.2	49.78
21.4	21.1	0.2	103.3	2.715	13.5	50.91
21.8	21.6	0.2	125.0	3.289	13.7	51.67
22.5	22.4	0.1	147.6	3.880	13.8	52.04

MODIFIED 5-SPOT PATTERN

OIL TYPE CWO

CONNATE WATER (%) = 30.2

RUN NO 45

INJECTION RATE/WELL (CC/HR) = 107.4

OBSERVED PRODUCTION DATA

INCREMENTAL PRODUCTION			CUMULATIVE PRODUCTION			
GROSS (CC)	WATER (CC)	OIL (CC)	GROSS (CC)	(PV)	OIL (CC)	(%INIP)
0.0	0.0	0.0	0.0	0.000	0.0	0.00
7.0	0.0	7.0	7.0	0.184	7.0	26.40
8.5	4.4	4.1	15.5	0.407	11.1	41.86
15.7	14.2	1.5	31.2	0.820	12.6	47.52
19.0	18.5	0.5	50.2	1.319	13.1	49.40
20.2	19.9	0.2	70.4	1.850	13.4	50.53
20.1	19.8	0.2	90.5	2.379	13.7	51.67
21.0	20.9	0.1	111.5	2.931	13.8	52.04
22.1	21.9	0.2	133.6	3.512	14.0	52.80

RUN NO 46

INJECTION RATE/WELL (CC/HR) = 342.9

OBSERVED PRODUCTION DATA

INCREMENTAL PRODUCTION			CUMULATIVE PRODUCTION			
GROSS (CC)	WATER (CC)	OIL (CC)	GROSS (CC)	(PV)	OIL (CC)	(%INIP)
0.0	0.0	0.0	0.0	0.000	0.0	0.00
6.0	0.0	6.0	6.0	0.157	6.0	22.62
15.7	11.3	4.4	21.7	0.570	10.4	39.22
18.5	16.8	1.7	40.2	1.056	12.1	45.63
18.9	18.2	0.7	59.0	1.553	12.8	48.27
21.0	20.4	0.6	80.1	2.106	13.4	50.53
21.4	21.1	0.2	101.5	2.668	13.7	51.67
20.6	20.4	0.2	122.0	3.210	13.9	52.42
21.6	21.5	0.0	143.6	3.778	14.0	52.80

MODIFIED 9-SPOT PATTERN

OIL TYPE CWD CONNATE WATER (%) = 30.2

RUN NO 47 INJECTION RATE/WELL (CC/HR) = 16.1

OBSERVED PRODUCTION DATA

INCREMENTAL PRODUCTION			CUMULATIVE PRODUCTION			
GROSS (CC)	WATER (CC)	OIL (CC)	GROSS (CC)	(PV)	OIL (CC)	(%IPIP)
0.0	0.0	0.0	0.0	0.000	0.0	0.00
7.8	0.0	7.8	7.8	0.205	7.8	29.41
13.0	9.9	3.1	20.8	0.546	10.9	41.11
18.8	18.1	0.7	39.6	1.041	11.6	43.75
19.0	18.4	0.6	58.6	1.540	12.2	46.01
18.0	17.4	0.6	76.6	2.013	12.8	48.27
18.4	17.7	0.7	95.0	2.497	13.5	50.91
20.5	20.0	0.5	115.5	3.036	14.0	52.80
21.0	20.7	0.3	136.5	3.588	14.3	53.93

RUN NO 48 INJECTION RATE/WELL (CC/HR) = 32.1

OBSERVED PRODUCTION DATA

INCREMENTAL PRODUCTION			CUMULATIVE PRODUCTION			
GROSS (CC)	WATER (CC)	OIL (CC)	GROSS (CC)	(PV)	OIL (CC)	(%IPIP)
0.0	0.0	0.0	0.0	0.000	0.0	0.00
2.0	0.0	2.0	2.0	0.052	2.0	7.54
8.4	2.1	6.3	10.4	0.273	8.3	31.30
11.0	9.0	2.0	21.4	0.562	10.3	38.84
15.5	13.7	1.8	36.9	0.970	12.1	45.63
19.3	18.6	0.7	56.2	1.477	12.8	48.27
19.5	18.9	0.6	75.6	1.990	13.4	50.53
20.0	19.6	0.4	95.6	2.516	13.8	52.04
20.6	20.5	0.0	116.2	3.057	13.9	52.42

MODIFIED 9-SPOT PATTERN

OIL TYPE CWO

CONNATE WATER (%) = 30.2

RUN NO 49

INJECTION RATE/WELL (CC/HR) = 53.6

OBSERVED PRODUCTION DATA

INCREMENTAL PRODUCTION			CUMULATIVE PRODUCTION			
GROSS (CC)	WATER (CC)	OIL (CC)	GROSS (CC)	(PV)	OIL (CC)	(%IOIP)
0.0	0.0	0.0	0.0	0.000	0.0	0.00
7.0	0.0	7.0	7.0	0.184	7.0	26.40
10.0	7.1	2.9	17.0	0.446	9.9	37.33
14.2	12.5	1.6	31.2	0.820	11.6	43.75
20.3	20.0	0.2	51.5	1.354	11.9	44.88
20.1	19.4	0.7	71.6	1.882	12.6	47.52
22.0	21.2	0.8	93.6	2.460	13.4	50.53
20.0	19.5	0.5	113.6	2.986	13.9	52.42

RUN NO 50

INJECTION RATE/WELL (CC/HR) = 150.0

OBSERVED PRODUCTION DATA

INCREMENTAL PRODUCTION			CUMULATIVE PRODUCTION			
GROSS (CC)	WATER (CC)	OIL (CC)	GROSS (CC)	(PV)	OIL (CC)	(%IOIP)
0.0	0.0	0.0	0.0	0.000	0.0	0.00
3.0	0.0	3.0	3.0	0.078	3.0	11.31
11.3	5.8	5.5	14.3	0.375	8.5	32.05
16.0	12.6	3.4	30.3	0.796	11.9	44.88
19.0	18.8	0.2	49.3	1.296	12.1	45.63
21.1	20.9	0.2	70.4	1.850	12.3	46.39
22.7	22.4	0.2	93.1	2.447	12.6	47.52
21.7	21.3	0.3	114.8	3.018	13.0	49.03
22.5	22.1	0.4	137.3	3.609	13.4	50.53

MODIFIED 9-SPOT PATTERN

OIL TYPE CWO CONNATE WATER (%) = 30.2

RUN NO 51 INJECTION RATE/WELL (CC/HR) = 214.3

OBSERVED PRODUCTION DATA

INCREMENTAL PRODUCTION			CUMULATIVE PRODUCTION			
GROSS (CC)	WATER (CC)	OIL (CC)	GROSS (CC)	(PV)	OIL (CC)	(%OIP)
0.0	0.0	0.0	0.0	0.000	0.0	0.00
3.0	0.0	3.0	3.0	0.078	3.0	11.31
10.5	4.0	6.5	13.5	0.354	9.5	35.83
19.3	17.8	1.5	32.8	0.862	11.0	41.48
20.2	19.7	0.5	53.0	1.393	11.5	43.37
20.1	19.8	0.2	73.1	1.921	11.8	44.50
21.6	21.0	0.5	94.6	2.489	12.3	46.76
20.8	20.5	0.2	115.4	3.036	12.6	47.89
20.8	20.0	0.7	136.3	3.583	13.4	50.91

APPENDIX C

Determination of Mobility Ratios

Fluid mobilities were defined at the residual saturations as suggested by Perkins and Collins (99). On this basis,

$$M = \frac{k_{wro}}{\mu_w} \times \frac{\mu_o}{k_{ocw}}$$

where

M = mobility ratio

k_{wro} = effective permeability to water at residual oil saturation

k_{ocw} = effective permeability to oil at residual water saturation

The permeabilities at the various residual saturations were determined using Muskat's five-spot equation outlined in Appendix A. The results were as follows:

Oil Type	μ_o/μ_w	S_{wi} (%)	S_{or} (%)	k_{wro} (darcys)	k_{ocw} (darcys)	M'
Kerosen	1.3165	36.0	8.0	5.15	2.57	2.63
KGO	8.6566	33.6	12.0	4.62	2.84	14.09
CWO	15.2206	30.2	15.0	4.29	3.17	20.61

APPENDIX D

Calculation of Scaling Coefficients

It will be recalled that the scaling coefficient proposed for the five and nine-spot floods was given by:

$$C = \frac{Q \mu_w}{\sigma \sqrt{K\phi}}$$

where

Q = production rate of pilot in bbls/day/ft

σ = oil-water interfacial tension in dynes/cm

K = absolute permeability of the porous medium in md

ϕ = fractional porosity

μ_w = water viscosity in cp

As pointed out earlier, for the five-spot

$$Q = q/h$$

where

q = injection rate per well, bbls/day

h = thickness of porous medium, ft

and for the nine-spot,

$$Q = 2 \frac{q_1}{h} + \frac{q_2}{h}$$

where

q_1 = injection rate of side well, bbls/day

q_2 = injection rate of corner well, bbls/day

In this study, uniform injection rates were used throughout; hence,

$$q_1 = q_2$$

The scaling coefficients were calculated at two viscosity ratios, 1.32 and 8.66. The results at a viscosity ratio of 15.22 were similar to those at 8.66 and as such, are not repeated here. The details of the calculations are given below.

Five-Spot Pattern, Viscosity Ratio = 1.32 (M = 2.63)

q (cc/hr/well)	Q (bbls/day/ft)	$C = \frac{Q\mu_w}{\sigma\sqrt{K\phi}}$	Oil Recovery at 1 PV (% IOIP)	Oil Recovery at 2 PV (% IOIP)
150.0	1.391	1.035×10^{-3}	91.0	116.7
214.3	1.987	1.478×10^{-3}	89.8	108.8
257.1	2.384	1.773×10^{-3}	89.0	105.0
342.9	3.179	2.365×10^{-3}	90.5	101.2
428.6	3.973	2.956×10^{-3}	90.2	79.9
514.3	3.768	3.547×10^{-3}	87.0	98.8

Nine-Spot Pattern, Viscosity Ratio = 1.32 (M = 2.63)

53.6	1.491	1.109×10^{-3}	126.2	162.0
64.3	1.788	1.330×10^{-3}	110.6	135.5
85.7	2.385	1.773×10^{-3}	105.0	124.0
107.1	2.979	2.216×10^{-3}	91.9	106.8
128.6	3.576	2.661×10^{-3}	86.5	100.6
171.4	4.767	3.547×10^{-3}	91.0	100.6
214.3	5.961	4.434×10^{-3}	87.0	98.0

Five-Spot Pattern, Viscosity Ratio = 8.66 (M = 14.09)

q (cc/hr/well)	Q (bbls/day/ft)	$C = \frac{Q\mu_w}{\sigma\sqrt{K\phi}}$	Oil Recovery at 1 PV (% IOIP)	Oil Recovery at 2 PV (% IOIP)
32.1	0.298	0.221×10^{-3}	55.0	63.0
85.7	0.795	0.590×10^{-3}	55.5	63.2
128.6	1.192	0.885×10^{-3}	53.4	60.5
171.4	1.589	1.179×10^{-3}	52.0	59.3
342.9	3.179	2.359×10^{-3}	53.0	59.4

Nine-Spot Pattern, Viscosity Ratio = 8.66 (M = 14.09)

16.1	0.448	0.332×10^{-3}	51.8	61.0
53.6	1.491	1.106×10^{-3}	51.8	60.0
150.0	4.172	3.096×10^{-3}	52.7	57.8
257.1	7.151	5.307×10^{-3}	55.5	61.8

It should be pointed out that the scaling coefficients calculated above are not in consistent units. The mixed units were adopted in order to facilitate the comparison of the present results with those in the literature. The units may, however, be made consistent by the application of an appropriate conversion factor.

To obtain the conversion factor, the various quantities which enter into the calculation of C should be expressed in consistent cgs units; that is, Q should be expressed in cc/sec-cm, μ_w in poise, σ in dynes/cm, and K in cm^2 . Thus,

$$C \equiv \frac{\text{bbl} \times \text{cp} \times \text{cm}}{\text{ft} \times \text{day} \times \text{dynes} \times \sqrt{\text{md}}} \equiv \gamma \frac{\text{cm}^3 \times \text{poise} \times \text{cm}}{\text{cm} \times \text{sec} \times \text{dynes} \times \sqrt{\text{cm}^2}}$$

where γ is the required conversion factor.

Noting that

$$1 \text{ ft} = 30.48 \text{ cm}$$

$$1 \text{ bbl} = 1.590 \times 10^5 \text{ cm}^3$$

$$1 \text{ cp} = 0.01 \text{ poise}$$

$$1 \text{ day} = 8.640 \times 10^4 \text{ sec}$$

$$1 \text{ md} = 9.869 \times 10^{-12} \text{ cm}^2$$

then,

$$C \equiv \frac{(1.590 \times 10^5)(0.01)}{(30.48)(8.640 \times 10^4)(3.141 \times 10^{-6})} \frac{\text{cm}^3 \times \text{poise} \times \text{cm}}{\text{cm} \times \text{sec} \times \text{dynes} \times \text{cm}}$$

$$\equiv 1.922 \times 10^2 \frac{\text{cm}^3 \times \text{poise} \times \text{cm}}{\text{cm} \times \text{sec} \times \text{dynes} \times \text{cm}}$$

Therefore,

$$\gamma = 1.922 \times 10^2$$

Thus, if consistent units are desired, the above values of C should be multiplied by 1.922×10^2 .